

Anti-TB Drug Leads From Diverse Natural Sources

BY

CHANG HWA HWANG

B.S., University of Illinois at Chicago, Chicago, 2003

DISSERTATION

Submitted as partial fulfillment of the requirements
for the degree of Doctor of Philosophy in Pharmacognosy
in the Graduate College of the
University of Illinois at Chicago, 2012

Chicago, Illinois

Defense committee:

Scott Franzblau, Chair and Advisor
Guido Pauli, Co-advisor
Brian Murphy
Birgit Jaki
Brent Friesen, Dominican University

DEDICATION

To

my parents; Jae Hun Hwang, Mi Joo Kim

my wife; Jung Yoo Hwang, and

my daughter; Olivia M. Hwang

ACKNOWLEDGEMENTS

This dissertation would not have been possible without the immeasurable supports from all the people around me. Especially, my foremost thanks go to my two academic Advisors, Dr. Scott Franzblau and Dr. Guido Pauli, who have provided great mentorship, trust, and patience over the time. Especially, the learning of persistence, exactitude, critical insights for the quality of science from Dr. Franzblau and Dr. Pauli will be always a great asset on my career.

I also owe sincere and earnest thankfulness to Drs. Birgit Jaki (the overall project guidance), Sanghyun Cho (high throughput screening and microbiology), David Lankin (NMR experiments), Jose Napolitano (PERCH software), Larry Klein (the synthesis of the four coumarins), James McAlpine (reviewing all three manuscripts and thesis along with great critical discussions), Shaonong Chen (chromatography), Maria F. Rodriguez-Brasco (spectroscopy) for sharing their scientific expertise and for countless redirecting me whenever I was lost.

I am grateful and privileged to have wonderful collaborators; namely Dr. Cedric Pearce and Mr. Paul Stamets, who providing me with a fungal extract library and the mushroom extracts, respectively. Without their continuous support, I would not have been able to make it this far.

The ITR staff, current/former students, and researchers also deserve countless thanks for their help throughout my time at UIC. Especially, I would like to thank Ms. Lorna Haubrich, Ms. Valsamma Abraham, and Dr. Bogdan Catalin for helping and solving almost 8 yrs of my human resource needs along with several VISA status changes. I also like to thank to Dr. Yeuhong Wang, Ms Baojie Wan, Geping Cai, Nan Zhang, Wei Gao, Hiten Gutka, Rene Ramos, Hacksoo Kang, Hyunjeong Kim, Aiyano Imai, Bethany Elkington, Kim Bean, Mathew Main, Feng Qiu, and Jahye Myung for our great friendship and for sharing my burden of science.

ACKNOWLEDGEMENTS (continued)

Lastly, I am truly indebted and thankful to Drs. Hyunwoo Lee, Hyunyoung Jeong, and Sungpil Cho for sharing their infinite interdisciplinary science and passion.

CHH

TABLE OF CONTENTS

<u>Chapter</u>	<u>page</u>
1 Introduction	2
1.1 Tuberculosis	2
1.1.1 Etology.....	3
1.1.2 Global TB facts.....	5
1.1.3 TB chemotherapy	6
1.2 Drug discovery and development	9
1.2.1 The process	9
1.2.2 Current TB drug discovery and challenges.....	11
1.2.3 Drug discovery from natural products.....	14
1.3 Statement of problem / hypothesis and specific aims	17
2 Aim 1: To find useful ethnobotanicals for TB drug lead discovery from the NAPRALERT database..	19
2.1 Background / scope of this study.....	20
2.2 Results and discussion.....	21
2.3 Limitation and suggested solution	30
3 Aim 2: Chemical and biological assessment of an anti-TB ethnomedicinal mushroom, <i>Fomitopsis officinalis</i> for anti-TB drug lead discovery	32
3.1 Background / scope of this study.....	33
3.2 Results and discussion.....	34
3.3 Materials and methods	42
4 Aim 3: To search for a new TB drug lead from fungal extract library	52
4.1 Aim 3a: High throughput screening of 12,905 fungal extracts library for anti-TB activity	53
4.1.1 Background / scope of this study.....	53
4.1.2 Results	55
4.1.3 Discussion.....	59
4.1.4 Materials and methods	61
4.2 Aim 3b: Isolation, identification, and biological evaluation of the anti-TB active principle	64
4.2.1 Background / scope of this study.....	64
4.2.2 Results	64
4.2.3 Discussion.....	74
4.2.4 Materials and methods	77
5 General conclusion, summary of aims, and future direction	81
References	89
APPENDICES	98
VITA	113

LIST OF FIGURES

<u>Figure</u>	<u>page</u>
Figure 1: A. <i>M. tuberculosis</i> cell wall structure. B. Phase of infection with <i>M. tuberculosis</i>	2
Figure 2: The pathogenesis of tuberculosis	3
Figure 3: Anti-tuberculosis drugs.....	8
Figure 4: Drug discovery and development process	10
Figure 5: Drugs in the clinical evaluation for tuberculosis	12
Figure 6: The 13 classes of antibiotics discovered.....	14
Figure 7: A. All new chemical entities, 1981 – 2006. B. Principal component analysis for chemical property distributions	15
Figure 8: Drugs derived from ethnobotanicals.....	19
Figure 9: Literature search and data mining scheme	21
Figure 10: Score index with the five criteria for prioritizing the 45 plants.....	23
Figure 11: Summary of NAPRALERT data mining	24
Figure 12: Anti-TB MICs of xanthenes	27
Figure 13: Falcarinol and phytol.	28
Figure 14: Two new naturally occurring coumarins (1 and 3) and their analogs (2 and 4).....	34
Figure 15: Key 2D correlations that were used for the structure determination of 1 and 2	35
Figure 16: NMR spectrum (225/900 MHz, MeOH-d ₄) comparison between synthesized and isolated compound 1 and 2.....	36
Figure 17: A. Distribution of growth inhibitory activity of 12,905 fungal extracts. B. Representative Z' factor	56
Figure 18: A. an MIC and cytotoxicity distribution of 460 extracts. B. Summary of high throughput screening results	57
Figure 19: Bio-activity guided isolation protocol of vermispurin from MSX105528. MICs for MSX105528 extract and the primary SPE fractions against <i>M. tuberculosis</i> H37Rv	66
Figure 20: A. Key results of the structure elucidation of the isolate and dereplication as vermispurin. COSY and HMBC correlations. B. 1D TOCSY upon selective excitation at δ 2.168 (H-3), δ 1.677 (H-4), and δ 1.468 (H-6) ppm. C. Observed NOE correlations for vermispurin.	68
Figure 21: Full ¹ H NMR spin analysis by PERCH iteration of 900 MHz data of vermispurin.....	71

LIST OF FIGURES (continued)

<u>Figure</u>	<u>page</u>
Figure 22: A. Possible tautomers of vermispurin and other tetramic acids. B. ^1H (900 MHz) and ^{13}C DEPTQ (225 MHz) NMR spectrum of vermispurin	75
Figure 23: Chiral centers in vermispurin.....	86
Figure 24: ^1H NMR spectrum of isolated 1	99
Figure 25: ^{13}C DEPTQ NMR spectrum of isolated 1	99
Figure 26: ^1H - ^1H COSY NMR spectrum of isolated	100
Figure 27: HSQC NMR spectrum of isolated 1	100
Figure 28: HMBC NMR spectrum of isolated 1	101
Figure 29: ^1H NMR spectrum of isolated 2	101
Figure 30: ^{13}C DEPTQ NMR spectrum of isolated 2	102
Figure 31: ^1H - ^1H COSY NMR spectrum of isolated 2	102
Figure 32: HSQC NMR spectrum of isolated 2	103
Figure 33: HMBC NMR spectrum of isolated 2	103
Figure 34: ^1H NMR spectrum of synthetic 1	104
Figure 35: ^{13}C DEPTQ NMR spectrum of synthetic 1	104
Figure 36: ^1H NMR spectrum of synthetic 2	105
Figure 37: ^{13}C DEPTQ NMR spectrum of synthetic 2	105
Figure 38: ^1H NMR spectrum of synthetic 3	106
Figure 39: ^{13}C DEPTQ NMR spectrum of synthetic 3	106
Figure 40: ^1H NMR spectrum of synthetic 4	107
Figure 41: ^{13}C DEPTQ NMR spectrum of synthetic 4	107
Figure 42: Full ^1H NMR spin analysis by PERCH iteration of 900 MHz data of the synthetic 1	108
Figure 43: Full ^1H NMR spin analysis by PERCH iteration of 900 MHz data of the synthetic 2	108
Figure 44: Full ^1H NMR spin analysis by PERCH iteration of 900 MHz data of the synthetic 3	109
Figure 45: Full ^1H NMR spin analysis by PERCH iteration of 900 MHz data of the synthetic 4	109
Figure 46: ^1H NMR spectrum of vermitrasporin.....	110
Figure 47: ^{13}C DEPTQ NMR spectrum of vermitrasporin	110

LIST OF FIGURES (continued)

Figure 48: ^1H - ^1H COSY NMR spectrum of vermitrasporin.....	111
Figure 49: HSQC NMR spectrum of vermitrasporin.....	111
Figure 50: HMBC NMR spectrum of vermitrasporin	112
Figure 51: ROESY NMR spectrum of vermitrasporin.....	112

LIST OF TABLES

<u>TABLE</u>	<u>Page</u>
TABLE I: CURRENT ANTI-TUBERCULOSIS DRUGS	8
TABLE II: DRUGS IN CLINICAL EVALUATION FOR TUBERCULOSIS	12
TABLE III: GROUP A	25
TABLE IV: GROUP B	25
TABLE V: GROUP C	26
TABLE VI: ¹ H AND ¹³ C NMR DATA OF COMPOUNDS 1 - 4	37
TABLE VII: ANTI-TB ACTIVITY PROFILES OF THE COUMARIN 1 - 4	40
TABLE VIII: SPECTRUM OF ACTIVITY AND NON-TUBERCULOUS MYCOBACTERIA ACTIVITY	41
TABLE IX: ANTI-TB ACTIVITY AND MAMMALIAN CELL CYTOTOXICITY FOR 13 PRIORITIZED EXTRACTS ..	59
TABLE X: OPTIMIZATION OF VARIOUS CULTURE CONDITIONS OF MSX105528 FOR ACTIVITY AGAINST <i>MYCOBACTERIUM TUBERCULOSIS</i> H37Rv	65
TABLE XI: NMR SPECTROSCOPIC DATA FOR VERMITRASPORIN (900/225 MHz, MeOH-d ₄)	71
TABLE XII: BIOLOGICAL EVALUATION OF VERMITRASPORIN	74

LIST OF ABBREVIATIONS

$[\alpha]_D$	Specific optical rotation
$^1\text{H NMR}$	^1H nuclear magnetic resonance
AIDS	acquired immune-deficiency syndrome
AMP	ampicillin
AMPH	amphotericin B
ATP assay	ATP TB bioluminescence assay
BGF	bioassay-guided fractionation
C18	Octadecyl derivatized silica
CDCl_3	deuterated chloroform
CHCl_3	chloroform
COSY	2D ^1H , ^1H -correlation NMR spectroscopy
CS	cycloserine
DMSO	dimethyl sulfoxide
FDA	United States Food and Drug Administration
GEN	gentamicin
HIV	human immunodeficiency virus
HMBC	heteronuclear multiple-bond correlation spectroscopy
HPLC	high performance liquid chromatography
HREIMS	high resolution electron ionization mass spectrometry
HRMS	high resolution mass spectrometry
HSQC	heteronuclear single quantum coherence spectroscopy
Hz	Hertz
IC50	inhibitory concentration which reduced activity by 50% relative to positive control
INH	isoniazid
ITR	Institute for Tuberculosis Research
KETO	ketoconazole
KAN	kanamycin
LORA	low oxygen recovery assay
MABA	microplate Alamar Blue assay
MDR-TB	multi-drug resistant tuberculosis
MeOH	methanol
MIC	minimum inhibitory concentration
NMR	nuclear magnetic resonance
NUTS	NMR simulation and processing tool used in the present work
rCS	cycloserine resistant <i>M. tuberculosis</i>
R _f	retention factor
rINH	isoniazid resistant <i>M. tuberculosis</i>
rKM	kanamycin resistant <i>M. tuberculosis</i>
RMP	rifampin
RMS	root means square
ROESY	rotating frame nuclear Overhauser effect spectroscopy
rRMP	rifampin resistant <i>M. tuberculosis</i>
rSM	streptomycin resistant <i>M. tuberculosis</i>
SM	streptomycin
TB	tuberculosis
TLC	thin-layer chromatography
UIC	University of Illinois at Chicago
UV	ultraviolet light

LIST OF ABBREVIATIONS (continued)

Vero	African green monkey kidney cell line
WHO	World Health Organization
XDR-TB	extensively drug resistant Tuberculosis
λ (nm)	wavelength in nanometer

INTRODUCTION: TUBERCULOSIS

1 Introduction

1.1 Tuberculosis

Tuberculosis (TB) is an infectious disease caused by the *Mycobacterium tuberculosis* (*M. tuberculosis*) complex including *M. bovis*, *M. africanum*, *M. canetti*, and *M. microti*. *M. tuberculosis* normally infects the human lung (pulmonary TB), but also can spread to other organs such as kidney, bones, and brain.^{1, 1b} *M. tuberculosis* is classified as a rod-shaped obligate aerobic acid-fast bacterium, which was first identified by Robert Koch in 1882.^{1b} The cell wall of this pathogen resembles that of Gram-positive bacteria, including a polysaccharide layer, a peptidoglycan layer, and lipids. In contrast to the typical Gram-positive bacterium, the cell wall has an additional layer with a waxy coat of fatty acids, more specifically, mycolic acids, as shown Figure 1A.² This distinctive thick cell wall likely makes this organism less susceptible to some antibiotics. In addition, *M. tuberculosis* divides slowly with a 20 – 24 hour doubling time, which contributes to long turnaround times in culture-dependent diagnosis and possibly to the need for the 6 – 9 months of treatment.^{1a}

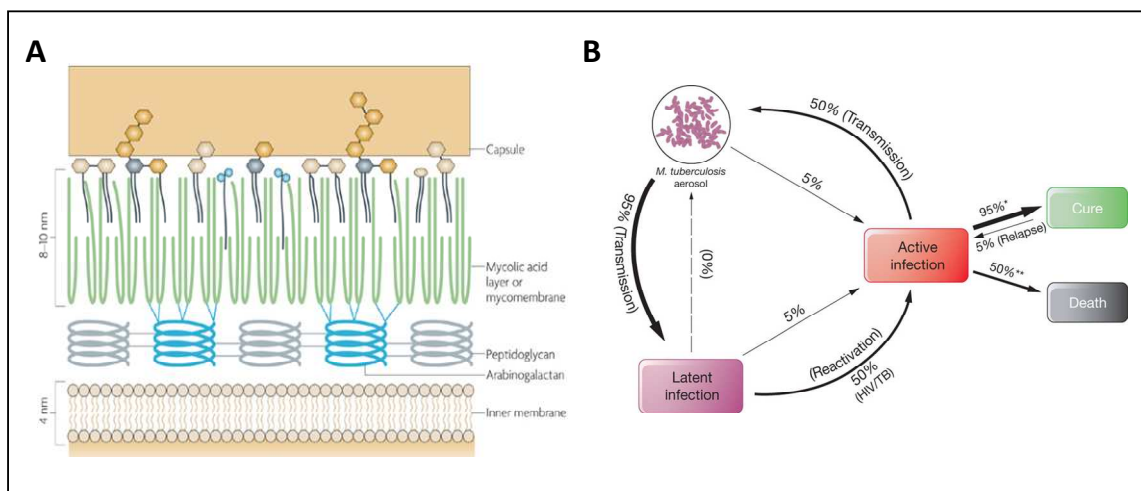


Figure 1. A *M. tuberculosis* cell wall structure. (Adapted from A Abdallah, *et al* Nature reviews, Microbiology, 5:883- 891, 2007) **B** Phase of infection with *M. tuberculosis*. (Adapted from Koul *et al.* Nature 469:483-490, 2011)

Most infections in humans result in an asymptomatic stage called latent infection, which presents no sign of illness such as chest pain, coughing up blood, weight loss, fatigue, and night sweats, until it progresses to the active disease. Patient with latent TB are not infectious, but these patients have a 10% chance of developing active TB at a later stage in their life, as shown Figure 1B.³

Individuals with immunosuppressive conditions such as HIV infection, diabetes, and silicosis have a higher chance of developing active TB.⁵

Active TB is mainly transmitted from people suffering from pulmonary TB by small particle aerosols from coughing, sneezing, speaking, and spitting. Those so exposed inhale these TB-containing aerosols, which are deposited in the alveolar space where the organism begins to replicate.⁴

To prevent and control TB, the Bacillus Calmete-Guerin (BCG) vaccine is used in the developing countries especially for infants.

1.1.1 Etiology

When aerosol droplets containing the infectious bacteria are inhaled and deposited in the walls of pulmonary cavities, the macrophages in the alveoli engulf the bacteria by phagocytosis, which results in infected macrophages. The infected macrophages then induce an inflammatory response that leads to infected macrophages being surrounded with immune cells (for example, mononuclear cells, uninfected macrophages, foamy giant cells, T lymphocytes, and B lymphocytes) from neighboring blood vessels.^{1b,6} These macrophages surrounded with immune cells form a small nodule called a granuloma, which prevents further bacterial spreading and provides a localized immune system environment. Healthy individuals with a successful immune response normally will seal off the lesion from surrounding tissue with a fibrotic capsule, and hence acquire a so-called latent or dormant TB infection.^{4,7}

When this containment fails because of a change in the immune status of the host, such as

malnutrition or HIV-co-infection, the center of the granuloma undergoes caseous necrosis enabling the bacteria to spill out into the airways in the lung. This eventually causes a productive cough that facilitates further infection within the lung as well as to other individuals.

During the normal process of infection, the bacteria in the macrophages are transported to regional lymph nodes, enter the bloodstream, and can establish sites of infection throughout the body such as the lungs, the lymph nodes, kidneys, brain, and bones. Figure 2 displays the pathogenesis of tuberculosis.^{6, 8}

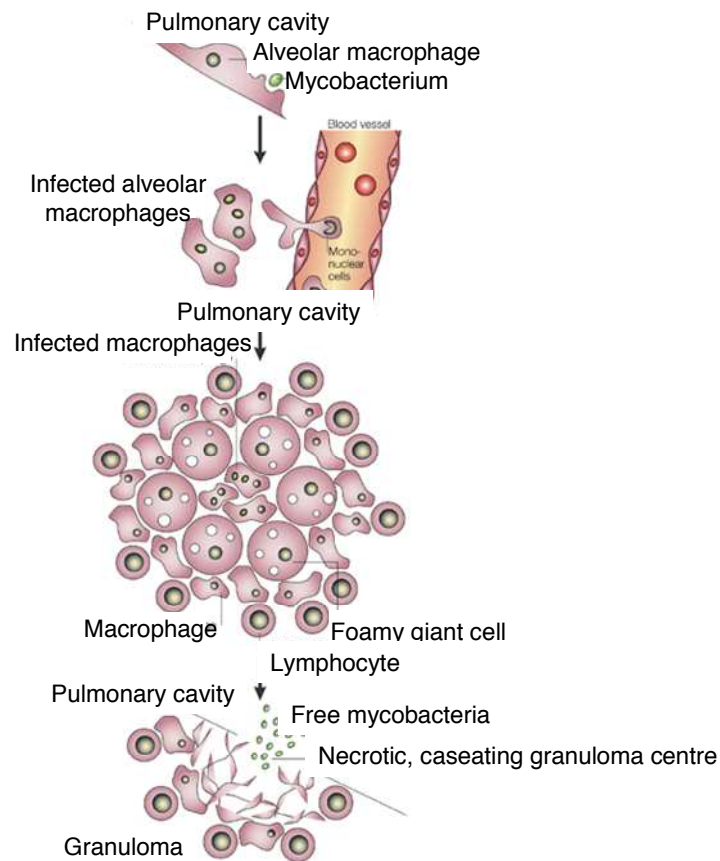


Figure 2. The pathogenesis of tuberculosis (Adapted from D Russell *et al.* *Nature, Molecular cell biology*, 2:1-9:2001)

1.1.2 Global TB facts

TB is an ancient disease of which the oldest trace of human TB was found in skeletal remains from prehistoric humans dated around 4000 BCE. Also, tubercular decay was found in the spine of Egyptian mummies from 3000 – 2400 BCE.⁹ In the 19th and early 20th century, TB was an endemic disease that led to the death of one-quarter of Europeans¹⁰ and was arguably the most widespread public threat in the world. Since the discovery of the BCG vaccine in 1921 and anti-TB drugs such as streptomycin¹¹ (1944), isoniazid (1952), and pyrazinamide (1952), the TB mortality rate has dramatically decreased worldwide.¹²

Currently, although the TB death rate has fallen by 35% since 1990, TB is considered a neglected disease in poor countries. The World Health Organization estimates that one third of the global population still are *M. tuberculosis* carriers.^{12a} In 2009, the WHO estimated 1.7 million people died from TB. In addition, there were 9.4 million new TB cases in 2009 including 0.3 million of multi-drug resistant TB (MDR-TB) and 1.1 million cases among people with HIV.¹³

MDR-TB is characterized by being resistant to the two conventional first line drugs, rifampin and isoniazid.¹⁴ More than 150,000 MDR-TB deaths were recorded from an estimated 440,000 MDR-TB cases in 2008.^{12b, 14} In 2009, 0.4 million people died of TB with HIV co-infection among 1.8 million HIV deaths worldwide. In short, TB with drug-resistance and HIV co-infection is a major threat to the public health.¹⁵ Especially, the WHO 2010 report estimates that the former Soviet Union, Africa, and South-East Asia account for approximately 85% of the global TB incidence and prevalence as well as mortality rate including MDR-TB and TB/HIV co-infection.¹³

In 2005, extensively drug-resistant TB (XDR-TB), which is resistant to more than three classes of second-line TB drugs (which include capreomycin, kanamycin, cycloserine, ethionamide, fluoroquinolones, and para-aminosalicylic acid) was first reported.¹⁶ In 2006, an XDR-TB outbreak in

KwaZulu Natal South Africa killed 52 out of 53 XDR TB patients within three weeks.¹⁷ The WHO confirmed that 69 countries had at least one case of XDR-TB between 2005 and 2010. In addition, there are an estimated 25,000 cases of XDR-TB emerging every year.¹⁵ Therefore, TB still remains a leading cause of human death among infectious diseases.

1.1.3 TB chemotherapy

Appropriate TB chemotherapy varies for patients with dormant/latent TB, active TB, MDR-TB, HIV co-infected TB, and XDR-TB. Due to the lengthy treatment duration, two to four antibiotics in combination are recommended in order to prevent drug resistance. Currently about 20 drugs are available for the treatment of TB, and they are categorized into first-line and second-line drugs (see Table 1). To treat patients with an active TB infection, the cocktail of isoniazid (INH), rifampin (RMP), pyrazinamide (PZA), and ethambutol (ETB) is used for the first 2 months, then INH and RMP for another 4 months.^{1a} For the treatment of a latent TB infection, 6 – 9 months of single drug therapy with INH is currently used and recent data suggests that 4 months of RMP will be equally effective. MDR-TB infections require up to two years of treatment with a cocktail of two to four second line drugs, which typically have more side-effects and less efficacy.¹⁴ XDR-TB treatment is highly individualized with relatively low cure rate and successful outcome depends on the extent of the drug resistance and the severity of the disease.¹⁶ It becomes even more complicated to treat HIV co-infected TB because RMP, the best current anti-TB drug on the market, diminishes antiviral efficacy of the most commonly used anti-HIV drugs (for example, HIV protease inhibitors) by inducing cytochrome P450 enzymes, which accelerate the metabolism of some HIV drugs, especially protease inhibitors.¹⁸ Therefore, non-nucleoside-reverse-transcriptase-inhibitor (NNRTI: nevirapine, delavirdine) containing regimens are given to minimize drug-drug interaction. However,

resistance to NNRTPIs tends to develop easily so that HIV co-infected TB patients become even more difficult to treat.^{16, 19}

In 1990, the WHO established the Directly Observed Treatment, Short-course (DOTS) strategy to better control and treat TB by focusing on the following five elements: (1) political commitment with increased and sustained financing, (2) diagnosis primarily by sputum-smear microscopy among patients, (3) direct observation of standardized treatment, (4) a definite supply of drugs and management system, and (5) systematic monitoring of cases and treatment outcomes. Since 1995, 41 million patients have been successfully treated through DOTS, and it remains the primary strategy to prevent and control TB.²⁰ Furthermore, the WHO extended the DOTS strategy in 1999 to DOTS-PLUS to manage MDR-TB, and this has now been proven to be effective, feasible, and a cost-effective intervention according to pilot studies in Estonia, the Russian Federation, the Philippines, and Peru.²¹

Currently, along with the Stop TB Partnership developed in 2000 by international, nongovernmental and governmental organizations, as well as patient groups worldwide, the WHO has established the Stop TB Strategy aimed at eradicating the global burden of TB by 2015.²²

TABLE I. CURRENT ANTI-TUBERCULOSIS DRUGS.

	Drugs	MIC ($\mu\text{g/mL}$)	Mechanisms of action	Targets	Genes involved in resistance
1 st line	Isoniazid	0.01 – 0.20	Inhibition of cell wall mycolic acid synthesis	Enoyl acyl carrier protein reductase (InhA)	<i>katG, inhA</i>
	Rifampin	0.05 – 0.50	Inhibition of RNA synthesis	RNA polymerase, β subunit	<i>rpoB</i>
	Pyrazinamide	20 – 100	Depletion of membrane energy	Membrane energy metabolism	<i>pncA</i>
	Ethambutol	1 – 5	Inhibition of cell wall arabinogalactan synthesis	Arabinosyl transferase	<i>embCAB</i>
	Streptomycin	2 – 8	Inhibition of protein synthesis	Ribosomal S12 protein and 16S rRNA	<i>rpsL, rrs</i>
2 nd line	Kanamycin	1 – 8	Inhibition of protein synthesis	16S rRNA	<i>rrs</i>
	Capreomycin	4	Inhibition of protein synthesis	16S rRNA, 50S ribosome, rRNA methyltransferase (TlyA)U	<i>rrs, tlyA</i>
	Fluoroquinolones	0.2 – 4.0	Inhibition of DNA synthesis	DNA gyrase	<i>gyrA, gyrB</i>
	Ethionamide	0.6 – 2.5	Inhibition of mycolic acid synthesis	Acyl carrier protein reductase (InhA)	<i>inhA, etaA/ethA</i>
	PAS	1 – 8	Inhibition of folate pathway and mycobactin synthesis	Thymidylate synthase (ThyA)?	<i>thyA</i>

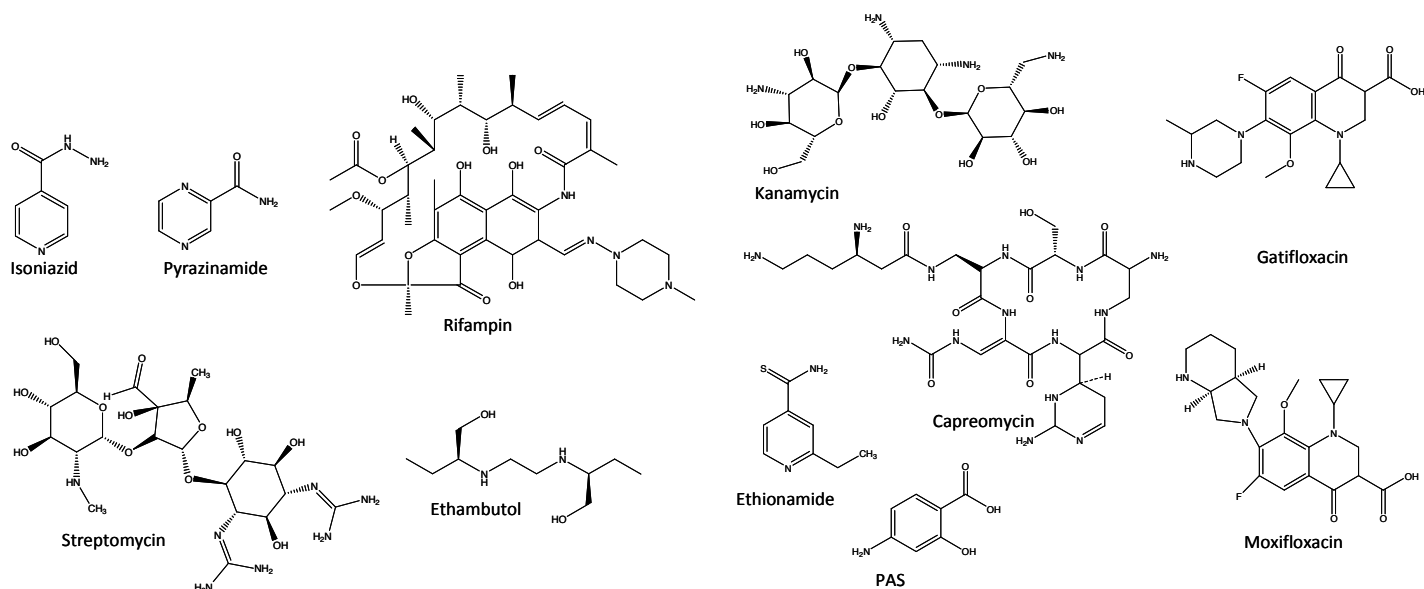


Figure 3. Anti-tuberculosis agents.

1.2 Drug discovery and development

Section 1.1 has described TB etiology and pathogenesis and explained the current global TB problem, and emphasized the significance of the urgent need for new anti-TB drug discovery. Section 1.2 describes how new drugs are discovered, issues specific to new TB drug discovery, and how natural products can assist with these problems.

1.2.1 The process of drug discovery and development²³

Drug discovery and development is the comprehensive and time consuming process of identifying drug candidates, synthesis, characterization, screening, and optimizing therapeutic efficacy in the field of bio-medical science. It is estimated to take around 10 - 15 years and cost 0.6 - 2 billion dollars to discover, develop and bring a new drug to the market only if there are no significant drawbacks during the overall process.^{23a} In general, it all begins from understanding the disease and the drug discovery to preclinical development process; the latter requiring around 4 - 6 years. This is followed by three stage of human clinical trials, which typically require 6-8 years to complete. Once these trials are completed, a New Drug Application (NDA) is assembled, filed and reviewed for approval by the USFDA, a process which takes up to three years, and then the drug would finally be released to the market. Thus, the overall process takes 10 - 15 years (Table II).

During the discovery process, a comprehensive basic and applied scientific knowledge (molecular and cellular biology, genomics, biochemistry, and pharmacology) is utilized to understand disease pathogenesis, which leads to identification of biological targets for the disease (the target could be a specific protein or a whole cell). Once the target is identified and validated, leads for the specific target are identified. The source for these leads could be either of natural or synthetic origin. Various high throughput screening methods can be applied. In addition, *in vitro* pharmacokinetics (PK) and –

dynamics (PD), toxicity, physiochemical properties, and stability of lead compounds will be assessed to predict behaviors in animal models prior to the clinical trial.

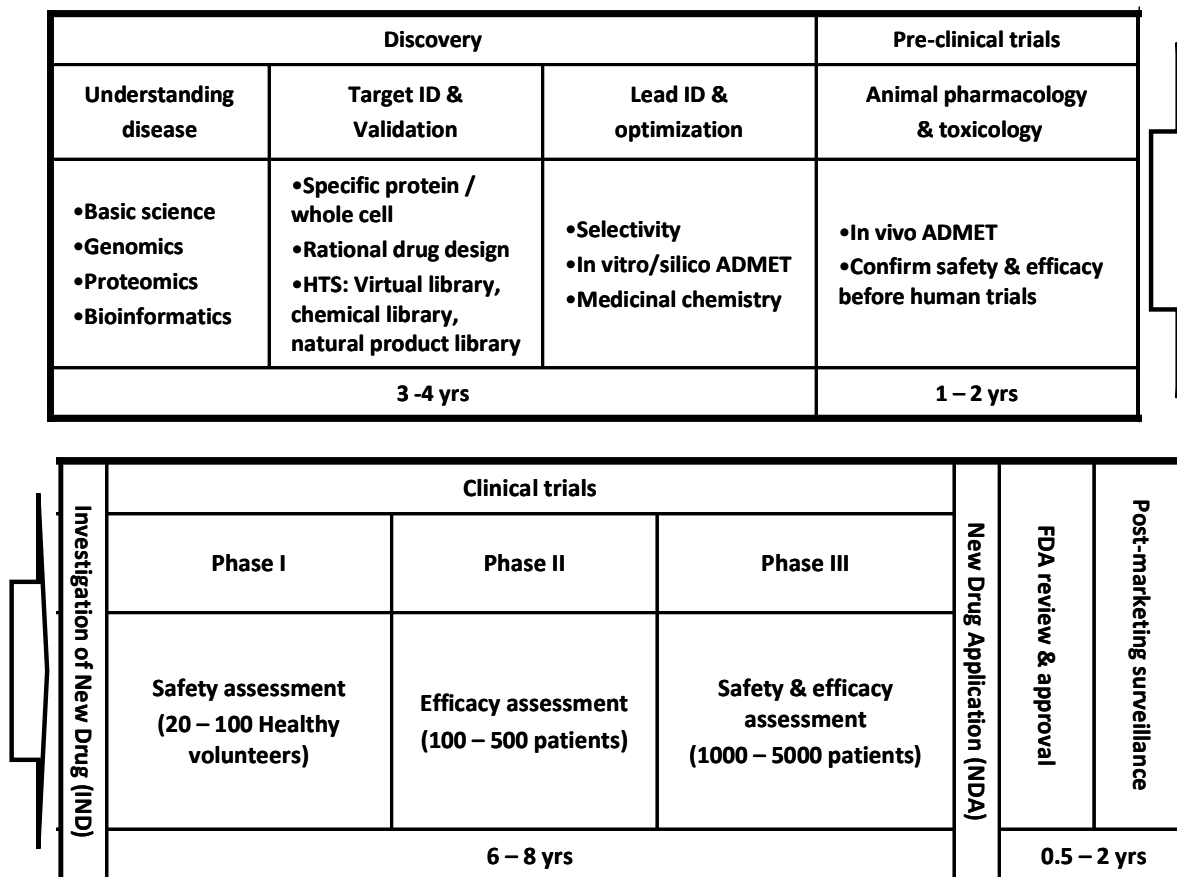


Figure 4. Drug discovery and development process

The preclinical development phase involves the assessment of the drug candidates with respect to animal pharmacology (PK and PD), bioavailability (Absorption, Distribution, Metabolism, Excretion; ADME) and toxicology (normally acute toxicity study from two weeks and long term toxicity study up to six months) to ensure safety and efficacy for the following human trials. In addition, an application for an investigational new drug (IND) is submitted to the FDA at this stage.

After 4 – 6 years of discovery and preclinical development, the 3 phases of human clinical trials begin, which together account for 85-90% of the drug discovery and development costs. The phase I clinical trial involves a small group of healthy volunteers (20 – 100 individuals) ensuring that the preclinical

data acquired in animals will translate to humans. The phase II clinical trial, which takes normally around 6 months to 3 yrs, mainly focuses on efficacy by testing a small group of patients (100 – 500 individuals), with the primary goal of defining an optimal efficacious dose. Finally, the phase III clinical trial (2 – 4 yrs) intends to ensure the safety and the efficacy by assessing a large group of patients (1000- 5000 individuals) and comparing the new drug with the best current treatment for the disease. It is imperative that there are enough patients to establish a statistically significant comparison. At the end of an effective clinical trial, a New Drug Application (NDA) is submitted to the FDA for approval.

1.2.2 Current TB drug discovery and challenges²⁴

Currently, there are about 20 antibiotics available for the treatment of TB, but the drugs in the standard TB treatment regimen (SM, INH, PZA, ETB, and RMP) were all discovered between the 1940s and the 1960s. Even though TB is still the cause of millions of deaths worldwide every year, until recently it was still considered a “neglected” disease. In addition, the relatively small predicted profit margins compared to high drug development costs resulted in diminished efforts in TB drug discovery by most pharmaceutical companies in the late 20th century. Consequently, no new class of drug has been introduced to the 1st line standard TB regimen for the last 40 years.

However, a rapidly increasing incidence of drug-resistant TB (MDR- and XDR-TB) together with the HIV pandemic has encouraged greater global efforts for TB drug discovery especially from academia and non-profit and governmental organizations. Since the establishment of the Global Alliance for TB Drug Development in 2000, efforts in finding new TB drugs have increased dramatically. Consequently, 13 existing and investigational new drugs have been or are currently undergoing clinical evaluation for the treatment of tuberculosis. These include three new chemical entities (NCE; TMC207, sudoterb, and SQ109), re-evaluation of rifamycins (high dose rifampin and rifapentine), fluoroquinolones (gatifloxacin

and moxifloxacin), nitroimidazoles (OPC-67683 and PA-824), and oxazolidinones (linezolid, PNU100480, and AZD584710).^{24a}

TABLE II. DRUGS IN CLINICAL EVALUATION FOR TUBERCULOSIS (adapted from A Ginsberg *et al.* 2010 *Drugs*, 70(17);2201-2214)

Drug	Category	Target	Clinical phase
TMC207	Novel	ATP synthase	II – III
Sudoterb (LL3858)	Novel	Unknown	II
SQ109	Novel	Cell wall and multi-target inhibitor	I
Rifapentine	Rifamycin	RNA polymerase	I - II
Rifampin	Rifamycin	RNA polymerase	I
Gatifloxacin	Fluoroquinolone	DNA gyrase	III
Moxifloxacin	Fluoroquinolone	DNA gyrase	III
Linezolid	Oxazolidinone	Protein synthesis inhibitor	II
PNU100480	Oxazolidinone	Protein synthesis inhibitor	I
AZD5847	Oxazolidinone	Protein synthesis inhibitor	I
Metronidazole	Nitroimidazole	Not determined for TB	II
OPC-67683	Nitroimidazole	Cell wall and multi-target inhibitor	II-III
PA-824	Nitroimidazole	Cell wall and multi-target inhibitor	II

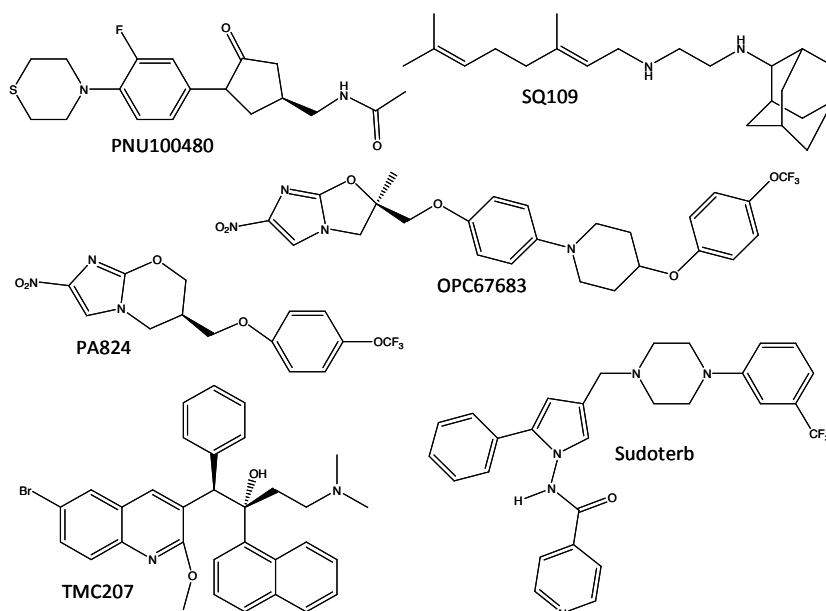


Figure 5. Drugs in clinical evaluation for tuberculosis

Although there has been a tremendous improvement in the TB drug discovery pipeline, the challenges for the effective control of TB still remain due to drug resistance and the HIV pandemic, the current TB treatment duration and toxicity associated with the current chemotherapy. To overcome these obstacles, discovery of a drug within a new chemical class and a new mode of action on a novel target might be necessary. However, only three out of thirteen drugs in the current TB drug pipeline are NCEs, whereas the majority is chemical modifications of existing drugs. Among the three NCEs, TMC207 is the only compound that is known to have a novel mode of action on a novel target. For the other two, the targets are still uncertain or are similar to existing targets, which are part of the cell wall.²⁵ This implies that drugs in the pipeline may not be sufficient to overcome the current challenges.

1.2.3 Drug discovery from natural products

Of the 13 drugs in the pipeline, rifampin and rifapentine are the only compounds of natural origin. The remaining 11 drugs are all synthetic compounds. This raises the question of why there is only one drug from a natural source in the current TB drug discovery pipeline.

On the other hand, the two most potent current anti-TB drugs in the first line regimen, RMP and INH, came from or were inspired by natural product scaffolds. INH is a synthetic drug based on the structure of nicotinamide (VitaminB2).¹¹ Rifampin is a derivative of rifamycin S, a metabolite of *Nocardia mediterranei*.²⁶ In addition, streptomycin (SM), the first antibiotic with clinical efficacy against TB, was discovered from *Streptomyces griseus* by Waksman and Schatz at Rutgers University in 1948.²⁷

In the mid 1900s, natural product sources such as fungi, plants, and actinomycetes were the major antibiotic producers in drug discovery.²⁸ Numerous novel drugs, which were discovered from natural sources for the treatment of human disease, are among the most effective drugs available. These include quinine and artemisinin for malaria treatment, paclitaxel for cancer treatment, lovastatin as a

lipid control agent, and morphine as an analgesic. In addition, more than two-thirds of the current antibiotics used in the clinic, including the beta-lactam class originated from natural sources.²⁸⁻²⁹

However, the relatively low profit margin compared to high development costs and the rapid development of drug resistance has restricted antibiotic discovery efforts in most pharmaceutical companies. In addition, researchers have repeatedly isolated the same compounds from natural sources because of a lack of efficient dereplication technology. Eventually, the relatively low cost associated with synthetic chemistry has placed it in a favored status compared to the time consuming and labor intensive nature of natural products as a source of drug discovery. Consequently, more than two-thirds of the antibacterial NCEs filed between 1980s and 2000s were synthetic derivatives of existing drugs.³⁰ Only two new classes of antibiotics, including oxazolidinones (linezolid) and lipopeptides (daptomycin) were discovered since the 1980s. (Figure 6)

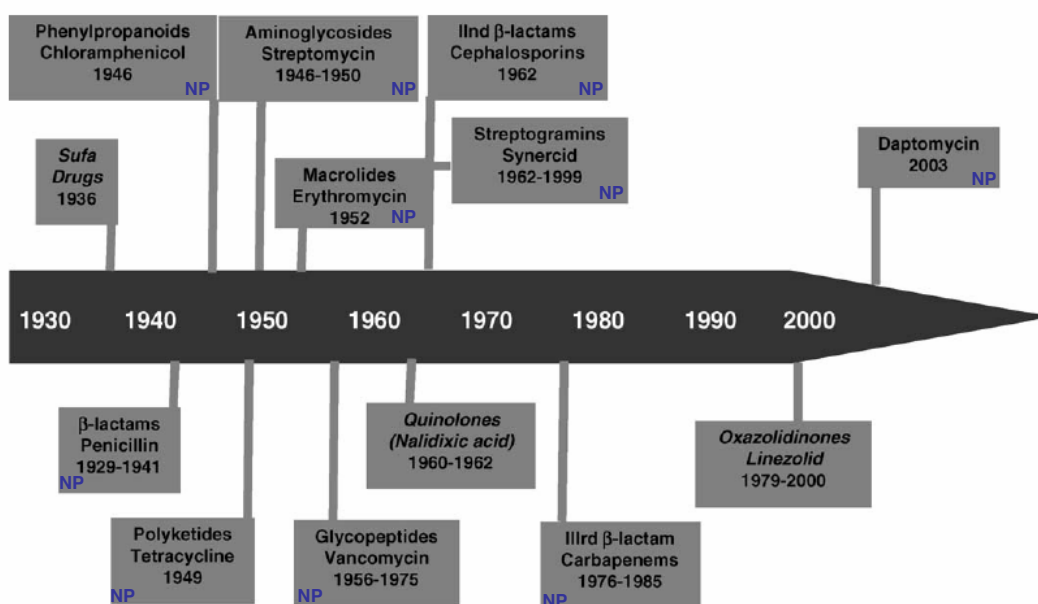


Figure 6. Timeline of introduction of 13 classes of antibiotics, NP: natural product origin.

Statistics have shown that natural products have remained a great source of pharmaceuticals. A total of 10 out of the 13 classes of antibiotics originate from natural products or are derivatives of natural products, as shown

Figure 6. Of all NCEs in all anti-infective (antibacterial, antifungal, antiparasitic, and antiviral) drugs, 60% came from either natural products or are natural product derivatives (Figure 7 A).³¹ In fact, the majority of natural product based-antibiotics including β -lactams (e.g., penicillin and cephalosporin), aminoglycoside (e.g., streptomycin), macrolides (e.g., erythromycin), and tetracyclines (e.g., tetracycline), were discovered from fungi or soil bacteria.²⁸⁻²⁹

In addition, natural sources provide more structural and chemical diversity, flexibility, complexity, and specificity toward a biological target compared to synthetic compounds.³² Also, the chemical properties (the number of

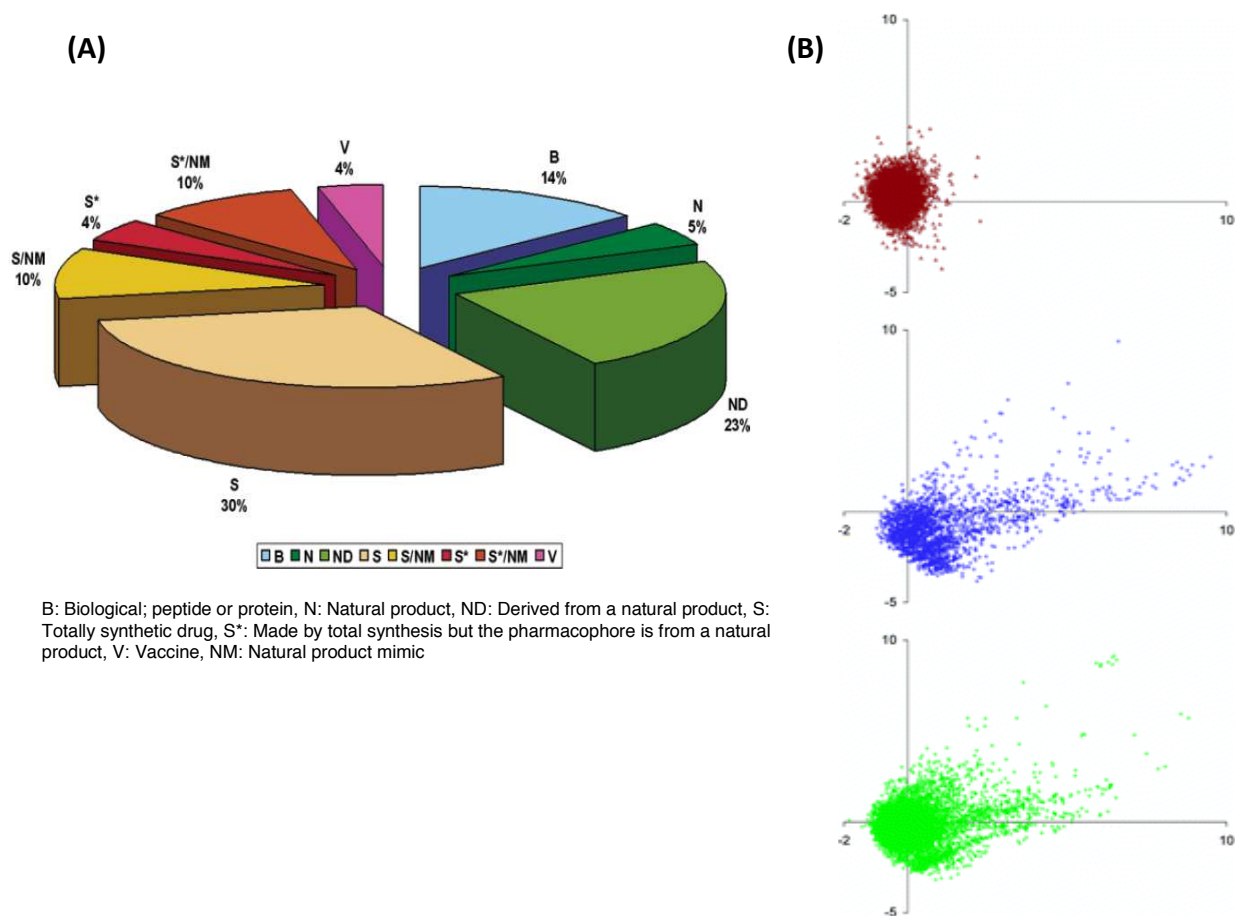


Figure 7. A All new chemical entities, 1981 – 2006 (adapted from Newman et al. 2007 JNP 70(3) 461-477). **B** Principal component analysis for chemical property distributions (brown: combinatorial compounds, n=13,506; blue: natural products, n=3287; green: drugs, n=10968, adapted from Feher et al. 2003 J. Chem. Inf. Comput. Sci. 43;218-227).

chiral centers, the prevalence of aromatic rings, the introduction of complex ring systems, the degree of the saturation of the molecules, and the ratios of different heteroatoms) of natural products display similar properties to that of commercially available drug molecules.³³ After all, these drug-like properties of natural products are presumably responsible for their historical success in drug discovery.

1.3 Statement of problem / hypothesis and specific aims

Although TB among the industrialized countries is considered a disease of the past, it still takes millions of people's lives every year worldwide and remains a leading cause of human deaths among infectious disease due to the lack of novel anti-TB agents, incidence of drug-resistant TB, reactivation of latent TB from HIV patients, and 6 – 9 month lengthy chemotherapy. A new TB drug is expected to contribute to the shortening of the total duration of treatment to less than 2 months, improving the treatment of MDR-TB and XDR-TB, improving an effective treatment of latent TB, and improving treatment of HIV/TB co-infection.²⁴ In order to fulfill these expectations, a new chemical compound class with a novel mechanism of the action is required.

Therefore, we hypothesize that natural products may be a superior source for novel anti-TB drug leads consisting of a new chemical compound class and mechanism of action. In order to support this statement, this study combines two approaches: (i) utilizing our ancestral indigenous ethnomedical knowledge and (ii) high throughput screening of a fungal extract library. In order to test this hypothesis, three specific aims were developed.

Aim1. Find useful ethnobotanicals for TB drug leads from the NAPTRALERT database

Aim2. Chemically and biologically assess an anti-TB ethnomedical mushroom, *Fomitopsis officinalis* with respect to anti-TB drug lead discovery

Aim3. Search for a new TB drug lead from a fungal extract library.

Aim 3 was further specified into two sub aims.

3a) Screen a library with 12,905 fungal extracts for anti-TB activity.

3b) Isolate, identify, and biologically evaluate anti-TB metabolites from a prioritized extract.

With these specific aims to test the hypothesis, this study utilized diverse natural sources, especially ethnomedical knowledge and a fungal extract library, to search for an anti-TB drug leads.

Chapter 2

Aim 1: Identify useful ethnobotanicals from the NAPRALERT database for TB drug lead discovery

2 Aim 1: Identify useful ethnobotanicals from the NAPRALERT database for TB drug lead discovery

2.1 Background and scope

Ethnomedicinal and folk medicinal information provide a great medical knowledge reservoir and have provided significant input on the discovery of modern pharmaceuticals. For example, of 119 plant-derived drugs used in modern medicine, 74% had the same or related uses in ethnomedicinal or folk medicine treatments: e.g. colchicine for gout, quinine for malaria, reserpine for high blood pressure, and pilocarpine for glaucoma.³⁶

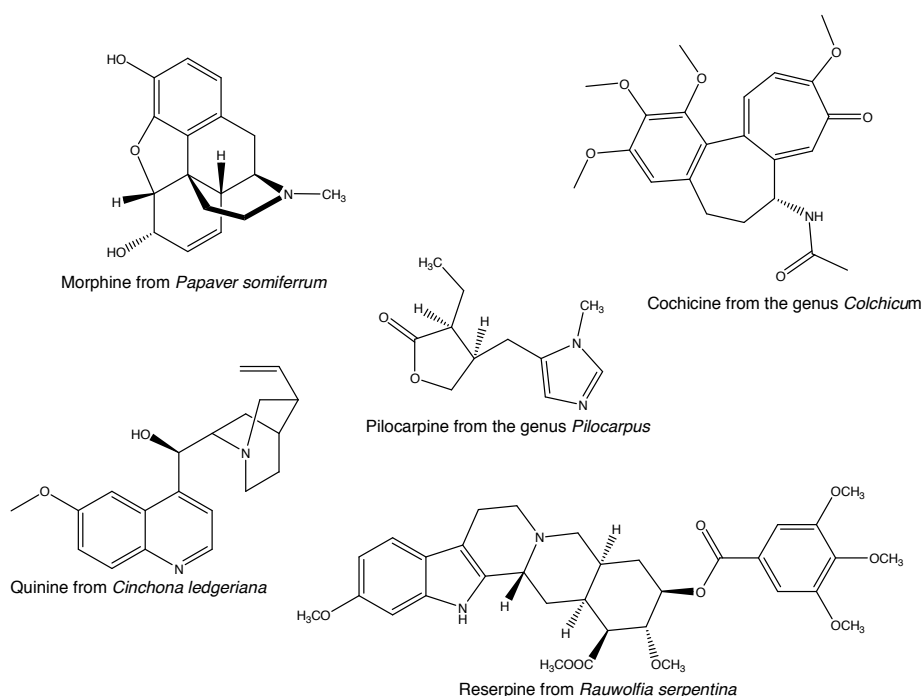


Figure 8. Drugs derived from ethnobotanicals

TB is an ancient disease, known for almost 9,000 years resulting in an abundance of ethnomedicinal information. Continuous usage of ethnomedicine over centuries suggests relative safety and efficacy. Recently, a study of ethnobotanical treatments for TB was conducted in Myanmar.³⁷ Soe *et al.* studied the potential role of Myanmar traditional herbal medicine in the treatment of multi-drug resistant pulmonary tuberculosis. Extracts of reputed medicinal plants used in Myanmar for the treatment of

lung disease were screened for *in vitro* / *in vivo* activity against *M. tuberculosis*. As a result, some medicinal plant extracts were found to possess significant *in vivo* anti-TB activity without any acute or sub-acute toxicity in mice (albino ddy strain) and rat (Wistar strain). Clinical data against fifteen MDR-TB patients for those medicinal plant extracts also indicate that traditional medicines from Myanmar could be a great value for finding leads for a new anti-TB agent.

Therefore, this study aims to utilize ethnomedical information to select plants that may contain novel anti-TB metabolites. A comprehensive literature search was conducted using the NAPRALERT database.³⁸ NAPRALERT is an online database produced by the Program for Collaborative Research in the Pharmaceutical Sciences (PCRPS) at the University of Illinois at Chicago. It manages bibliographic and factual data on natural products including information on pharmacology, biological activity, taxonomic distribution, ethnomedicine, and chemistry of plant, microbial, and animal extracts.

2.2 Results and discussion

The keywords “Antimycobacterial Activity” were used for the initial search on NAPRALERT, resulting in a total of 1225 references from the 1950s to 2003. These 1225 references could be allocated (non-exclusively) to three areas, as shown in Figure 9, of which: (1) 243 references for ethnomedical usage of plants, (2) 283 references for *in vitro* and *in vivo* activity of plant extracts, and (3) 819 references for anti-mycobacterium activity of compounds from natural products including plants, fungi, marine organisms, and soil microbes (as shown in Figure 9).

The 243 ethnomedical references contained 409 reports for the treatment of TB. The latter were associated with 334 species belonging to 103 plant families. Since (2) and (3) contain the information for antimycobacterial activity, anti-TB specific data were sorted out. The 283 references of antimycobacterial plant extracts (2) contained 1867 activity data entries against *M. tuberculosis*. The

819 references for compounds tested against mycobacteria (3) contained 1058 data entries for *M. tuberculosis*.

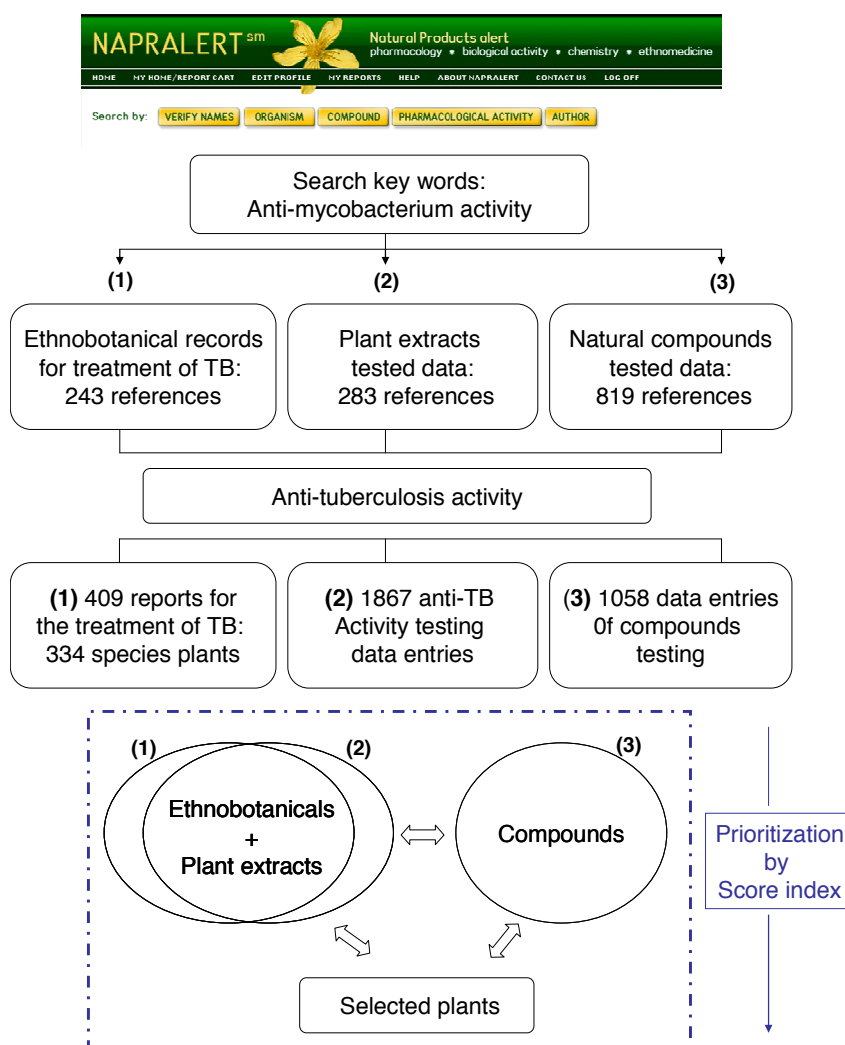


Figure 9. Literature search and data mining scheme

Anti-TB active plant extracts were prioritized for further evaluation based on their anti-TB activity. Testing concentrations for anti-TB activity for extracts are not always defined in NAPRALERT, but data sets for this activity were categorized as: strongly active, active, weakly active, and inactive. In addition, for those specifying defined concentrations related to their anti-TB activity, various testing

methods were used, such as the microplate dilution method, disc diffusion assay, and agar plate assay. Consequently, anti-TB activity of extracts alone could not serve as the main prioritization method due to variability in the methods and undefined testing concentrations.

Therefore, for these anti-TB active plant extracts, correlations were sought between *in vitro* / *in vivo* anti-TB active plant extracts (2) and ethnomedical records (1). In addition, an investigation was made to determine whether the anti-TB active plants having ethnomedical usage records also contain any known anti-TB active compounds or not (3). We were less interested in the plant that had already contained many known anti-TB compounds.

Based on the above strategy, 46 anti-TB plants were initially selected, based on the availability of information regarding both anti-TB activity of the extract *in vitro* or *in vivo* from (2) and ethnomedical usage (1).

Because of the lack of uniformity in testing methods and undefined testing concentrations for the extract activity data, the 46 plants were subdivided into three groups (A, B, and C) based on activity and the presence or absence of defined concentrations. Group A contains 19 plants for the activities with defined concentrations. Group B includes 7 plants that were reported as strongly active but without defined testing concentrations or a testing concentration that exceeded 5 mg/ml. Group C contains 20 plants, which didn't have defined concentrations but were reported as active. In addition, a list of all compounds isolated from each of the 46 plants using the (3) information was obtained from a secondary search of the NAPRALERT database. In short, ethnobotanical usage data, extract activity data, and the number of isolated compounds were investigated for each of the 46 plant extracts.

For the further assessment of the information available for the 46 priority plants, an arbitrary scoring index system was developed for a rational approach to prioritize the search results. The score index contains five criteria (S1 – S5) yielding a score from 0 to 3 points for each criterion. First, a plant extract

with reported ethnomedical data along with anti-TB activity received the highest score (S1). Second, one of two possible scores was assigned for the anti-TB activity based on whether the concentration defined or not defined (S2). For those concentration-defined extracts, MICs of ≤ 100 $\mu\text{g/ml}$, $>100 \leq 500$ $\mu\text{g/ml}$, and >500 $\mu\text{g/ml}$ received 3, 2, and 1 points, respectively. For extracts with undefined concentrations, “strongly active” scored 2 points; “active” scored 1 point (S2).

S1. Ethnomedical Report		S2. AntiTB Activity		
Score	No. of Reports	Score	Conc Defined	Conc Not Defined
1	1	1	MIC > 500 $\mu\text{g/mL}$,	Active
2	2	2	$100 < \text{MIC} \leq 500$	Strong active
3	3	3	MIC ≤ 100 $\mu\text{g/mL}$	-

S3. No. of Isolated Compound		S4. The Presence of AntiTB Compound	
Score	No. Compd Isolated	Score	Anti-TB Compd
1	> 50	0	Present (Fatty Acid, Essential Oil, Phenolic)
2	$>10, \leq 50$	1	Present (Others)
3	≤ 10	2	Not Present

S5. Activity in Compound vs. Extract	
Score	# Anti-TB Compd Isolated
1	-
2	Extract = AntiTB Compd
3	Extract $>$ AntiTB Compd

Figure 10. Score index with the five criteria for prioritizing the 45 plants

The number of compounds isolated from each plant was an important parameter because plants with more reported constituents might be less likely to yield a novel active constituent. Therefore, a plant that has been studied less and for which less compounds were identified received a higher score (S3). For instance, plants with <10 , $10 - 50$, or >50 isolated compounds received score of 3, 2, and 1, respectively. In addition, plants with compound known to have unfavorable pharmacological properties, such as fatty acids, ursolic acid, betulinic acid, ergosterol, essential oils, or phenolics received zero points (S4).³⁹ Finally, extracts with better activities than the compounds isolated from them received an additional 3 points because this phenomenon suggests a possible synergistic effect within the extract although synergy is not a primary consideration for this lead discovery project (S5).

Understanding synergy within a complex matrix of extract could be a challenge, but it could also be a great scientific achievement.

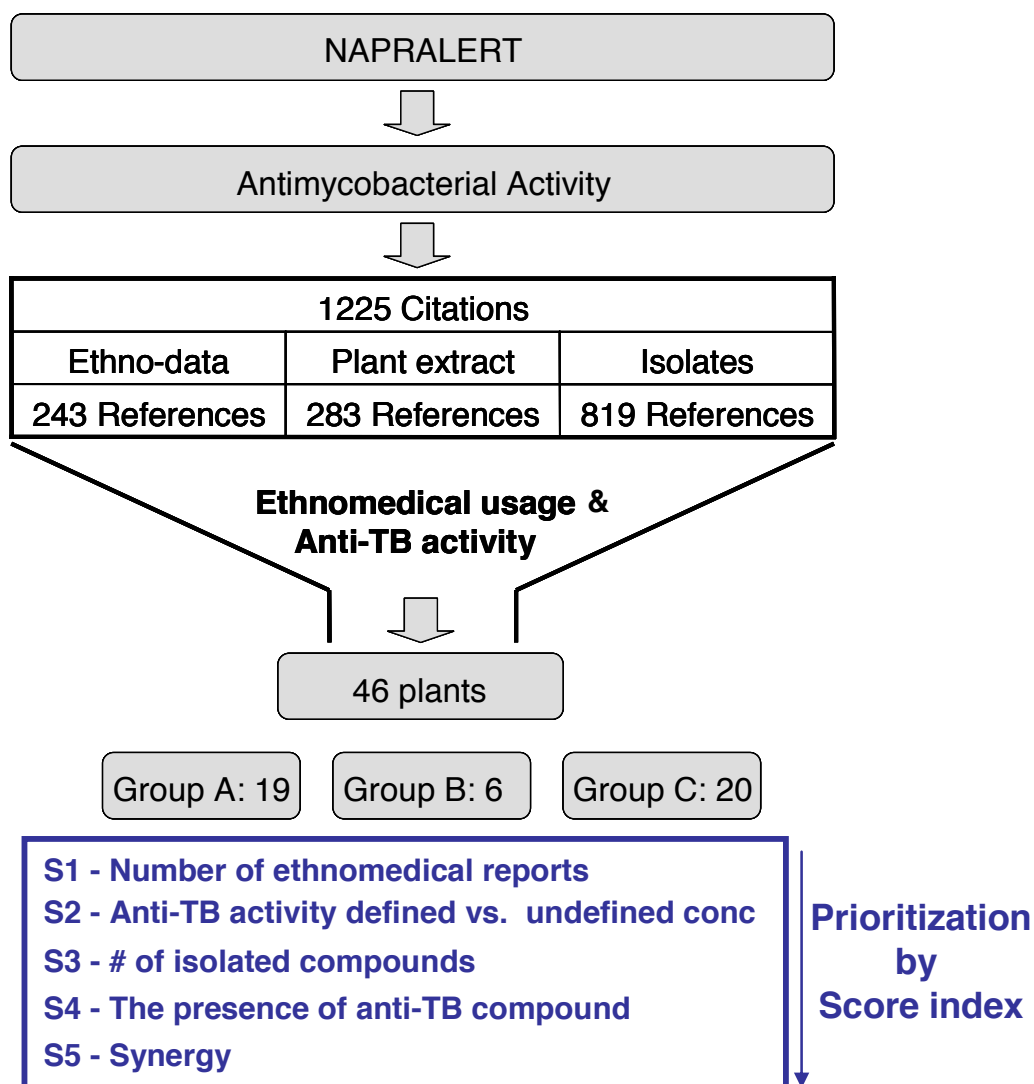


Figure 11. Summary of NAPRALERT data minding for selecting useful ethnobotanicals for searching anti-TB drug leads.

TABLE III. GROUP A: PLANTS (CONCENTRATION DEFINED)

Group A: plant, extract part, origin	Test conc (µg/ ml)	Score	Reference
<i>Nidorella anomala</i> (Asteraceae) dried entire plant, South Africa	100	9	Lall (1999) ⁴⁰
<i>Canscora decussata</i> (Gentianaceae) entire plant, India	10	9	Ghosal (1975) ⁴¹
<i>Croton pseudopulchellus</i> (Eupobiaceae) dried aerial parts, South Africa	100	9	Lall (1999) ⁴⁰
<i>Polygala myrtifolia</i> (Polygalaceae) dried aerial parts, South Africa	100	9	Lall (1999) ⁴⁰
<i>Acacia xanthophloea</i> (Fabaceae) dried bark, South Africa	500	8	Lall (1999) ⁴⁰
<i>Cryptocarya latifolia</i> (Lauraceae) dried bark, South Africa	500	8	Lall (1999) ⁴⁰
<i>Allium sativum</i> (Amaryllidaceae) essential oil, India	0.5	7	Jain (1998) ⁴²
<i>Combretum molle</i> (Combretaceae) dried bark, South Africa	500	7	Lall (1999) ⁴⁰
<i>Ekebergia capensis</i> (Meliaceae) dried bark, South Africa	100	7	Lall (1999) ⁴⁰
<i>Euclea natalensis</i> (Ebenaceae) dried root, South Africa	100	7	Lall (1999) ⁴⁰
<i>Iboza riparia</i> (Lamiaceae) dried leaf, Rwanda	500	7	Van Puyvelde (1994) ⁴³
<i>Acorus calamus</i> (Acoraceae) rhizome essential oil, India	10	6	Chopra (1957) ⁴⁴
<i>Inula helenium</i> (Asteraceae) fresh root, USA-OR	100	6	Fischer (1999) ⁴⁵
<i>Maytenus senegalensis</i> (Celastraceae) dried aerial parts, South Africa	500	6	Lall (1999) ⁴⁰
<i>Morinda citrifolia</i> (Rubiaceae) dried leaf, Philippines	100	6	Saludes (2002) ⁴⁶
<i>Helichrysum odoratissimum</i> (Asteraceae) dried entire plant, South Africa	500	5	Lall (1999) ⁴⁰
<i>Bidens pilosa</i> (Asteraceae) dried leaf, Rwanda	500	4	Van Puyvelde (1994) ⁴³
<i>Chenopodium ambrosioides</i> (Chenopodiaceae) dried aerial parts, South Africa	500	4	Lall (1999) ⁴⁰
<i>Thymus vulgaris</i> (Lamiaceae) dried aerial parts, South Africa	500	4	Lall (1999) ⁴⁰

TABLE IV. GROUP B: (STRONG ACTIVE, CONCENTRATION NOT DEFINED)

Group B: plant, extract part, origin	Test conc µg/ ml	Score	Reference
<i>Fatsia horrida</i> (Araliaceae) dried part, not specified, Canada-BC	NA	8	Mc Cutcheon (1997) ⁴⁷
<i>Empetrum nigrum</i> (Empetraceae) dried part not specified, Canada-BC	NA	5	Mc Cutcheon (1997) ⁴⁷
<i>Glehnia littoralis</i> (Apiaceae) dried part not specified, Canada-BC	NA	4	Mc Cutcheon (1997) ⁴⁷
<i>Petasites japonicus</i> (Asteraceae) fresh flowers, USA	NA	4	Frisbey (1953) ⁴⁸

<i>Allium cepa</i> (Liliaceae) fresh seed, USA	NA	4	Frisbey (1953) ⁴⁸
<i>Pinus nigra</i> (Pinaceae) fresh stem, USA	NA	4	Frisbey (1953) ⁴⁸

TABLE V. GROUP C: PLANTS (ACTIVE, CONCENTRATION NOT DEFINED OR RELATIVELY HIGH TESTING CONCENTRATION)

Group C: plant, extract part, origin	Test conc µg/ ml	Score	Reference
<i>Rapanea melanophloeos</i> (Myrsinaceae) dried bark, South Africa	5000	7	Lall (1999) ⁴⁰
<i>Euphorbia heterophylla</i> (Euphorbiaceae) dried flowers, leaf, South Africa	NA	7	Watt (1962) ⁴⁹
<i>Pentas longiflora</i> (Rubiaceae) dried root, Rwanda	1000	6	Van Puyvelde (1994) ⁴³
<i>Haematoxylum campechianum</i> (Fabaceae) part not specified	NA	6	Grange (1990) ⁵⁰
<i>Cetraria islandica</i> (Parmeliaceae) dried thallus	NA	6	Dopp (1950) ⁵¹
<i>Eriodictyon californicum</i> (Hydrophyllaceae) dried leaf and stem, USA	NA	6	Salle (1951) ⁵²
<i>Cassine papillosa</i> (Celastraceae) dried bark, South Africa	1000	5	Lall (1999) ⁴⁰
<i>Alnus rubra</i> (Betulaceae) part not specified	NA	5	Grange (1990) ⁵⁰
<i>Adhatoda vasica</i> (Acanthaceae) dried part not specified, India	NA	5	Frisbey (1953)
<i>Glycyrrhiza glabra</i> (Fabaceae) part not specified	NA	4	Grange (1990) ⁵⁰
<i>Juniperus communis</i> (Cupressaceae) part not specified	NA	4	Grange (1990) ⁵⁰
<i>Equisetum arvense</i> (Equisetaceae) fresh plant juice, USA-CA	NA	4	Azarowicz (1959) ⁵³
<i>Tussilago farfara</i> (Asteraceae) entire plant	1250	3	Fitzpatric (1954) ⁵⁴
<i>Brassica oleracea</i> (Brassicaceae) fresh aerial parts	NA	3	Albert-Puleo (1983) ⁵⁵
<i>Calotropis gigantea</i> (Asclepiadaceae) part not specified	NA	3	Grange (1990) ⁵⁰
<i>Echinacea purpurea</i> (Asteraceae) dried root	NA	3	Dopp (1950) ⁵¹
<i>Ginkgo biloba</i> (Ginkgoaceae) fruit, China	NA	3	Schramm (1956) ⁵⁶
<i>Humulus lupulus</i> (Cannabaceae) entire plant	NA	3	Gottshall (1949) ⁵⁷
<i>Salvia officinalis</i> (Lamiaceae) leaf	NA	3	Gottshall (1949) ⁵⁷
<i>Salix alba</i> (Salicaceae) part not specified	NA	1	Grange (1990) ⁵⁰

Within the NAPRALERT database, anti-TB active ethnobotanicals were extensively searched and 45 ethnobotanicals selected that may have significant potential for containing anti-tuberculosis drug leads, especially those highly scored botanicals in each group, as shown in Table 3, 4, and 5.

For example, from group A, *Canscora decussata*, commonly called Shankhpushpi, is a well known Indian traditional medicinal plant, which contains anti-inflammatory,⁵⁸ immunomodulatory,⁵⁹ antioxidant,⁶⁰ and antitubercular properties.⁴¹ It is an erect annual herb growing well in moist areas and also commonly found in Southeast Asia. Among the various biological activities, anti-TB MICs of polyoxygenated xanthenes were reported to be as low as MIC 5 µg/ml, (Figure 12). However, there were no subsequent reports of selectivity and pharmacological properties.

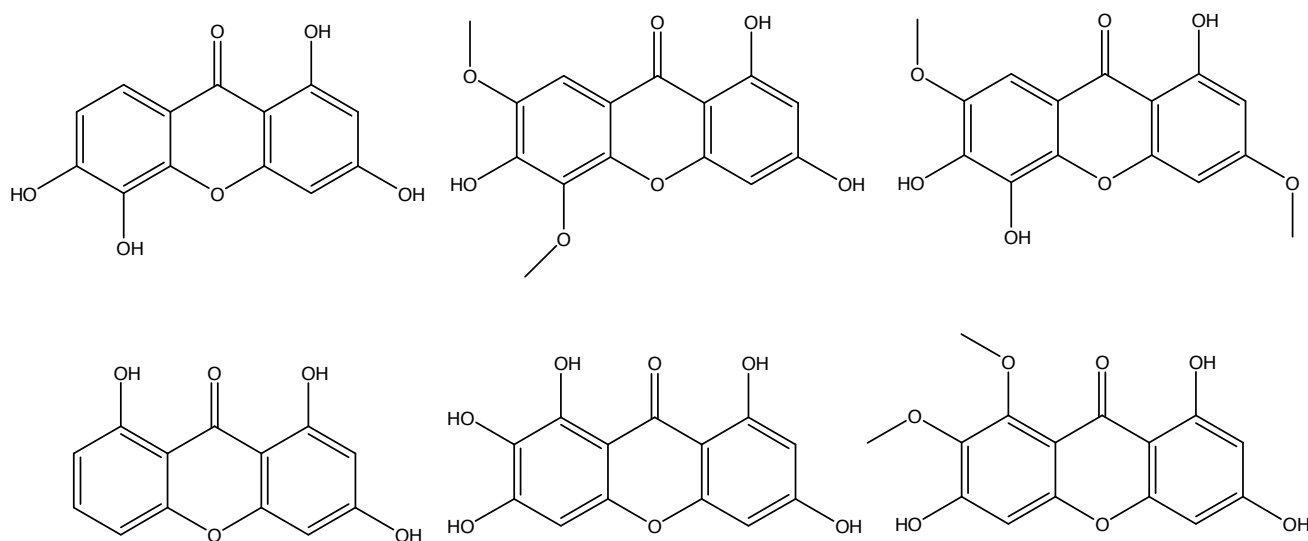


Figure 12. Anti-TB MICs of xanthenes.

Another group A plant, *Croton pseudopulchellus* had a score of 9. *C. pseudopulchellus* is a shrub that is fairly widely distributed in East and South-central Africa. Ethnomedically, the Croton genus has been used for the treatment of TB, asthma, cold, gonorrhoea, and syphilis and as an insecticidal.^{40, 61} In

addition, currently anti-cancer (*C. lechleri*), antiparasitic (*C. cajucara* oils), antiviral (*C. lechleri*), anti-inflammatory (*C. lechleri*), and anti-diarrhea (*C. lechleri*) activities, are widely studied within the *Croton* genus.⁶² An essential oil containing linalool, caryophyllene oxide, γ -terpinene, 1-methylpyrrole, was isolated from *C. pseudopulchellus* and showed an insect repellent activity.⁶³ However, only a few studies have been reported for *C. pseudopulchellus* compared to other *Croton* species. From the only reported study against TB, dried aerial parts of *C. pseudopulchellus* were reported as having an MIC of 100 $\mu\text{g/ml}$.⁴⁰ A compound isolated from *C. pseudopulchellus* has not been reported yet. Therefore, *C. pseudopulchellus* has great potential to be further explored for anti-TB active components.

Nidorella anomala (Asteraceae) from group A also scored 9. It is mostly distributed through South Africa. Only a few studies have been reported for this plant; e.g. the anti-TB activity of the crude extract (MIC 100 $\mu\text{g/ml}$) and one ethnomedical report for the treatment of TB.⁴⁰ In addition, previously, phytol, obliquine, and dehydrofalcarinone derivatives were isolated from this genus.⁶⁴ Although phytols⁶⁵ and falcarinols⁶⁶ are well known anti-TB active compounds from studies of other medicinal plants, (Figure 13), no compound isolation report is available from *N. anomala*. Therefore, a further search for anti-TB active constituents may be fruitful.

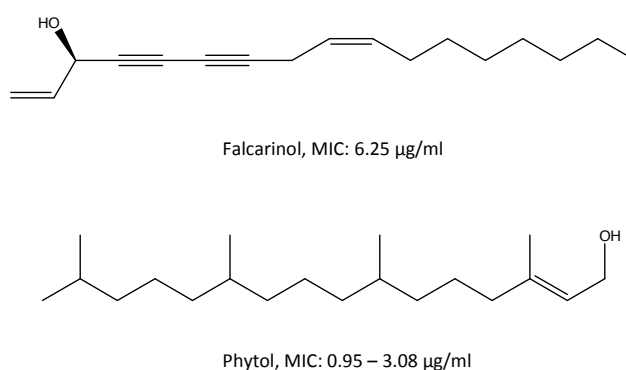


Figure 13. Falcarinol and phytol

Fatsia horrida from group B scored 8 points and has been re-classified as *Oplopanax horridus*, Devils Club. This plant was traditionally used by Native Americans to treat diabetes, tumors, and respiratory ailments including tuberculosis. Recently, extensive research on anti-TB activity has been performed with this plant at the Institute for Tuberculosis Research (24).^{39b, 66a} Two anti-TB active compounds, oplopandiol (MIC 61.5 µg/ml) and falcarindiol (MIC 6.2 µg/ml), were isolated along with two new sesquiterpenes, neroplomacrol (MIC > 128 µg/ml) and neroplofurol (MIC 128 µg/ml).^{66a}

Rapanea melanophloeos from group C scored 7 points. It is a small shrub that is widespread in Kenya, particularly in upland dry forests and rocky hillsides.⁶⁷ Historically, it has been widely used as an anthelmintic in humans and livestock in Africa. The bark or roots are used for respiratory problems, as well as for stomach, muscular, and heart problems.⁶⁸ A recent study showed that the bark of the plant exhibits some anti-TB activity against drug sensitive and resistant TB although the test concentration of the extract was relatively high (5 mg/ml).⁴⁰ However, no further study against TB has been reported.

As examples, plants with the highest scored from each group were introduced, and resulting in those high scored 45 plants with extract testing data (2) implies an evidence of valid practices of ancestors' ethnobotanicals. It also indicates that ethnobotanicals can yield more confidence for the isolation anti-TB active metabolites compared to random screening of available plants because of historical usages for TB treatment of the former. In addition, associating the 45 selected plants with the known anti-TB compounds isolated from natural sources (3) can help to avoid isolating previously known anti-TB active compounds especially those with poor solubility, absorption, bioavailability, and metabolic stability.

There is little doubt that ethnobotanical records provide a huge reservoir of knowledge about the medicinal values of plants. Although among the industrialized countries TB is considered a disease of

the past, it still takes millions of lives every year in the developing countries. Many undeveloped countries still rely on these ethnobotanicals for the treatment of tuberculosis.

2.3 Limitations and suggested solutions.

Upon a closer examination of the above cited botanicals, their usage for the treatment of TB by our ancestors is validated. The results also demonstrate that the NAPRALERT database is a valuable source for the investigation of ethnobotanicals.

However, the NAPRALERT database only fully covers the literature up to 2003. *Fatsia horrida* could be a good example of a limitation of the NAPALERT because an extensive phytochemical and biological study against TB was reported after 2003. Considering the data obtained from the more recent studies, it would not be the highest scored botanical in group B. Therefore, it is crucial to perform a literature search for 2003 to present by using other databases, such as Scifinder Scholar, Pubmed, and the Dictionary of Natural Products. For instance, the Dictionary of Natural Products provides the chemical, physical, bibliographic, and structural information on over 139,000 natural products, virtually every natural product isolated and reported in the literature. Besides, the book, Native American Medicinal Plants by Moerman, contains a remarkable amount of knowledge on medicinal plant use by Native Americans. It includes more than 2,500 species of medicinal plants. Therefore, the utilization of these additional search tools will aid the comprehensive literature search for this project, together with NAPRALERT.

The Score Index needs to be further developed. Initially, the five criteria for the score index were developed by characteristics that are favored for TB drug discovery. Each criterion of the score index in the preliminary data is an independent aspect for the selection of a candidate. Thus, a criterion may or may not correlate with another criterion. However, it could be meaningful when an extract

positively correlates to all of the independent criteria. Therefore, further development of the score index needs to be conducted, considering elements such as host immune stimulation, cytotoxicity, host pathogen interactions, as well as the aspect of conservation/sustainability.

Another anticipated problem is the limited polarity range of traditionally prepared water extracts (decoctions). Therefore, an ethnomedical record for an extract that is reported as inactive might be a false negative result. For instance, inactivity might be observed due to an inadequate extract preparation (aqueous vs. organic solvent extraction). With 283 references for antimycobacterial plant extracts, the polarity range of the preparation of those plant extracts will therefore be assured and the correlation of ethnomedical records with *in vitro* anti-TB activity of extracts will be carefully conducted.

Finally, most of these selected ethnobotanicals are only available outside of United States, such as Southern Africa and Asia, which leads to difficulties to access these materials. The conservation of natural resources is also an important aspect for drug discovery from medicinal plants which cannot be neglected. Prior to the further investigation of those selected ethnobotanicals, therefore, the availability, conservation, and the bio-cultural perspective also needs to be taken into consideration.

Chapter 3

Aim 2: Chemical and biological assessment of an anti-TB ethnomedical mushroom, *Fomitopsis officinalis* for anti-TB drug lead discovery

3 Aim 2: Chemical and biological assessment of an anti-TB ethnomedical mushroom, *Fomitopsis officinalis* for anti-TB drug lead discovery

As explained with previous chapter (Aim 1), 45 useful ethnobotanicals were selected to search for anti-TB drug leads. However, most of these plants were only available in Africa and South East Asia, which represents a major difficulty to access materials. While this project was underway, the Institute for Tuberculosis Research established a collaboration with a mushroom company, Fungi Perfecti, LLC., Washington. One of the company's mushroom collections has numerous ethnomedical reports for the TB treatment, mostly from journals that are not in indexed journals. This means that this mushroom had not been entered in the NAPRALERT database with anti-mycobacterium activity. However, ethnomedical reports for an anti-inflammatory effect and the treatment of cold and cough were available from NAPRALERT. In addition, there was no *in vitro/in vivo* anti-TB activity data available from the current literature search, such as PubMed, SciFinder, and NAPRALERT. Therefore, to continue to adapt ancestor's ethnomedical knowledge, the ethnomedical mushroom, *F. officinalis* was obtained and assessed biologically and chemically for anti-TB drug lead discovery in this Aim 2.

3.1 Backgrounds and scope of this study

F. officinalis is a wood rotting fungus known as a medicinal mushroom for the treatment of tuberculosis, pneumonia, cough, and asthma.⁶⁹ It is found in the old growth forests of Oregon and Washington in the Pacific Northwest United States, and British Columbia in Canada as well as in the northern regions of China and Europe.^{69a, 69d} While *F. officinalis* has known to be a rich source of unusual triterpenoids, only a few chemical studies have been reported, mostly on the isolation of terpenes and no anti-TB activity report available.^{69d, 70}

There were several anti-TB active triterpenes reported previously such as ergosterol from *Ajuga remota*, and saringosterol from *Lessonia nigrescens* as MICs as low as 0.25 µg/ml. Generally, these terpenoids are

known to possess relatively potent anti-mycobacterium activity due to their relatively non-polar characteristic, which may associate to a possible mode of action on non-polar mycobacterium cell wall. However, this is also considered the main cause of a poor pharmacological characteristic for drug development.

We obtained a mycelial culture extract (EtOH) of *F. officinalis* and isolated two new anti-TB active metabolites from the extract. The structures of the two metabolites were confirmed by chemical synthesis, together with the synthesis of two analogs. For the unambiguous chemical and biological characterization of the four compounds, we completely resolved all their *J*-couplings and chemical shifts by full spin analysis using PERCH software to facilitate future dereplication of these lead structures. Also, we extensively assessed their biological activity, focusing on *M. tuberculosis*.

3.2 Results and discussion

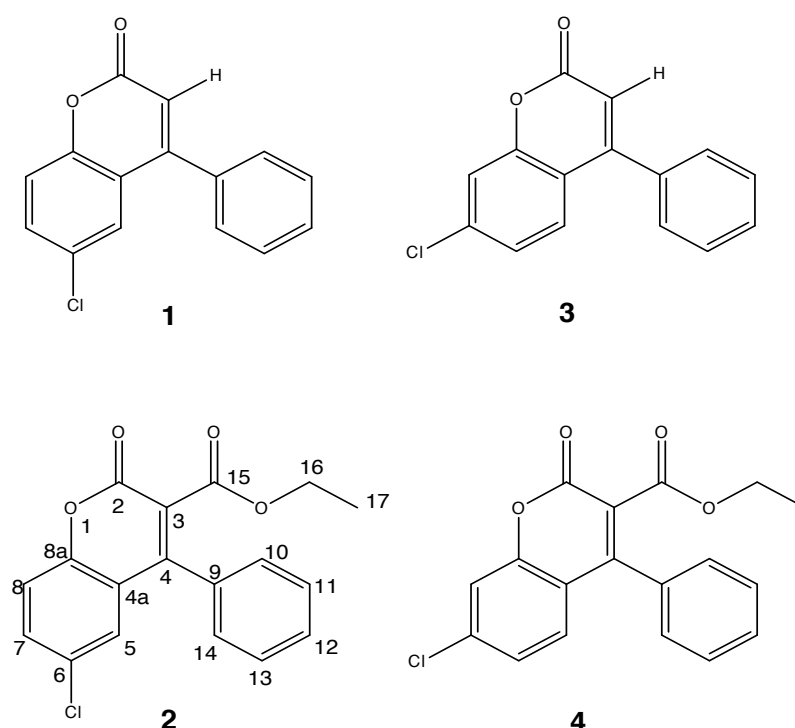


Figure 14. Two isolated coumarins (**1** and **2**) and their analogs (**3** and **4**)

Two new coumarins, **1** (0.5 mg dry wt) and **2** (0.2 mg dry wt), were isolated from an EtOH extract of the polypore mushroom *F. officinalis*. For **1**, the HRMS measurement indicated the presence of one chlorine in the molecule with a molecular ion peak at m/z 257.0372 $[M+H]^+$ corresponding to a molecular formula of $C_{15}H_9ClO_2$. The ^{13}C DEPTQ, and HSQC NMR (MeOH- d_4) spectra at 225/900 MHz confirmed the presence of 6 quaternary carbons (δ 160.5, 155.1, 120.2, 129.4, 152.6, and 134.6 ppm) and 9 methine carbons (δ 115.5, 125.9, 131.8, 118.6, two at 128.2, two at 128.8, and 129.8 ppm). HRMS measurement and the ^{13}C and DEPTQ NMR confirmed the molecular formula of $C_{15}H_9ClO_2$. The 1H , 1H - 1H COSY, ^{13}C DEPTQ, HSQC, and HMBC NMR spectra for the isolated **1** are provided in the Appendix, Figure 23-27. The aromatic region of the 1H NMR spectrum clearly showed the presence of one AMX and one AA'BB'C spin system, indicative of a tri- and a mono-substituted aromatic rings, respectively, which was confirmed by the COSY correlations (Figure 15). In addition, the IR spectrum presented a strong carbonyl absorption band at 1731 cm^{-1} , which was consistent with an ester carbonyl corresponding to the quaternary carbon C-2 (δ 160.5).

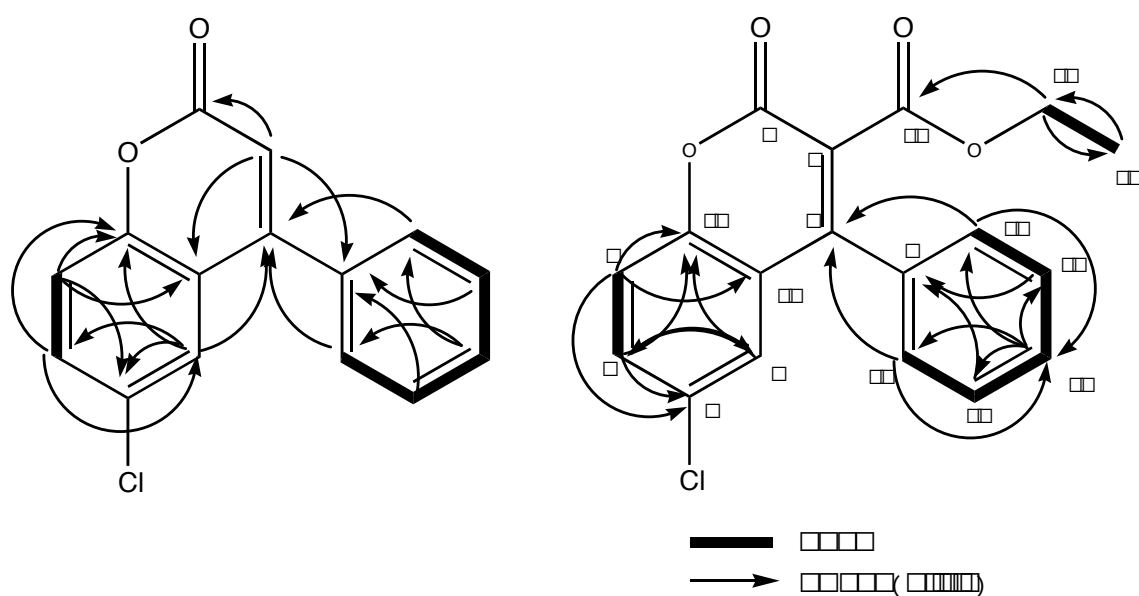


Figure 15. Key 2D NMR correlations that were instrumental for the structure determination of **1** and **2**

Long-range ^1H , ^{13}C couplings from both aromatic protons H-10/H-14 (δ 1.036) on the stated phenyl ring to a quaternary carbon C-4 (δ 155.1) confirmed the phenyl substitution at C-4. HMBC correlations from the olefinic proton H-3 (δ 6.405) to C-2 (δ 160.5), C-4a (δ 120.2), and C-9 (δ 134.6) also provided evidence for phenyl substitution at C-4. The AMX splitting pattern for H-7 (dd, 8.84, 2.50 Hz) was consistent with meta-coupling to H-8 and ortho-coupling to H-5, suggesting the chlorine substitution to be at C-6 (δ 129.4). Additional HMBC correlations of H-5 (δ 7.433) to C-8a (δ 152.6) and C-4 as well as H-7 to C-8a and C-5 confirmed the remaining coumarin skeleton. Isolated **1** turned out to be synthetically accessible compound, 6-chloro-4-phenyl-2H-chromen-2-one. Since only sub-milligram quantities of could be isolated, the compound was synthesized in order to gain more material for the subsequent chemical and biological evaluation. The isolated and the synthetic product resulted in an identical ^{13}C DEPTQ spectrum, as shown in Figure 16.

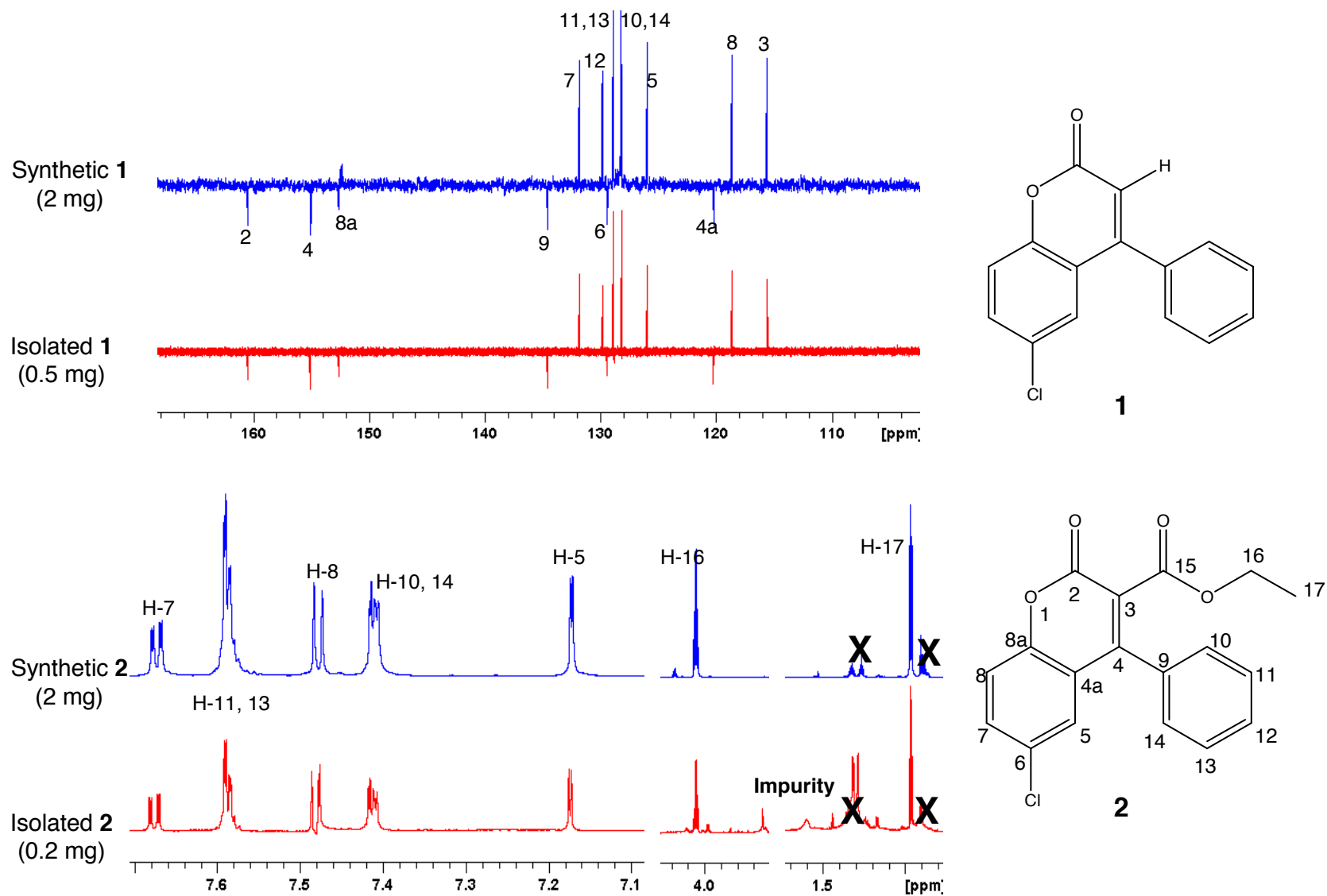


Figure 16. Demonstration of congruence between the synthetic and isolated compounds **1** and **2** by ^{13}C DEPTQ and ^1H NMR respectively, (225/900 MHz, $\text{MeOH-}d_4$)

TABLE VI. ¹H AND ¹³C NMR DATA OF COMPOUNDS 1 - 4.

Position	1^b				2^b				3^b				4^b			
	δ_{H}	multi (<i>J</i> in Hz) ^e	δ_{C} ^c	multi	δ_{H}	multi (<i>J</i> in Hz) ^e	δ_{C} ^c	multi	δ_{H}	multi (<i>J</i> in Hz) ^e	δ_{C} ^c	multi	δ_{H}	multi (<i>J</i> in Hz) ^e	δ_{C} ^c	multi
2	-	-	160.5	C	-	-	159.1	C	-	-	161.1	C	-	-	158.9	C
3	6.405	s	115.5	CH	-	-	121.8	C	6.382	s	115.1	CH	-	-	119.2	C
4	-	-	155.1	C	-	-	153.7	C	-	-	156.3	C	-	-	155.1	C
4a	-	-	120.2	C	-	-	123.5	C	-	-	118.4	C	-	-	122.3	C
5	7.433	dd (2.50, 0.41)	125.9	CH	7.176	dd (2.50, 0.44)	128.4	CH	7.494	dd (8.58, 0.76)	125.3	CH	7.250	dd (8.61, 0.22)	126.5	CH
6	-	-	129.4	C	-	-	131.4	C	7.322	dd (8.58, 1.98)	128.8	CH	7.326	dd (8.61, 2.05)	131.0	CH
7	7.632	dd (8.84, 2.50)	131.8	CH	7.677	dd (8.87, 2.50)	134.3	C	-	-	135.5	C	-	-	134.0	CH
8	7.455	dd (8.84, 0.41)	118.6	CH	7.495	dd (8.87, 0.44)	120.1	CH	7.504	dd (1.98, 0.76)	117.7	CH	7.548	dd (2.05, 0.22)	118.3	CH
8a	-	-	152.6	C	-	-	153.5	C	-	-	155.1	C	-	-	154.2	C
9	-	-	134.6	C	-	-	133.8	C	-	-	138.3	C	-	-	140.0	C
10	7.527	dddd (2.04, 7.66, 1.25, 0.64)	128.2	CH	7.422	dddd (1.92, 7.67, 1.25, 0.62)	130.0	CH	7.512	dddd (2.24, 7.67, 0.33, 1.30)	128.9	CH	7.395	dddd (1.63, 7.68, 0.63, 1.06)	129.5	CH
11	7.599	dddd (7.66, 0.64, 1.25, 7.55)	128.8	CH	7.591	dddd (1.25, 7.57, 0.72, 7.67)	130.2	CH	7.570	dddd (7.76, 0.33, 1.33, 7.54)	129.4	CH	7.559	dddd (7.68, 0.63, 1.28, 7.49)	130.0	CH
12	7.592	dd (1.25, 7.55)	129.8	CH	7.588	dd (7.57, 1.25)	131.2	CH	7.566	dd (1.30, 7.54)	130.4	CH	7.565	dd (7.49, 1.06)	130.5	CH
13	7.599	dddd (7.66, 0.64, 1.25, 7.55)	128.8	CH	7.591	dddd (1.25, 7.57, 0.72, 7.67)	130.2	CH	7.570	dddd (7.76, 0.33, 1.33, 7.54)	129.4	CH	7.559	dddd (7.68, 0.63, 1.28, 7.49)	130.0	CH
14	7.527	dddd (2.04, 7.66, 1.25, 0.64)	128.2	CH	7.422	dddd (1.92, 7.67, 1.25, 0.62)	130.0	CH	7.512	dddd (2.24, 7.67, 0.33, 1.30)	128.9	CH	7.395	dddd (1.63, 7.68, 0.63, 1.06)	129.5	CH
15	-	-	-	-	-	-	165.3	C	-	-	-	-	-	-	165.3	C
16	-	-	-	-	4.052	q (7.01)	61.5	CH ₂	-	-	-	-	4.040	q (7.12)	62.9	CH ₂
17	-	-	-	-	0.966	t (7.01)	12.6	CH ₃	-	-	-	-	0.957	t (7.12)	14.0	CH ₃

^b. ¹H NMR data were obtained from the synthetic compounds.

^c. ¹³C NMR chemical shifts were obtained from DEPTQ.

^e. The *J*-coupling values resolved from iterative full ¹H spin analysis using PERCH and are given with 10 MHz precision.

In order to differentiate from a possible chlorine substitution at C-7, we also synthesized compound 7-chloro-4-phenyl-2H-chromen-2-one, **3**. The ^1H and ^{13}C DEPTQ NMR spectra of **3** are available in the Appendix, Figure 37 and Figure 38. In addition, a full spin analysis of the ^1H NMR spectra was carried out for both synthetic compounds **1** and **3** by using the PERCH iteration software^{66a,71}, resulting in the full assignment of the ^1H resonances including their multiplicities, as shown in Table 6 and the Appendix (Figure 41 and Figure 43).

Compound **2**, ethyl 6-chloro-2-oxo-4-phenyl-2H-chromen-3-carboxylate, displays very similar ^1H and ^{13}C NMR peak patterns compared to **1**, exhibiting AMX and AA'BB'C spin systems as well. The HRMS measurement also indicated the presence of one chlorine in the molecule by affording a molecular ion peak at m/z 329.0614 $[\text{M}+\text{H}]^+$ for the ^{35}Cl isotope, which had 72 amu difference from **1**. The ^{13}C DEPTQ, HSQC, and HMBC spectra were obtained at 225/900 MHz (MeOH- d_4 , 3 mm and 1.7 mm), but showed poor signal-to-noise due to the small amount (approx. 0.2 mg) of sample. The ^1H , ^1H - ^1H COSY, ^{13}C DEPTQ, HSQC, and HMBC NMR spectra for the isolated compound **2** are provided in the Appendix, Figure 28-31. Despite these limitations, we were still able to confirm that **2** possessed a coumarin skeleton with a chlorine at C-6 (δ 131.4) and phenyl substitution at C-4 (δ 153.7). In addition, **2** clearly did not have an olefinic proton at C-2, but rather had an ethoxycarbonyl moiety with H-17 (2H, δ 4.052) and H-18 methyl protons (3H, δ 0.966). The ^1H - ^1H COSY confirmed the correlation between H-17 and H-18. Deshielding of both the carbon and the proton of C-17/H-17 (δ 61.5/ δ 4.052) indicated close proximity to an electronegative oxygen atom. Long-range couplings from H-17 (δ 4.052) to a quaternary carbon C-15 (δ 165.3) in the HMBC confirmed the presence of the ethyl ester moiety, which also accounted for the 72 amu difference. Therefore, **2** was shown to possess an ethyl ester moiety at C-3 (δ 121.8) in **1**. Thus, **2** was deduced as ethyl 6-chloro-2-oxo-4-phenyl-2H-chromen-3-carboxylate, which was also accessible by synthesis. In order to confirm the structure, **2** was synthesized and shown

to have an identical ^1H NMR spectrum to the isolated material, as shown in Figure 16. In addition, the analog with chlorine substitution at C-7, ethyl 7-chloro-2-oxo-4-phenyl-2H-chromen-3-carboxylate, **4** was synthesized to rule out this positional isomer. The ^1H and ^{13}C DEPTQ NMR spectra for the **4** are available in the Appendix, Figure 39 and Figure 40. In addition, full ^1H NMR spin analysis was carried out for both **2** and **4** using the PERCH iteration software, which resulted in Table 6 and the Appendix, Figure 42 and Figure 44. The overall deviation between the simulated and the experimental spectrum for synthetic **1** – **4** was represented by total Root Mean Square value (total RMS = 0.05, 0.19, 0.04, and 0.05%, respectively), which indicated an excellent simulation.

Biological evaluation

The anti-TB activity of the four coumarins, **1** – **4**, was assessed by the microplate Alamar Blue assay (MABA) and the low oxygen recovery assay (LORA), as shown in Table 7. MABA is used to measure the activity against replicating *M. tuberculosis*, while LORA is designed to assess the activity against non-replicating *M. tuberculosis*.

MABA and LORA MICs resulted in similar anti-TB activities as the MIC ranged from 20 to 50 $\mu\text{g}/\text{ml}$, except for compound **1** (>100 $\mu\text{g}/\text{ml}$). The 7-chloro congener **4** of the ethyl ester had superior anti-TB activity. The olefinic proton substitution (**3**) of the two 7-chloro variations (**3** and **4**) seemed to be slightly more active than the ethyl ester variation, but this might be insignificant due to the minor difference in the MIC values (less than two-fold). On the other hand, in the 6-chloro variation (**1** and **2**), the ethyl ester substitution (**2**) seemed to have stronger anti-TB activity. Based on these structure-activity relationship (SAR) observations, it can be deduced that the structural variation containing an ethyl ester is of superior anti-TB activity if it contains a chlorine in position 6, while it is less active with a 7-chlorine substitution. In summary, out of the four structural variations (**1-4**), compound **3**, was the most active against replicating and non-replicating *M. tuberculosis* with MICs of 23.9 and 21.9 $\mu\text{g}/\text{ml}$, respectively. Furthermore, activity in the LORA assay

indicated that these coumarins might have the potential for shortening the duration of therapy through efficient killing of the non-replicating persister. Activity against a panel of mono drug-resistant isolates was determined by the MABA assay and resulted in a similar susceptibility profile of MABA and LORA, indicating that there is no significant difference in the anti-TB activity for an ethyl ester with 7-chloro substitution, while once more a better activity was observed with 6-chloro moiety, as shown in Table 7. To understand the spectrum of activity of the four coumarins (**1-4**), MICs of a small panel of 8 bacterial species, *S. aureus*, *E. coli*, *C. albicans*, *E. faecalis*, *P. aeruginosa*, *A. baumannii*, *S. pneumoniae*, and *M. smegmatis* were determined, revealing that all four compounds were inactive at the highest testing concentration, 100 µg/ml. In addition, activity against other mycobacteria was assessed with *M. chelonae*, *M. abscessus*, *M. marinum*, *M. kansasii*, *M. avium*, and *M. bovis*. The latter having the closest gene homology to *M. tuberculosis* showed the most similar susceptibility profile to that of *M. tuberculosis*. Compounds **2** and **3** were weakly active against *M. marinum* and *M. kansasii*, respectively, with MICs of 97.1 µg/ml and 49.3 µg/ml, respectively. Otherwise, no activity was observed at 100 µg/ml. The spectrum and non-tuberculosis mycobacterium activities are available in Table 8.

TABLE VII. ANTI-TB ACTIVITY PROFILES OF THE COUMARINS, 1 – 4.

	MIC (µg/ml)						
	MABA ^a	LORA ^b	rRMP ^c	rINH ^c	rSM ^c	rKAN ^c	rCS ^c
1	> 100	> 100	> 100	> 100	> 100	> 100	> 100
2	44.7	37.1	46.6	44.7	49.5	> 100	> 100
3	23.9	21.9	45.4	76.5	46.9	47.4	47.3
4	35.9	23.2	44.7	31.7	46.9	43.9	47.3
rifampin	0.08	<0.05	>3.29	0.04	0.09	0.02	0.02
isoniazid	0.03	-	0.03	>2.19	0.03	0.07	0.04
streptomycin	-	1.07	0.47	0.56	>9.31	1.48	0.53
PA824	0.02	0.25	0.07	0.05	0.17	0.34	0.18
kanamycin	-	-	0.73	0.72	0.76	> 25	1.12
cycloserine	-	-	4.8	5.0	4.9	4.9	>10.2

^a. Determined by the MABA for replicating *M. tuberculosis*, ^b. Determined by LORA for non-replicating *M. tuberculosis*, ^c. *M. tuberculosis* strains resistant to rifampin (rRMP), isoniazid (rINH), streptomycin (rSM), and kanamycin (rKAN)

TABLE VIII. SPECTRUM OF ANTIMICROBIAL AND NON-TUBERCULOUS MYCOBACTERIA ACTIVITY.

	MIC ($\mu\text{g/ml}$)						
	<i>S. aureus</i>	<i>A. baumannii</i>	<i>P. aeruginosa</i>	<i>E. faecalis</i>	<i>E. coli</i>	<i>C. albicans</i>	<i>M. smegmatis</i>
1	> 100	> 100	> 100	> 100	> 100	> 100	> 100
2	> 100	> 100	> 100	> 100	> 100	> 100	> 100
3	> 100	> 100	> 100	> 100	> 100	> 100	> 100
4	> 100	> 100	> 100	> 100	> 100	> 100	> 100
Ampicillin	1.07	-	-	-	8.75	-	-
Gentamicin	0.28	0.74	0.68	11.84	1.60	-	-
Doxycycline	-	0.11	-	-	-	-	-
Demeclocycline	-	0.17	-	-	-	-	-
Minocycline	-	0.39	-	-	-	-	-
Kanamycin	-	1.45	-	-	-	-	-
Ciprofloxacin	-	-	0.15	0.55	0.61	-	< 0.39
Ofloxacin	-	-	0.81	1.14	1.14	-	0.84
Rifampin	-	-	10.3	-	-	-	45.0
Vancomycin	-	-	-	-	0.15	-	-
Moxifloxacin	-	-	-	-	-	-	0.12
Amphotericin B	-	-	-	-	-	0.89	-
Ketoconazole	-	-	-	-	-	<0.01	-

	MIC ($\mu\text{g/ml}$)					
	<i>M. chelonae</i>	<i>M. abscessus</i>	<i>M. marinum</i>	<i>M. kansasii</i>	<i>M. avium</i>	<i>M. bovis</i>
1	> 100	> 100	> 100	> 100	> 100	> 100
2	> 100	> 100	97.1	> 100	> 100	49.7
3	> 100	> 100	> 100	49.3	> 100	44.7
4	> 100	> 100	> 100	> 100	> 100	47.3
Rifampin	-	-	0.05	0.16	> 0.29	0.02
Moxifloxacin	0.10	5.10	0.19	0.10	2.77	< 0.02

3.3 Materials and methods

General experimental procedures

The UV-vis spectra were obtained with a SpectraMax Plus 384 at 25 °C. Optical rotations $[\alpha]_D$ were measured on a Perkin-Elmer 242 polarimeter at 25 °C. The infrared spectra were measured on a Thermo Nicolet 6700 FT-IR spectrometer. All NMR experiments were obtained at either 600 or 900 MHz and performed on Bruker AVANCE-600 or AVANCE II-900 instruments respectively, each equipped with a cryogenic sensitivity-enhanced triple-resonance 5mm inverse TCI cryoprobe. The samples were dissolved in 99.96% MeOH- d_4 and transferred to 3 mm or 1.7 mm NMR tubes. ^{13}C DEPTQ experiments were obtained at 225 MHz on Bruker AVANCE II-900. All NMR experiments were performed using standard Bruker pulse sequences and the temperature was maintained at 25 °C (298 K). High-resolution ESI mass spectra were obtained using a Shimadzu IT-TOF LC mass spectrometer. The ^1H NMR full spin analysis was performed with PERCH NMR software (v.2010.1, PERCH Solutions Ltd., Kuopio, Finland). The ^1H NMR spectra were processed with NUTS (Acorn NMR Inc.), imported into PERCH as JCAMP-DX files, and subjected to baseline correction, peak picking, and integration. The ^1H NMR parameters in MeOH- d_4 were predicted using the PERCH Molecular Modeling System (MMS). After a manual examination of the ^1H assignments, the calculated ^1H chemical shifts, signal line widths, and J -couplings were refined by using the integral-transform (D) and total-line-fitting (T) modes until an excellent agreement between the observed and simulated spectra was attained ($\text{RMS} \leq 5.4\%$). Viability was assessed by the measurement of fluorescence, luminescence, or absorbance with the Victor3 multilabel reader (PerkinElmer Life Sciences).

Organism collection, identification, culture, and extraction

Fomitopsis officinalis was collected from Morton, WA in September 2001. The tissue culture and stock cultures are maintained at Fungi Perfecti Research Laboratories in Shelton, WA. Partial sequence of 18S and 28S ribosomal RNA genes established the identification of *Fomitopsis officinalis*. Sequence data are available on Genbank (EU854436.1).

Mycelial cultures were grown in sterile Petri dishes containing sterilized antibiotic malt extract yeast agar. After three weeks of colonization in a clean room laboratory at temperatures between 21 – 24 °C, the cultures were aseptically transferred into a 1000 ml Eberbach™ stirrer containing 800 ml sterilized water. The Eberbach™ container was activated using a Waring™ blender base and the mycelium was fragmented in a process known as liquid fragmentation (the dissociated fragmented mycelial mass allows for a multiple loci inoculation, resulting in accelerated colonization). Approximately 50 – 100 ml myceliated broth was then transferred into a polypropylene incubation bag containing approximately 3 kg of moistened sterilized rice (approximately 45 -50% moisture content). These bags of freshly inoculated rice were then incubated for 60 – 120 days in a class 100 clean room. Once colonization was determined to be sufficient, the mycelium-colonized rice was transferred to glass containers for extraction. The mycelium was covered with an equal weight of 95% EtOH. The mixture was agitated and then allowed to macerate at room temperature.

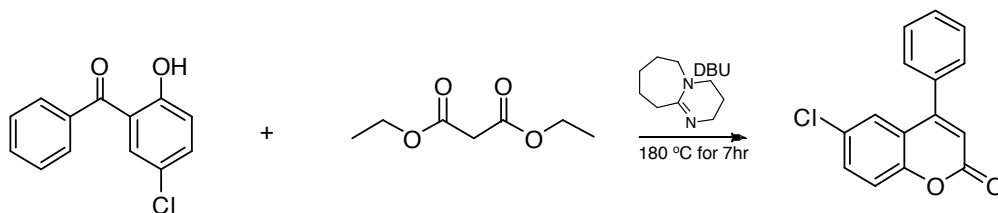
Isolation

The *Fomitopsis officinalis* mycelium culture extract (1.75 L, 95% EtOH) was evaporate under vacuum to give 17 g of dried crude extract. The extract was redissolved in 1 L of 75% EtOH and partitioned with petroleum ether, hexane, CHCl₃, EtOAc, and n-BuOH (1:1, v/v) to give 474, 30, 4270, 48, and 8569 mg of extracts, respectively. The CHCl₃ partition fraction was further separated on Isolera™ Flash

purification system (SNAP 100 g, 30 ml/min) with a linear solvent gradient of CHCl₃/MeOH (100:0, v/v) to 100% MeOH over 100 min, to afford 135 fractions (25ml/fraction). The fractions were recombined into 22 subfractions based on their TLC (silica, CHCl₃:MeOH, 85:15) profile. From the 22 fractions, fractions 11, 12, and 13 were later recombined (300 mg) for further separation on the Isolera™ Flash purification system (SNAP 10 g, 9 ml/min) with a linear solvent gradient of CHCl₃/MeOH (90:10, v/v) to 15% MeOH over 28 min, affording 85 sub-fractions (3ml/fraction). The total of 85 sub-fractions was recombined into 7 fractions based on TLC profile and dried to yield 17, 9, 6, 24, 31, 37, and 17 mg, respectively. The first combined fraction (17 mg) was further fractionated using reverse-phase HPLC on a Waters Delta 600 system with a Waters 996 photodiode array detector using a semi-preparative column (Waters, C18, 5 μm, 250 x 10 mm, 3 ml/min). Five separated injections with a linear solvent gradient of MeOH/H₂O (80:20, v/v) to 100% MeOH over 25 min afforded 0.2 mg of **2** at 15 min and 0.5 mg of **1** at 17 min. General fraction monitoring for chromatographic separation was done by TLC analysis with precoated Alugram SIL G/UV plates (Macherey-Nagel, Duren, Germany).

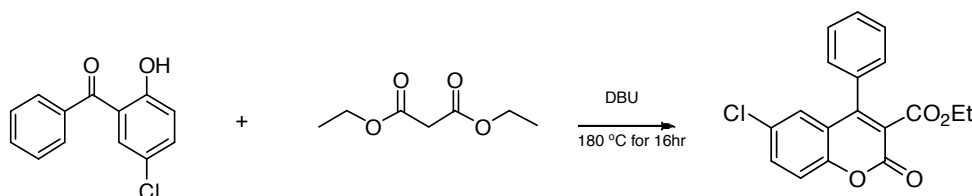
Synthesis of 1, 2, 3, and 4

¹H NMR and ¹³C NMR spectra were recorded on Bruker spectrometer at 400 MHz equipped with a 5 mm QNP probe with temperature maintained at 25 °C (298 K). Chemical shifts are reported in parts per million (ppm) downfield from tetramethylsilane (TMS, 0.00 ppm). HRMS were run on the Shimadzu LCMS-ITTOF ionization (ESI) mode. Chromatographic purifications were performed using an HPFC BioTage SP1 system using prefilled KP-Sil (normal phase) SNAP cartridges with UV detection at 235 and 254 nm utilizing Hexane/EtOAc gradients. CEM Explorer 48/72/96 automated microwave synthesizer was used for microwave heated reactions with an external computer loaded with the Synergy application software (Version 1.1).

6-Chloro-4-phenyl-2H-chromen-2-one⁷², (**1**)

5-Chloro-2-hydroxybenzophenone (0.25 g, 1.08 mmol), DBU (82 mg, 0.54 mmol) and diethyl malonate (0.26 g, 1.60 mmol) were combined in a 10 ml vessel and heated to 180 °C via microwave for 7 min. After the starting material was not detectable on TLC (10% EtOAc:Hex), the crude residue was collected in dichloromethane (DCM) and washed with sat. NH_4Cl . The organic layer was separated and dried over sodium sulfate, and the solvents were evaporated. The crude product was purified via BioTage silica gel Flash cartridge 12 L using 7.5% Et/Hex to give 58.3 mg (24%) as a white solid from the pure fractions.

White, amorphous powder, $[\alpha]_{\text{D}}^{25}$ 0 (c 0.001, MeOH); UV/Vis (MeOH) λ_{max} (log ϵ) 257 (2.87), 264 (3.09), 288 nm (3.42); IR (neat) ν_{max} 2359, 2341, 1731 cm^{-1} ; $^1\text{H}/\text{DEPTQ}$ ^{13}C NMR (900/225 MHz, MeOH- d_4), see Table 6; HRMS m/z 256.0274 $[\text{M}+\text{H}]^+$ (calculated for $\text{C}_{15}\text{H}_9\text{ClO}_2$, 256.0291)

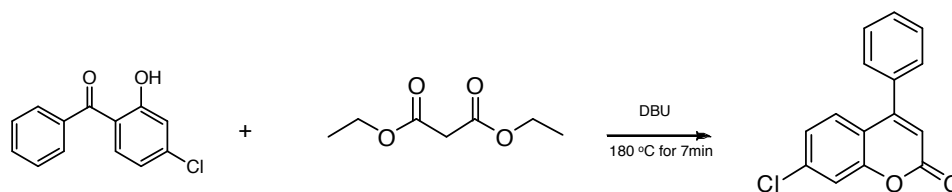
Ethyl 6-chloro-2-oxo-4-phenyl-2H-chromene-3-carboxylate⁷³, (**2**)

5-Chloro-2-hydroxybenzophenone (0.20 g, 0.86 mmol), DBU (13 mg, 0.09 mmol) and diethyl malonate (0.27 g, 1.72 mmol) were combined in a 10 ml vessel and heated to 180 °C via microwave for 7 min.

After the starting material was not detectable on TLC (10% EtOAc:Hex), the crude residue was collected in dichloromethane (DCM) and washed with sat. NH_4Cl . The organic layer was separated and dried over sodium sulfate, and the solvents were evaporated. The crude product was purified via BioTage silica gel Flash cartridge 12 L using 10% Et/Hex to give 94.4 mg (35%) as a white solid from the pure fractions.

White, amorphous powder, $[\alpha]_{\text{D}}^{25}$ 0 (c 0.001, MeOH); UV/Vis (MeOH) λ_{max} (log ϵ) 257 (3.16), 265 (3.52), 289 (3.95), 294 nm (3.94); IR (neat) ν_{max} 1745, 1724, 1599, 1244, 1039 cm^{-1} ; $^1\text{H}/\text{DEPTQ}$ ^{13}C NMR (900/225 MHz, MeOH- d_4), see Table 6; HRMS m/z 328.0515 $[\text{M}+\text{H}]^+$ (calculated for $\text{C}_{18}\text{H}_{13}\text{ClO}_4$, 328.0502)

7-Chloro-4-phenyl-2H-chromen-2-one⁷², (3)

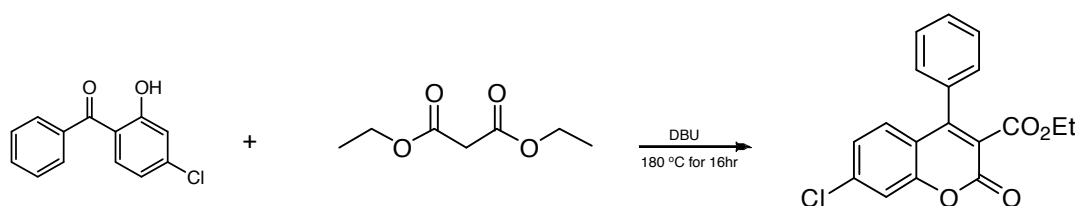


4-Chloro-2-hydroxybenzophenone (0.2 g, 0.86 mmol), DBU (65 mg, 0.43 mmol), and diethyl malonate (0.21 g, 1.29 mmol) were combined in a 10 ml vessel and heated to 180 °C via microwave for 7 min. After the starting material was not detectable on TLC (EtOAc:Hex 1:3), the crude residue was collected in DCM and washed with sat. NH_4Cl . The organic layer was separated and dried over sodium sulfate, and the solvents were evaporated. The crude product was purified via BioTage silica gel Flash cartridge 12 L using 7.5% Et/Hex to give 54 mg (24%) white solid from the pure fractions.

White, amorphous powder, $[\alpha]_{\text{D}}^{25}$ 0 (c 0.001, MeOH); UV/Vis (MeOH) λ_{max} (log ϵ) 257 (3.17), 265 (3.55), 289 (3.89), 294 nm (3.89); IR (neat) ν_{max} 1743, 1725, 1601, 1279, 1037 cm^{-1} ; $^1\text{H}/\text{DEPTQ}$ ^{13}C NMR

(900/225 MHz, MeOH-d₄), see Table 6; HRMS m/z 256.0298 [M+H]⁺ (calculated for C₁₅H₉ClO₂, 256.0291)

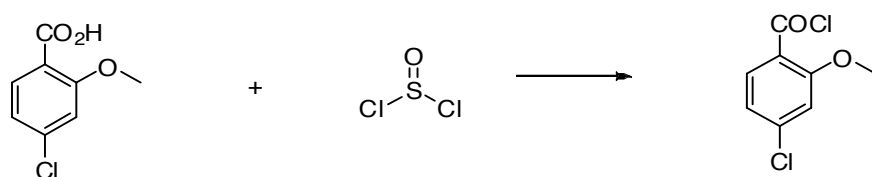
Ethyl 7-chloro-2-oxo-4-phenyl-2H-chromene-3-carboxylate⁷³, (**4**)



4-Chloro-2-hydroxybenzophenone (0.2 g, 0.86 mmol), DBU (13 mg, 0.086 mmol), and diethyl malonate (0.275 g, 1.72 mmol) were combined in a 10 ml flask and heated in an oil bath at 160 °C for 16 h. After the starting material was not shown on TLC (10% EtOAc:Hex), the crude residue was collected in DCM and washed with sat. NH₄Cl. The organic layer was separated and dried over sodium sulfate, and the solvents were evaporated. The crude product was purified via BioTage silica gel Flash cartridge 12L using 10% Et/Hex to give 132 mg (47%) of white solid.

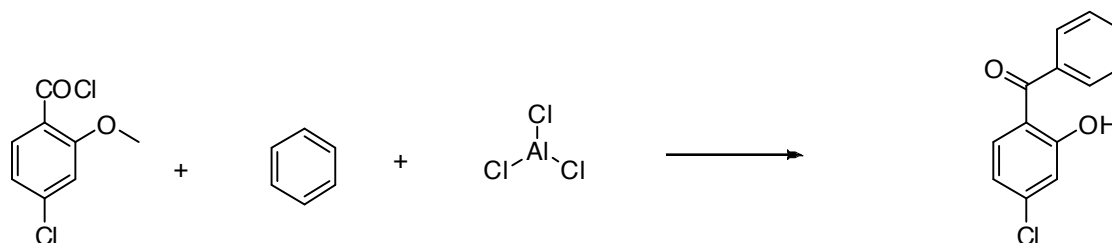
White, amorphous powder, $[\alpha]_D^{25}$ 0 (c 0.001, MeOH); UV/Vis (MeOH) λ_{\max} (log ϵ) 257 (3.17), 265 (3.55), 289 (3.89), 294 nm (3.89); IR (neat) ν_{\max} 1743, 1725, 1601, 1279, 1037 cm⁻¹; ¹H/DEPTQ ¹³C NMR (900/225 MHz, MeOH-d₄), see Table 6; HRESIMS m/z 328.0516 [M+H]⁺ (calculated for C₁₈H₁₃Cl₂O₄, 328.0502)

Synthesis of 4-chloro-2-methoxybenzoyl chloride⁷⁴



2-Methoxy-4-chlorobenzoic acid (2 g, 10.72 mmol) was treated with thionyl chloride (2.93 g, 25 mmol)

and DMF (1 drop) and heated at reflux for 2 h. The thionyl chloride was evaporated, and the crude residue was used directly for the next reaction.



The acid chloride from above was dissolved in benzene (15 ml). Aluminum chloride (1.57 g, 11.8 mmol) was added portion-wise over 10 min to this solution, and the resulting suspension was refluxed for 1 h (initial vigorous gas evolution upon heating). The mixture was cooled to room temperature, poured into ice (100 g) and con. HCl (20 ml). The organic layer was separated, and the aqueous layer extracted with EtOAc (3x40 ml). The combined organic layer was washed with water (3x20 ml), dried over Na₂SO₄, and the solvents were evaporated to give 2.33 g (crude yield 50%) crystallizing tan solid.

Bacterial strain preparation for anti-TB bioassay and Minimum Inhibitory Concentration (MIC)

M. tuberculosis H₃₇Rv ATCC 27294 was purchased from the American Type Culture Collection (ATCC) and cultured to late log phase in the 7H12 media, Middlebrook 7H9 broth supplemented with 0.2% (vol/vol) glycerol, 0.05% Tween80, and 10% (vol/vol) oleic acid-albumin-dextrose-catalase (OACD, Fischer). The culture was harvested and resuspended in phosphate-buffered saline. Suspensions were then filtered through 8 μm pore size membranes and frozen at -80°C. Prior to use of bacterial stocks for the anti-TB assay, CFU were determined by plating on 7H11 agar media. The MIC is defined here as the lowest concentration resulting in ≥90% growth inhibition of the bacteria being tested. MIC against replicating *M. tuberculosis* was measured by the MABA.⁷⁵

Low oxygen recovery assay

The luciferase reporter gene *luxAB* recombinant *M. tuberculosis* was prepared as previously reported.⁷⁶ The bacteria was adapted to low oxygen during culture in a BioStatQ fermentor. The low oxygen-adapted culture was exposed to the extracts in 96-well microplates for 10 days at 37°C in a hypoxic environment created with an Anoxomat (WS-8080, MART Microbiology). The cultures were then transferred to a normoxic environment at 37°C for 28 hours. Viability was assessed by the measurement of luciferase-mediated luminescence. The LORA MIC was defined as the lowest concentration effecting a reduction of luminescence of ≥90% relative to untreated cultures.

Cytotoxicity

Cytotoxicity^{65a,77} was assessed using Vero (ATCC CRL-1586) cells. Vero cells were cultured in 10% fetal bovine serum (FBS) in Eagle minimum essential medium. The culture were incubated at 37°C under 5% CO₂ in air and then diluted with phosphate-buffered saline to 10⁶ cells/ml. In a transparent 96-well plate (Falcon Microtest 96), 2-fold serial dilutions of testing samples with a final volume of 200 µl cell culture suspension was prepared. After 72 h incubation at 37°C, the medium was removed and monolayers were washed twice with 100 µl of warm Hanks' balanced salt solution (HBSS). One hundred µl of medium and 20 µl of MTS-PMS (Promega) were added to each well. Plates were then incubated for 3 hours, and cytotoxicity was determined by the measurement of absorbance at 490 nm.

MIC against drug-resistant *M. tuberculosis* Isolates

M. tuberculosis strains resistant to rifampin (RMP, ATCC 35838), isoniazid (INH, ATCC 35822), streptomycin (SM, ATCC 35820), and kanamycin (KAN, ATCC 35827) were obtained from the American Type Culture Collection (ATCC). Inocula were prepared and MICs determined as described above for

the pan-sensitive H₃₇Rv strain (ATCC 27294).

MIC against non-tuberculosis Mycobacteria

Mycobacterium abscessus (ATCC19977), *Mycobacterium chelonae* (ATCC35752), *Mycobacterium avium* (ATCC15769), *Mycobacterium marinum* (ATCC927), *Mycobacterium kansasii* (ATCC12478), and *Mycobacterium bovis* BCG (ATCC35734) were purchased from ATCC. Cultures were prepared and MICs against non-tuberculosis Mycobacteria were determined by the MABA assay as described above for *M. tuberculosis* H37Rv. *M. abscessus* was incubated with 7H12 media at 37°C for 3 days and incubated an additional 4 hours after adding 12 µl of 20% Tween80 and 20 µl of Alamar Blue dye. *M. bovis* was incubated with 7H12 media at 37°C for 7 days and an additional 1 day of incubation period after adding 12 µl of 20% Tween80 and 20 µl of Alamar Blue dye. *M. chelonae* was incubated with 7H9 media at 30°C for 3 days, plus an additional 6 days of incubation period after adding 12 µl of 20% Tween80 and 20 µl of Alamar blue dye. *M. marinum* was incubated with 7H9 media at 30°C for 5 days and additional 1 day of incubation after adding 12 µl of 20% Tween80 and 20 µl of Alamar blue dye. *M. avium* and *M. kansasii* were incubated with 7H9 media at 37°C for 6 days, plus an additional 1 day of incubation period after adding 12 µl of 20% Tween80 and 20 µl of Alamar blue dye. Viability was assessed by measuring fluorescence with the Victor3 (PerkinElmer).

Spectrum of activity

Staphylococcus aureus (ATCC29213), *Candida albicans* (ATCC90028), *Escherichia coli* (ATCC25922), *Mycobacterium smegmatis* MC²155, *Streptococcus pneumoniae* (ATCC49619), *Enterococcus faecalis* (ATCC29212), and *Pseudomonas aeruginosa* (ATCC27853) were purchased from ATCC, and the activity of coumarins 1 to 4 was tested against these organisms by broth micro dilution with a

spectrophotometric readout at 570 nm (*S. pneumonia* at 490 nm) as described by the National Committee on Clinical Laboratory Standards.⁷⁸ The activity against *M. smegmatis* was determined by MABA, incubating 3 days at 37°C, plus an additional 4 hours of incubation period after adding 12 µl of 20% Tween80 and 20 µl of Alamar Blue dye. Viability was assessed by the measurement of fluorescence with the Victor 3

Chapter 4

Aim 3: Searching for a new TB drug lead from a fungal extract library

4 Aim 3: Searching for a new TB drug lead from a fungal extract library

4.1 Aim 3a: High throughput screening of 12,905 fungal extracts library for anti-TB activity

4.1.1 Background / scope of this study

Within the past few decades, technology and tools for drug discovery have improved dramatically. Molecular, cellular, and genomic techniques now allow identification of new molecular targets and purification of target proteins that can be assessed in high throughput screening.⁷⁹ HTS technology includes an automated screening with modern robotic instruments that enables the testing of hundreds of thousands of compounds with minimized labor and cost.⁸⁰ HTS has recently been applied to TB drug discovery as well. The Molecular Libraries Screening Center Network (MLSCN) and Penn Center for Molecular Discovery (PCMD) performed target-based HTS with 201,368 compounds to search for a new cell wall inhibitor of *M. tuberculosis*.⁸¹ As a result, triazinoindol-benzimidazolones were identified as inhibitors of the *M. tuberculosis* enzyme, RmlC (TDP-6-deoxy-D-xylo-4-hexopyranosid-4-ulose3,5-epimerase). In addition, the Tuberculosis Antimicrobial Acquisition and Coordinating Facility (TAACF) along with the MLSCN assessed 100,997 chemicals purchased from ChemBridge Corporation and 215,110 chemicals from the NIH small molecule repository (SMR) with whole-cell-based HTS.⁸² This study revealed specific classes of compounds with potential as leads for new TB drug development. Also, new classes of *M. tuberculosis* alanine racemase inhibitors were identified by target-based HTS of 53,000 compounds at the National Screening Laboratory for Regional Centers of Excellence for Biodefense and Emerging Diseases Research (NSRB) at Harvard Medical School.⁸³ A peptide, fellutamide B18,⁸⁴ was discovered by HTS to be the most potent inhibitor of *the M. tuberculosis* proteasome from the Analyticon Discovery GmbH bacterial and plant-derived natural compound library. In short, global HTS has been an important tool for TB drug discovery during the last decade.

To date, HTS in TB drug discovery has been predominantly directed toward molecular targets (vs. whole cells) and has employed chemical compound libraries (vs. screening of extracts/compounds from natural sources). Creating a sizeable synthetic chemical library is much less technically challenging than doing so with natural products although the chemical diversity of the former is limited.^{33, 79} Consequently, there are no reports in the last 10 years of HTS of a large-scale natural product library against *M. tuberculosis*.

While target-based HTS aims to identify active principles that work directly on a given target, whole-cell-based HTS cannot distinguish the mode of action of an active principle without extensive follow-up research. Isolation and identification of pure compounds from natural products present additional obstacles. However, historically, the majority of the natural product-based drugs including cyclosporin, paclitaxel, and camptothecin derivatives were first discovered by traditional cell-based in vitro assays before their molecular biological targets were identified.⁸⁵

Statistics prove that natural products have always been a valuable source for pharmaceuticals.^{31-32, 86} Of all anti-infective drugs which can be classified as new chemical entities (NCEs), 60% are natural products or derived from them.^{31b} Most current antibiotics were discovered from fungi or soil bacteria, and these micro-organisms may still represent the best source for discovering new antibiotics.^{31a, 31c} In addition, the two most potent first-line anti-TB drugs, rifampin (RMP) and isoniazid (INH), came from or were inspired by natural products.

Since the Global Alliance for TB Drug Development was established in 2000, efforts for finding new TB drugs have increased, and 13 investigational new drugs are currently undergoing clinical evaluation. These include three NCEs (TMC207, Sudoterb, and SQ109), a re-evaluation of rifamycins (high dose rifampin and rifapentine), fluoroquinolones (gatifloxacin and moxifloxacin), nitroimidazole analogs (OPC-67683 and PA-824), and oxazolidinones (linezolid, PNU100480, and AZD5847).^{24a} TMC207 (HTS of

synthetic chemical library) and SQ109 (HTS of a combinatorial library of ethambutol pharmacophore) are especially successful examples identified from phenotypic whole-cell-based HTS screening.

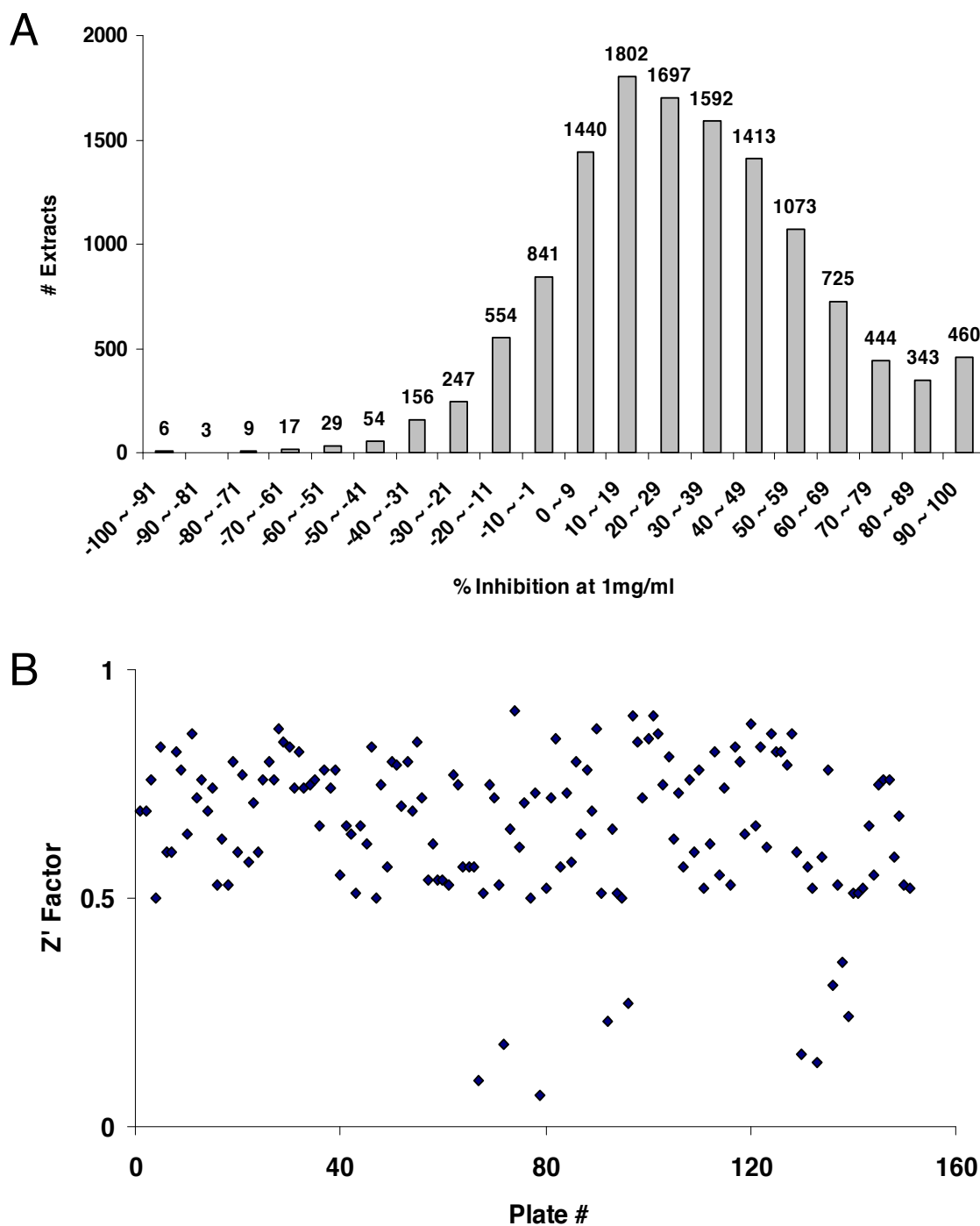
During the golden antibiotic discovery era (1940s-1960s), screening soil bacteria and fungi for antibiotic activity by pharmaceutical companies resulted in the discovery of many antibiotics, including beta-lactams, tetracyclines, aminoglycosides, macrolides, chloramphenicol, vancomycin, and rifamycins. However, *M. tuberculosis* was not in the primary target screening panel. Considering that *M. tuberculosis* has a drug susceptibility profile that is unique relative to Gram-positive and negative bacteria, it is likely that many TB-specific compounds were missed. Therefore, it is prudent to now reexamine soil microorganisms with modern HTS for TB drug discovery.

In this study, 12,905 fungal extracts were screened for anti-TB activity by whole-cell based phenotypic HTS and biologically characterized.

4.1.2 Results

Primary screening

The percentage of *In vitro* growth inhibition of the 12,905 fungal extracts against *M. tuberculosis* resulted in a normal distribution (Figure 17A). To validate the quality of the HTS results, the Z' factor calculation was used. Bacteria-only and media-only controls from 151 96-well plates yielded an average Z' factor of 0.7, which indicates an excellent assay (Figure 17B). Extracts with $\geq 90\%$ inhibition were classified as hits. A total of 460 (3.6%) extracts out of 12,905 effected $\geq 90\%$ inhibition at 1.0 mg/ml.



MIC and selectivity of hits

MICs of the 460 extracts ranged from 19 $\mu\text{g/ml}$ to 1.0 mg/ml. Toxicity against Vero cells at 1.0 mg/ml was determined to assess relative selectivity (Figure 18A). To determine a reasonable number of extract candidates for further prioritization and assessment, MIC and cytotoxicity cutoffs were set at $<300 \mu\text{g/ml}$ and $<30\%$ inhibition at 1 mg/ml respectively, and 52 extracts meeting these criteria were selected for further biological evaluation.

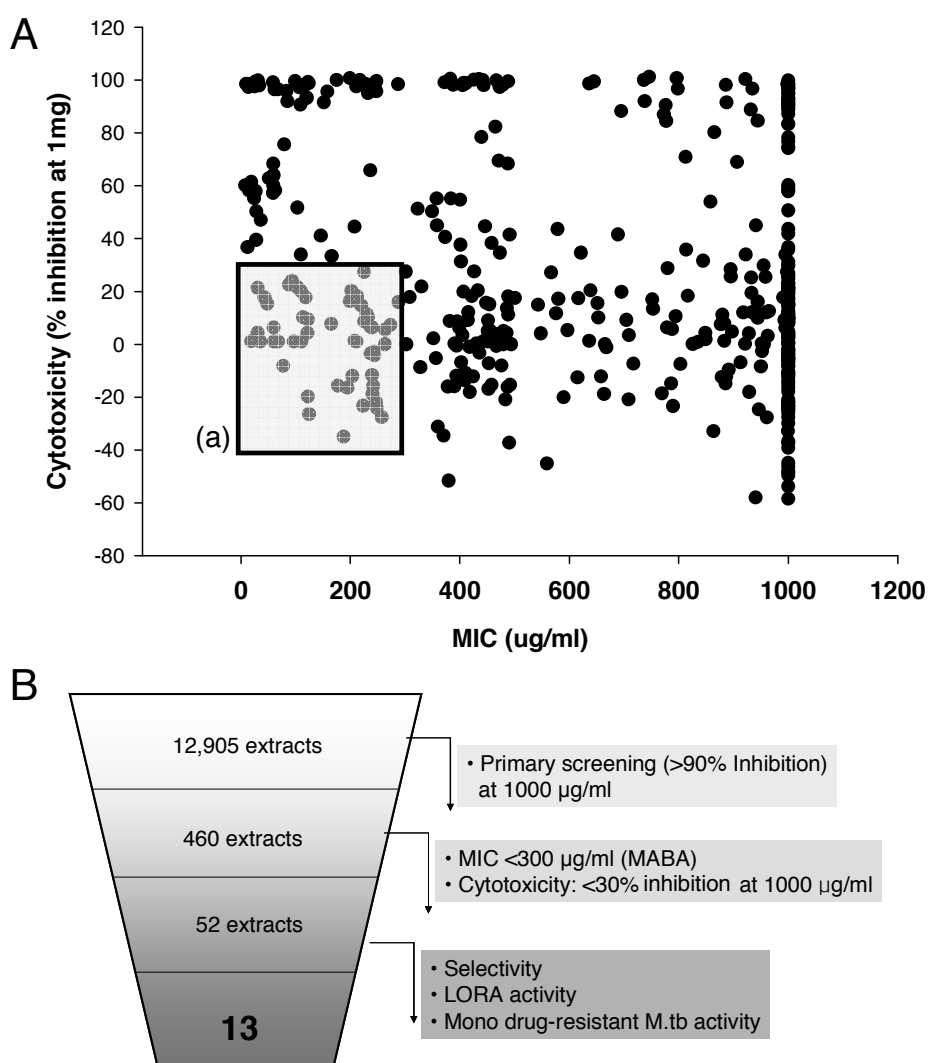


Figure 18. **A** MIC and cytotoxicity distribution of 460 extracts. **(a)** Represents 52 selected fungal extracts with MIC $<300 \mu\text{g/ml}$ and $\text{IC}_{50} <30\%$ inhibition at 1000 $\mu\text{g/ml}$. **B** Summary of high throughput screening result. Finally, 13 extracts were selected from 12,905 fungal extracts.

MIC against mono drug-resistant *M. tuberculosis* and non-replicating cultures

To aid in the prioritization of fungal extracts for further bioassay-guided fractionation, MICs against mono-drug resistant isolates and activity against non-replicating *M. tuberculosis* were determined. The latter utilized the LORA and may identify compounds that have the potential for shortening the duration of therapy. DD003955F6, DD003955E6, DD003954F6, and DD003954E6 were active against both replicating and non-replicating *M. tuberculosis*. DD004008A8 was active against replicating *M. tuberculosis*, but displayed strong cross resistance with SM-resistant *M. tuberculosis*. This may indicate a mechanism of the action similar to that of SM, which inhibits protein synthesis by inhibiting the binding of formyl-methionyl-tRNA to the 30S subunit.

Prioritization of hits

Of the 52 prioritized fungal extracts, 13 with MICs against replicating *M. tuberculosis* of less than 100 µg/ml were selected and classified into three groups according to selectivity and activity against non-replicating *M. tuberculosis* and mono drug-resistant *M. tuberculosis* (Table 9). Group A (7 extracts) showed the highest activity and selectivity against both replicating and non-replicating TB, as well as no cross resistance against drug resistant TB isolates. Despite its relatively poor LORA activity, DD004008B9 was still included in group A due to strong activities against mono drug-resistant *M. tuberculosis* isolates. The five extracts in Group B also showed good activity and selectivity against replicating TB, but relatively weak activity against non-replicating TB. Finally, DD004008A8 was assigned to group C due to its strong cross-resistance to SM-resistant *M. tuberculosis*.

TABLE IX. ANTI-TB ACTIVITY AND MAMMALIAN CYTOTOXICITY FOR 13 PRIORITIZED EXTRACTS.

Priority	Fungal ID	MIC (ug/ml)						Vero cytotoxicity
		MABA	LORA	rRMP	rINH	rSM	rKM	% inhibition at 1.0 mg/ml
A	DD004009B9	19	498	18	52	16	18	1
A	DD003955F6	31	64	27	77	249	51	4
A	DD003954F6	60	107	58	155	N/A	N/A	6
A	DD003954E6	78	52	62	222	60	61	-8
A	DD003955E6	43	107	30	84	36	30	18
A	DD004003B9	49	481	29	58	27	25	15
A	DD004008B9	55	>1000	1	3	2	2	18
B	DD004009B8	36	>1000	31	73	60	31	22
B	DD004002B7	88	>1000	59	189	59	59	23
B	DD004003B8	99	>1000	61	149	104	56	15
B	DD004009D5	60	>1000	36	108	31	31	1
B	DD004002B9	68	>1000	59	128	62	58	1
C	DD004008A8	93	>1000	57	124	>1000	694	1

4.1.3 Discussion

HTS with 12,905 fungal extracts has identified several extracts which possibly harbor novel anti-TB lead compounds. Of the 460 extracts effecting a reduction of $\geq 90\%$ in the primary screening (Figure 17), this level of inhibition was confirmed in 320 of the extracts when performing subsequent MIC determinations, yielding a confirmation rate of 70%. If the re-test inhibition cutoff was set instead at $\geq 80\%$ at 1.0 mg/ml, then 94% of the extracts would have confirmed, which is considered good for HTS. The $\geq 90\%$ inhibition hit rate in this study was 3.6%, which obviously is impacted by the selected extract concentration, assay type (cellular), percent inhibition threshold, and library type. Subsequent determination of MIC reveals approximate hit rates of 1.6, 0.6, and 0.4% had the primary screen been conducted at 500 $\mu\text{g/ml}$, 200 $\mu\text{g/ml}$, or 100 $\mu\text{g/ml}$, respectively. Because the extracts contain compounds from both the mycelium and culture medium, we opted to conduct primary screening at relatively high concentration in order to detect activity of relatively minor constituents. The resulting number of hits were manageable, therefore, in retrospect the primary screening concentration appears to be appropriate for a whole cell-based screen of this size. In comparison, hit rates of 1.2%⁸¹ and 0.9%⁸³ were recently reported for *M. tuberculosis* target-based HTS and 1.8%⁸² for whole-cell-

based HTS.

Selective toxicity, which is often assessed only in fractions or compounds from bioassay-guided isolation schemes, was assessed as early as possible in this HTS (by screening against a mammalian cell line) because in our experience failure to consider selectivity in mixtures most often leads to isolation of non-selective compounds. However using this criterion when evaluating mixtures does run the risk of de-prioritizing extracts in which different compounds are responsible for the anti-TB and cytotoxic activities. Of the hits, 83, 132, and 163 extracts showed ≥ 90 , ≥ 50 , and $\geq 30\%$ inhibition in Vero cell toxicity, respectively. Based on the selectivity of 460 extracts, anti-TB MICs of $< 500 \mu\text{g/ml}$ with $< 50\%$ inhibition of Vero cells at 1 mg/ml , MICs of $< 300 \mu\text{g/ml}$ with $< 50\%$ inhibition of Vero cells at 1 mg/ml , and MICs of $< 300 \mu\text{g/ml}$ with $< 30\%$ inhibition of Vero cells at 1 mg/ml selected 71, 60, and 52, extracts respectively.

From the latter, 10 extracts were found to have MICs of $< 100 \text{ ug/ml}$ against replicating *M. tuberculosis*, and of these 6 also were active against non-replicating *M. tuberculosis*. Overall, 28 of 52 extracts did not display any detectable activity against non-replicating *M. tuberculosis*. At this stage of evaluation, DD003955F6 and DD003954E6 are the most promising extracts with strong anti-TB activity against both replicating and non-replicating *M. tuberculosis* as well as against four mono-drug resistant *M. tuberculosis* isolates (Table 9).

Kanamycin and streptomycin, aminoglycoside antibiotics, are involved in the inhibition of protein synthesis. There was a similar response of the SM and KM-resistant isolates to most of the 52 extracts ($R^2 = 0.93$) in terms of MIC whereas activity against these strains varied significantly in comparison with H₃₇Rv ($R^2 = 0.09$ and 0.08 , respectively). DD004008A8 was unique in demonstrating activity against the KM-resistant but not the SM-resistant isolate. The 13 fungal isolates prioritized from this study can subsequently be scaled up, and bio-assay-guided fractionation can be performed according to the

priority order for the isolation and structural elucidation of anti-TB compounds.

According to the Stop-TB Working Group on New TB Drugs (www.newtbdrugs.org), pharmaceutical companies, such as AstraZeneca, GlaxoSmithKline, and the Lilly TB drug discovery initiative, recently added whole-cell based phenotypic screening to their HTS campaigns where target-based HTS was previously the dominant modality. Although natural products are generally considered superior with respect to diversity, flexibility, complexity, and specificity to biological target, it is not clear at this time if there is the willingness to include extract libraries in such HTS campaigns since these would require subsequent bioassay-guided isolation of active principles. The results presented here suggest that the inclusion of even a modest microbial extract library within a larger HTS campaign is likely to yield a manageable number of hits with biological profiles worthy of the effort required for bioassay-guided isolation.

4.1.4 Materials and methods

Fungal isolation

Fungi for this project were from the Mycosynthetix collection and the organisms used for this project were isolated from various sites within the continental United States. Plant material from a variety of ecosystems were subjected to their standard fungus isolation protocol. All isolates are maintained in the Mycosynthetix culture collection on slants of malt agar medium (agar 1.8%, malt 1%), and corresponding relevant information is stored in the Mycosynthetix database.

Fungal culture

Fungi were grown in a liquid medium (YESD) containing dextrose (2%), soy peptone (2%) yeast extract (1%). After 7 days incubation at 23 °C with agitation, the mycelia were inoculated into six-well plates

containing, each well containing one of following: potato dextrose agar (PDA); dilute soy agar(DSA); agar 1.8%, mannitol 0.5%, soy grits (0.2%); dextrose-yeast extract agar (DYA) agar (1.8%), glucose (1%), yeast extract (0.1%), casein (0.2%); Czapek agar (CZA) Czapek agar Fisher brand 233910; (Mycological low pH agar, LPHA) Fisher brand DF0305173; Oatmeal agar (OMA) oatmeal agar, Fisher brand. Plates were incubated at 23 °C for 11 days and then frozen at -80 °C.

Fungal extracts

The plates containing the frozen cultures were lyophilized overnight. A custom robotics system was used to add methanol to freeze dried cultures and to dispense extracts into 96 well plates. Plates were bar coded to facilitate tracking and minimize errors. Methanol (10 ml) was placed into each well containing the freeze dried culture and left to soak overnight. The following day the methanol was removed and aliquots placed into 96-well plates and dried. Typically between 25-100 mg of extract was isolated from a 10 ml culture, depending on both the organism and the medium used for growth.

Primary screening

Screening of primary extracts at 1.0 mg/ml was assessed in terms of percent inhibition. For primary screening, the extracts were prepared in 96-well plate format in 1.0 mg/ml concentration with a final volume of 200 µl bacterial culture in Middlebrook 7H12 broth. Extracts effecting greater than 90% inhibition were subsequently tested to determine for minimum inhibitory concentration (MIC) at 2-fold serial dilutions using the MABA.

Statistics

The Z' factor calculation, $3(\text{standard deviations of positive control} + \text{standard deviations of negative control}) / (\text{mean of positive control} - \text{mean of negative control})$, was used for quality assessment of

assay conditions. The value $Z' = 1$, $1 > Z \geq 0.5$, and $0.5 > Z > 0$ indicate ideal, excellent, and marginal assays, respectively while $Z \leq 0$ means that screening is essentially impossible.

The methods below were described in materials and methods, Chapter 3

Bacterial strain preparation for screening (page 48)

Minimum inhibitory concentration (page 48)

Low Oxygen Recovery Assay (LORA) (page 49)

MIC against drug-resistant isolates (page 49)

Cytotoxicity (page 49)

4.2 Aim 3b: Isolation, identification, and biological evaluation of an anti-TB active tetramic acid derivative

4.2.1 Background / scope of this study

The fungal culture MSX105528 was selected from 13 selected fungal extracts based on the relative activity and selectivity (Aim 3a). Using a bioassay-guided procedure, the anti-TB active tetramic acid derivative was isolated and characterized, indicating one of possible stereoisomers of vermispurin a previously known natural product with a tetramic acid skeleton and isolated from the fungi *Ophiobolus vermispuris*,⁸⁷ *Phoma*, and *Alternaria* species.⁸⁸ The previous study⁸⁷ stated biological activities of vermispurin against gram-positive bacteria and anaerobic bacteria. However, to our knowledge, activity data against *Mycobacterium* species have not been reported to date. In addition, none of the literature reported a comprehensive chemical characterization for vermispurin as well as any of vermispurin stereoisomers. In this study, an extensive chemical and biological assessment was performed to elaborate on the new finding of a stereoisomer of vermispurin, named here as vermitrasporin, having significant anti-TB activity.

4.2.2 Results

Fermentation

MSX105528 was cultured on six different media (Czapek-Dox agar, low pH agar, oatmeal agar, potato dextrose agar, diluted soy agar, and dextrose yeast extract agar), and the anti-TB activity of the MeOH extracts was confirmed. The potato dextrose agar medium produced the most potent extract with an MIC of 48 µg/ml. Further optimization of anti-TB activity for MSX105528 was conducted by applying different fermentation temperatures (4, 25, and 37°C) and times (5, 10, 15, and 22 days), as shown in Table 10. Overall, culturing MSX105528 on potato dextrose agar media at room temperature (25 °C) for 3 weeks (22 days) yielded the most potent anti-TB activity with an MIC of 11 µg/ml.

TABLE X. ACTIVITY OPTIMIZATION FOR VARIOUS CULTURING CONDITIONS OF MSX105528 against *MYCOBACTERIUM TUBERCULOSIS* H₃₇Rv.

MSX105528	MIC (µg/ml)	
Agar media, 14 days fermentation	Czapek-Dox	>100
	Low pH (pH 2.5)	94
	Oatmeal	93
	Potato dextrose	48
	Diluted soy	>100
	Dextrose yeast extract	85
Different temperatures, 14 days fermentation, potato dextrose agar	4 °C	>260
	25 °C	63
	37 °C	>280
Different fermentation durations, potato dextrose agar at 25 °C	5 days	>228
	10 days	196
	15 days	12
	22 days	11

Bioassay-guided fractionation and isolation

In order to isolate the anti-TB active principle, a bioassay-guided fractionation (BGF) protocol was conducted using a combination of solid phase extraction (SPE) and high pressure liquid chromatography (HPLC) for fractionation. The bioactivity was monitored with the microplate Alamar blue assay (MABA) (see Figure 19).

The freeze dried MSX105528 culture (500 mg) was extracted with MeOH and separated by C18 SPE, resulting in 6 primary fractions by elution with 20, 40, 60, 80, 100% MeOH, and 100% CHCl₃ (300, 58.5, 0.5, 69.6, 26.0, and 3.0 mg, respectively). MABA MICs were determined by MABA as 60.5, 182.9, 30.1, 47.1, 0.9, and 188.8 µg/ml, respectively, (Figure 19). Normal phase thin layer chromatography (NP-TLC) with CHCl₃:MeOH (95:5, v/v) and staining with vanillin sulfuric acid reagent visualized anti-TB active primary fractions, displaying orange colored spots ($R_f = 0.3$) which might represent the active ingredient in the 100% MeOH fraction. Therefore, 26 mg of the 100% MeOH fraction was fractionated by RP-HPLC. The UV 290 nm chromatogram presented one major peak at 50.8 min (t_R), flanked by a

few minor peaks, which were collected into three sub-fractions, leading to the conclusion that the major peak collected in fr5-3 (6.0 mg), was the active component with a MIC of 0.74 $\mu\text{g/ml}$ against *M. tuberculosis*.

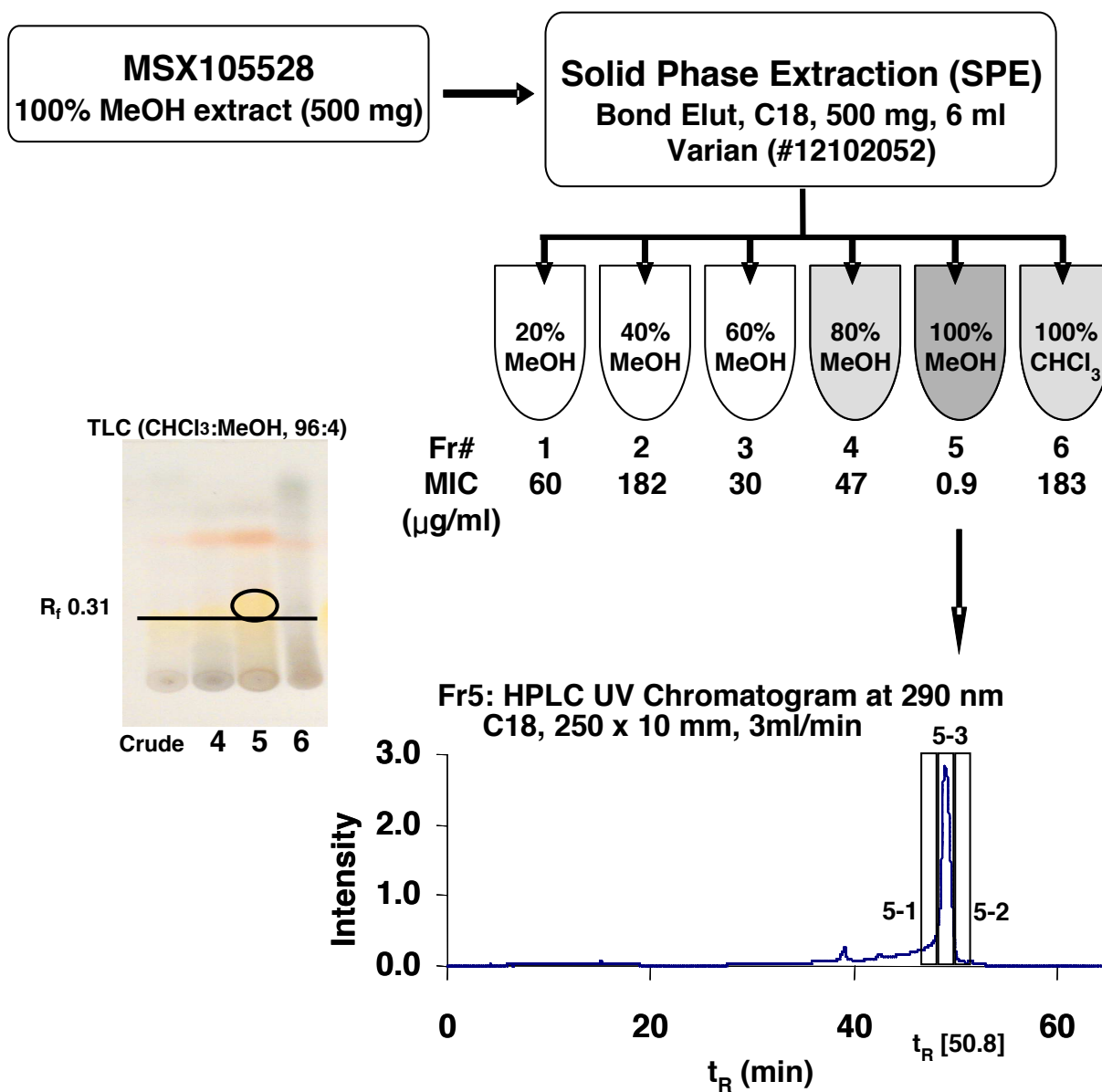


Figure 19. Bio-activity guided isolation protocol of the anti-TB active vermitrasporin from MSX10528. MICs for MSX10528 extract and the primary SPE fractions against *M. tuberculosis* H₃₇Rv.

Structure elucidation of vermitrasporin

Fraction 5-3 was subject to comprehensive structural analysis as follows. The molecular formula was deduced by HRESIMS measurement along with the ^{13}C and the broad-band decoupled DEPTQ-135 ^{13}C NMR spectra, indicating $\text{C}_{25}\text{H}_{37}\text{NO}_4$ at m/z 415.5743 $[\text{M}+\text{H}]^+$; calculated 415.5723. The ^{13}C DEPTQ NMR ($\text{MeOH}-d_4$) spectrum at 225 MHz NMR confirmed the presence of seven methyl (δ 13.0, 14.1, 17.5, 19.1, 22.7, 23.0, and 28.2 ppm), two methylene (δ 39.6 and 40.0 ppm), eleven methine (δ 31.2, 35.0, 39.7, 39.9, 41.8, 43.9, 54.5, 61.4, 71.5, 126.9, and 135.3 ppm), and five quaternary carbons (δ 67.3, 105.4, 176.7, 196.1, and 200.1 ppm), including three carbonyl carbons (δ 176.7, 196.1, and 200.1 ppm). The ^1H NMR spectrum showed signals of 36 protons, three of which were assigned to an NCH_3 group corresponding to a singlet at δ_{H} 2.872 (δ_{C} 28.2 ppm). The infrared spectrum showed absorption bands for hydroxyl (3378 cm^{-1}) and amide (1673 cm^{-1}) groups. Because the ^1H NMR in $\text{MeOH}-d_4$ detected only 36 of the 37 hydrogens, there must be one exchangeable proton. Therefore, the 17 amu difference to $\text{C}_{25}\text{H}_{36}\text{NO}_3$ was assigned to a free OH-group. The HSQC, HMBC, and COSY spectra established relationships between proton and carbon atoms and indicated the presence of a tetramic acid with decalin moiety, as shown in Figure 20A.

Due to significant signal overlap, correlations within the A ring were obscured in both the 1D and 2D spectra. This part of the structure could only be assigned with the help of ^1H selective 1D TOCSY spectra: exciting the resonances at δ 2.168, 1.677, and 1.468 ppm (Figure 20D) resolved H-5 $_{\alpha}$ (δ 1.297) and H-5 $_{\beta}$ (δ 1.213) (see Figure 20D1), as well as two methyls, C-14 and C-15 at δ 23.1 (doublet) and δ 22.7 (doublet) ppm, respectively. Long-range couplings in the HMBC spectrum from the methyl protons H-6' (δ 1.036, d) and H-7' (δ 1.005, d) to methine carbon C-5' (δ 31.2) and C-4' (δ 71.5) established the *iso*-propyl moiety. In addition, long-range couplings from the methyl proton H-17 (δ 1.275, d) to the quaternary carbon C-12 (δ 67.3), and from the methyl proton H-16 (δ 1.239, s) to the methine carbon C-11 (δ 54.5) established the 2,3-dimethyl oxirane moiety. In summary, the 1D/2D NMR and HRMS data were compatible with the structure of vermisporin, CAS:122301-98-9. However, the dereplication of this compound was complex.

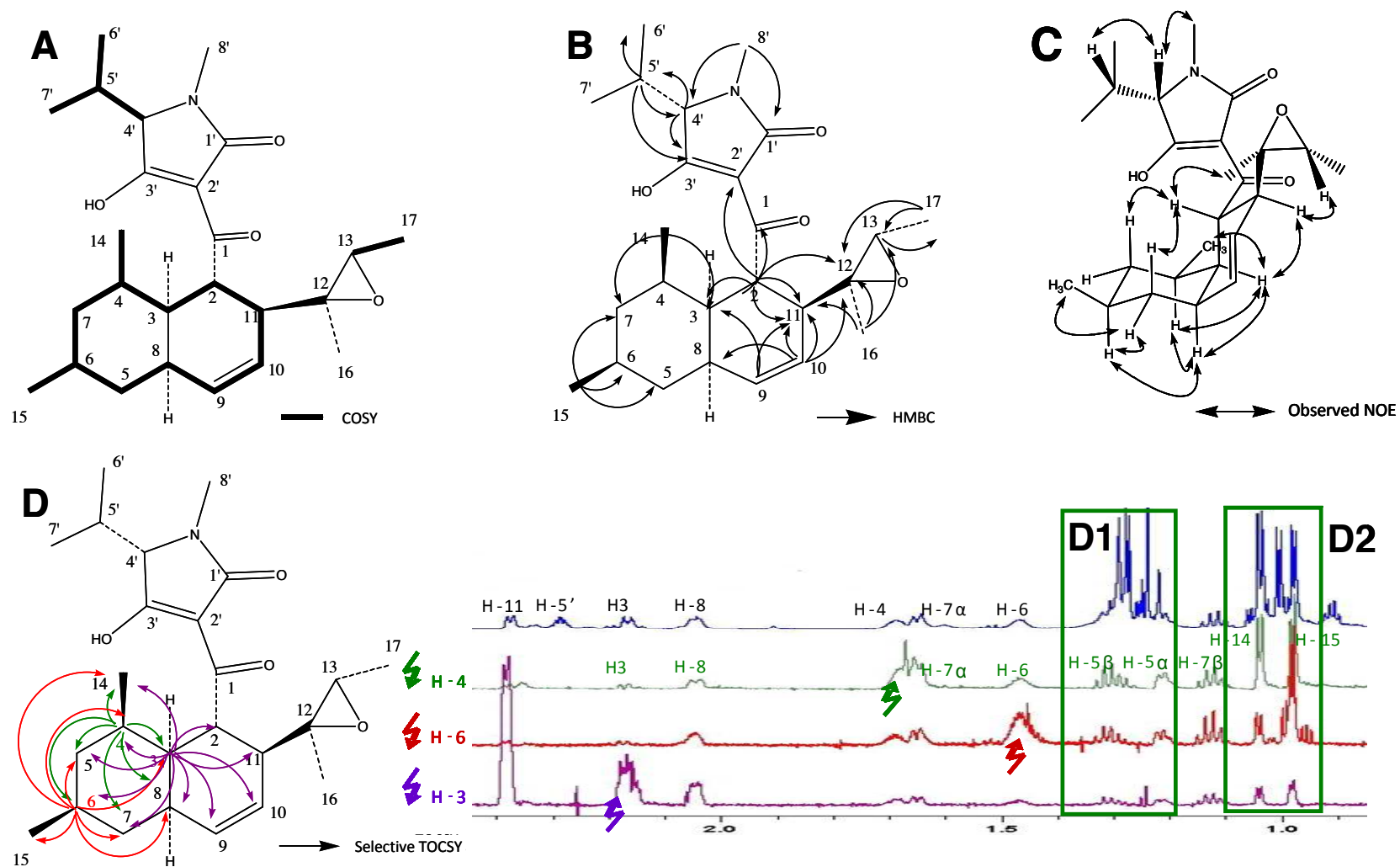


Figure 20. Key results of the structure elucidation of the isolate and dereplication for vermitrasporin, one of stereoisomers of vermispurin. Observed COSY (**A**), HMBC (**B**), and NOE (**C**) correlations. **D** shows the result of selective TOCSY experiments ($T_{\text{mix}} = 90$ ms, 900 MHz, 3 mm tube, 0.5 mg in 200 μl MeoH- d_4) upon selective excitation at δ 2.168 (H-3), δ 1.677 (H-4), and δ 1.468 (H-6) ppm. This revealed H-5 α and 5 β , H-7 β , H-14, and H-15 (as shown in D1 and D2).

Previously, Minowa *et al.*⁸⁸ deduced the absolute configuration of the decalin ring of vermispurin by X-ray crystallography of the degradation products of vermispurin. Later, Koyama *et al.*⁸⁹ reported isolation of vermispurin along with analogs, spylidone and PF1052, but no structural dereplication information of vermispurin was available. In the present study, the *cis*-ring fusion of the decalin moiety was determined from the magnitude of the scalar coupling between the bridge hid protons, H-3 and H-8, as $J_{H3eq-H8ax} = 3.7$ Hz. This was confirmed by a ROESY experiment (600 MHz, MeOH- d_4 and DMSO- d_6 , $T_{mix} = 200$ msec), as shown in Figure 20C. The presence of a strongly coupled doublet of a doublets ($J = 10.09$ and 11.25 Hz) showed the *trans*-diaxial arrangement of H-3 and H11, which corroborated the equatorial oriented atom of the oxirane moiety attached to C-11. The NOEs among H-2, H-7 β , and H-5 β as well as H-4, H-6, H-8, and 7 α also supported the relative configuration of the decalin, as depicted in Figure 20C.

In order to provide further support for the relative configuration, a full spin analysis of the 900 MHz 1H NMR spectrum was carried out using the PERCH iteration software. This resulted in the full assignment of all 1H resonances including their multiplicities. The methodology of full 1H NMR spin analysis has been previously documented and was adopted accordingly.^{66a, 71} The result is summarized in Table 11 and Figure 21. The overall deviation between the simulated and the experimental spectrum was represented by total Root Mean Square value (total RMS = 0.21%), which indicated an excellent simulation.

TABLE XI. NMR SPECTROSCOPIC DATA FOR VERMITRASPORIN (900/225 MHz, MeOH-*d*₄) INCLUDING FULL ¹H NMR SPIN PARAMETERS FROM A FULL SPIN ANALYSIS.

position	vermitrasporin						
	δ_C	mult	δ_H	mult	<i>J</i> in Hz	COSY	HMBC (H→B)
1	200.1	C	-	-			
2	39.9	CH	4.611	dd	(11.25, 10.09)	H-11, H-3	C-1, C-2', C-3, C-11, C-12
3	43.9	CH	2.166	dddd	(11.25, 3.72, 3.48, 0.95, 0.51)	H-2, H-8, H-4	
4	39.7	CH	1.689	dddq	(12.63, 6.99, 0.94, 3.48)	H-14, H-7, H-3	
5	40.0	CH ₂	1.297	dddd	(-11.32, 4.59, 3.78, 0.94, 0.95)		
			1.213	ddd	(-11.32, 9.99, 12.63)		
6	35.0	CH	1.469	dddd	(4.59, 9.99, 11.56, 3.76, 6.56)	H-7, H-5, H-15	
			1.649	ddd	(3.76, -13.23, 1.25, 0.51)		
7	39.6	CH ₂	1.120	ddd	(11.56, -13.23, 12.32)		
8	41.7	CH	2.046	dddd	(12.32, 1.25, 3.72, -1.14, 5.46)	H-3, H-5, H-9	
9	135.3	CH	5.811	ddd	(5.46, -2.88, 9.95)	H-8, H-10	C-3, C-11, C-10
10	126.9	CH	5.357	ddd	(-1.15, 1.95, 9.95)	H-9, H-11	C-8, C-9, C-11, C-12
11	54.5	CH	2.375	ddd	(10.09, 1.95, -2.88)	H-2, H-10	C-10, C-12, C-16
12	67.3	C	-	-			
13	61.4	CH	2.913	q	(5.79)	H-17	C-17
14	23.1	CH ₃	1.039	d	(6.99)	H-4	C-3, C-5
15	22.7	CH ₃	0.978	d	(6.55)	H-6	C-6, C-5, C-7
16	13.0	CH ₃	1.239	s			C-11, C-12, C-13
17	14.1	CH ₃	1.275	d	(5.79)	H-13	C-12, C-13
1'	176.6	C	-	-			
2'	105.4	C	-	-			
3'	196.1	C	-	-			
4'	71.5	CH	3.459	d	(2.70)	H-5'	C-1', C-3', C-5'
5'	31.2	CH	2.285	dqq	(2.70, 7.66, 7.15)	H-4', H-6', H-7'	C-3', C-4', C-6'
6'	17.6	CH ₃	1.036	d	(7.66)	H-5'	C-4'
7'	19.1	CH ₃	1.005	d	(7.15)	H-5'	C-4'
8'	28.2	CH ₃	2.872	s			C-1', C-4'

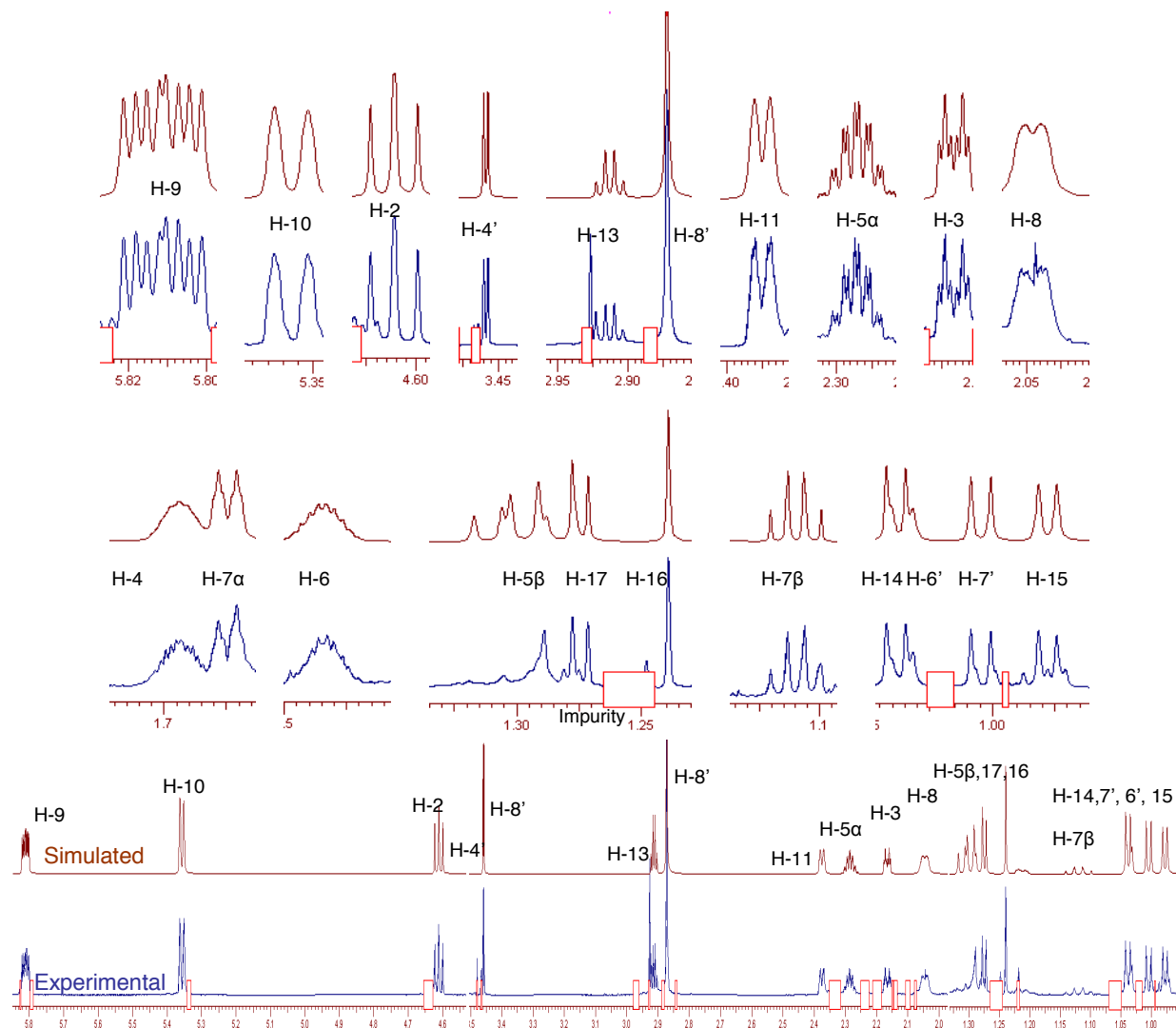


Figure 21. Full ^1H NMR spin analysis by PERCH iteration of the 900 MHz spectrum of vermitrasporin using the PERCH iterator (simulated spectra in red: experimental spectra in blue). The total RMS = 0.21% (excellent) for the full spectrum iteration. Impurities, which were covered by the red square boxes (\square), were not accounted for iteration during the simulation.

Biological evaluation of vermitrasporin

The MIC of vermisporin against *M. tuberculosis* was determined using three different phenotypic assays: the microplate Alamar blue assay (MABA), the low oxygen recovery assay (LORA), and the TB bioluminescence assay (ATP), each in triplicate. MABA and ATP assess the activity against replicating *M. tuberculosis*, while LORA is designed to detect compounds that may have the potential for shortening the duration of therapy through efficient killing of the non-replicating persistor (NRP) population. In addition, the MBC of vermitrasporin was determined in triplicate against replicating *M. tuberculosis*. As shown in Table XII, the MIC of vermitrasporin was 0.74 (± 0.01) in the MABA, 0.56 (± 0.23) in the ATP, and 1.50 (± 0.37) $\mu\text{g/ml}$ in the LORA. The MBC of vermisporin was determined as 0.50 (± 0.13) $\mu\text{g/ml}$. To assess the anti-TB selectivity of vermitrasporin, general cytotoxicity was measured with Vero and J774A.1 cell lines. The observed IC_{50} values of 1.8 and 9.3 $\mu\text{g/ml}$, respectively, indicated a limited selectivity with selective indices value of 3.6 and 18.6, respectively.

MABA MICs against all five of mono drug resistant isolates were ≤ 1.0 $\mu\text{g/ml}$ (Table XII). The lack of cross resistance activity against mono drug-resistant *M. tuberculosis* isolates implies that the mode of action of vermitrasporin may be different from current anti-TB agents, especially isoniazid (INH), rifampin (RMP), streptomycin (SM), kanamycin (KM), and cycloserine (CS). Accordingly, the target of vermitrasporin might be exploited to target drug resistant TB.

To understand the spectrum of activity of vermitrasporin, MICs were determined against a mini panel of four microbial species, *S. aureus*, *E. coli*, *C. albicans*, and *M. smegmatis* were determined (Table XII).

TABLE XII. BIOLOGICAL PROFILE OF VERMITRASPORIN.

		vermitrasporin	RMP ^a	INH ^a	SM ^a	KAN ^a	CS ^a	AMP ^b	GEN ^c	KETO ^d	AMPH ^e
Anti-TB activity/cytotoxicity											
MIC (µg/ml)	MABA	0.74	0.05	0.06	0.12	0.65	-	-	-	-	-
	ATP	0.56	0.05	0.05	-	-	-	-	-	-	-
	LORA	1.50	0.35	>70.2	-	-	-	-	-	-	-
	MBC (µg/ml)	0.50	0.05	0.03	-	-	-	-	-	-	-
IC50 (µg/ml)	Vero	1.80	65.7	-	-	-	-	-	-	-	-
	J774A.1	9.30	53.1	-	-	-	-	-	-	-	-
Mono drug-resistant <i>M. tuberculosis</i> activity											
MIC (µg/ml)	rINH ^a	0.68	0.01	>1.10	0.28	-	-	-	-	-	-
	rRMP ^a	0.73	>0.82	0.06	0.42	-	-	-	-	-	-
	rSM ^a	0.71	0.02	0.03	>4.65	-	-	-	-	-	-
	rKM ^a	<0.39	0.02	0.77	1.82	>24.2	-	-	-	-	-
	rCS ^a	<0.39	0.01	0.06	0.52	-	>10.2	-	-	-	-
Spectrum of activity											
MIC (µg/ml)	<i>S. aureus</i>	1.80	-	-	-	-	-	0.29	0.31	-	-
	<i>E. coli</i>	11.9	-	-	-	-	-	2.28	1.12	-	-
	<i>C. albicans</i>	2.90	-	-	-	-	-	-	-	0.03	0.02
	<i>M. smegmatis</i>	16.7	36.6	13.5	-	-	-	-	-	-	-

^a *M. tuberculosis* strains resistant to rifampin (rRMP), isoniazid (rINH), streptomycin (rSM), kanamycin (rKAN), cycloserine (rCS), ^bampicillin, ^cgentamicin, ^dketoconazole, ^eamphotericin B

4.2.3 Discussion

Vermitrasporin is one of possible stereoisomers of vermispurin, a known naturally occurring tetramic acid with a tenuazonic acid type skeleton and a decalin moiety. Tetramic acid containing natural products, such as tenuazonic acid, α/β -cyclopiazonic acid, erythrokyrine, and streptolydigin are structurally very diverse and exhibit remarkable activities against bacteria, viruses, cancer and fungi.⁸⁹ However, tetramic acids exist in the different tautomeric forms depending on physicochemical conditions, such as crystal state, solvent, or temperature. Therefore, it is important to consider tautomerization as a factor during the structural analysis, as shown Figure 22 A. In solution, vermispurin may exist as four different tautomers, such as external tautomers (a, b \leftrightarrow c, d; interconversion of *cis-trans*) and internal tautomers (a \leftrightarrow b, c \leftrightarrow d; interconversion of a hydroxyl proton along the intramolecular hydrogen bond).

Previous reports⁹⁰ concluded that internal tautomerization is too fast to determine major tautomers over the NMR time scale. On the other hand, external tautomerization could occur slowly enough so that predominant tautomers could be deduced by NMR spectroscopy due to an outstanding characteristic of resonances doubling by conformational and tautomeric interchange. For instance, Yamaguchi *et al.*^{90b} and Jones *et al.*⁹¹ have shown that naturally occurring and synthetic tetramic acid (e and f) exist mainly in the endo-enol form (Figure 22 A). However, Nolte *et al.*⁹² concluded that the synthesized form (e) exists mainly in the exo-enol form from their study. A recent study showed that the tautomeric equilibrium of a tetramic acid in solution is also strongly affected by the N-substitution and by the acyl group.⁹³

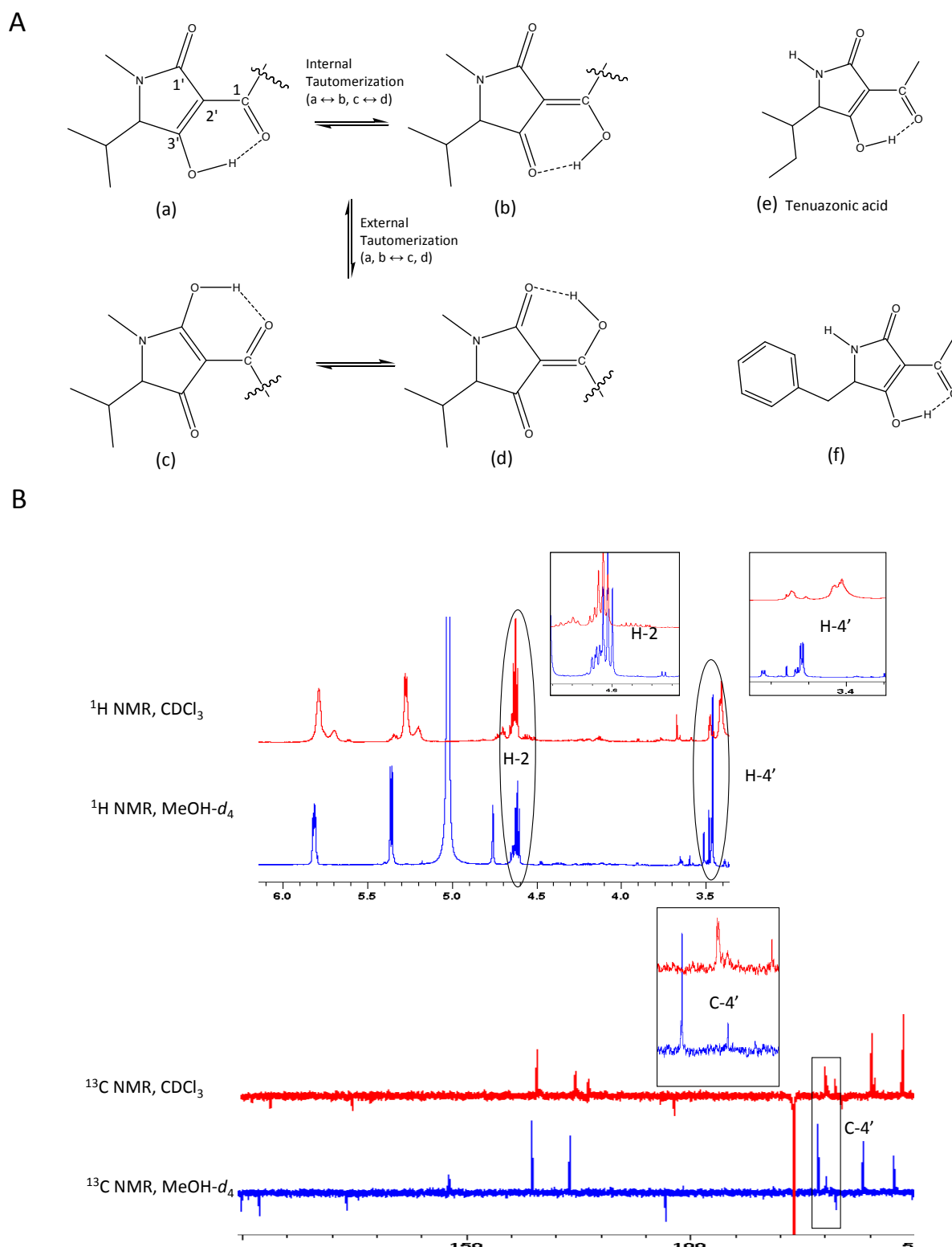


Figure 22. Investigation of the tautomerization of vermitrasporin. The four possible tautomers, a-d, of vermitrasporin and related tetramic acids (A). Observed the doubling of resonances at H-2 and H-4' as well as at C-4' due to possible tautomerization effect in the ^1H (900 MHz) and ^{13}C DEPTQ (225 MHz) NMR spectra of vermitrasporin (CDCl_3 and $\text{MeOH-}d_4$) (B).

The nature of tautomers is interchangeable with a very low energy barrier. The population of each will vary with different solution, temperature, substituent groups, and physiochemical state. As for vermitrasporin, we observed a possible doubling of resonance peaks in ^{13}C and ^1H NMR spectrum in both CDCl_3 and MeOH-d_4 at especially C-1, C-1', C-3', C-4', H-2, and H-4'. Their chemical shifts split into double or triple resonances due to possible tautomeric effect rather than impurities,^{92, 94} as shown Figure 22 B. Nolte *et al.* and Steyn *et al.* observed the doubling of the resonances in the ^1H and ^{13}C NMR spectrum for the tenuazoic acid on the external tautomerization due to the anisotropic effect of neighboring enolization or ketolization.^{92, 95}

In order to determine the possible predominant tautomer of vermitrasporin, the CSEARCH NMR database, developed by Wolfgang Robien of the University of Vienna, was utilized.⁹⁶ Based on over 193,000 ^{13}C NMR data, CSEARCH predicts ^{13}C NMR chemical shifts and calculates differences between predicted and observed ^{13}C chemical shift of a given structure. CSEARCH is also able to differentiate its predictions based on the stereochemistry in the molecule. The 4 possible tautomers of vermitrasporin were assessed with the CSEARCH prediction tool. Structure (a), the endo-enol form, gave the best match in the ^{13}C chemical shift. The ^{13}C NMR chemical shift differences between the predicted and experimental resonances of C-1, C-1', C-2', and C-3' was 0.6, 3.8, 2.3, and 0.7 ppm, respectively.

However, these data cannot explain if the observed differences result from tautomerization or other conformational changes in the molecule. In order to understand the tautomerization of vermitrasporin fully, further extensive studies such as X-ray crystallography, a relative energy calculation of each tautomer, and more elaborate NMR spectroscopy will have to be performed. In order to accomplish these assessments, significantly more material would be required, and this is currently outside the scope of this project.

In conclusion, the isolated anti-TB active principle, vermitrasporin, was shown to be one of possible stereoisomers of vermisporin. The relative configuration of vermitrasporin was unambiguously established, and the first comprehensive biological assessment was conducted with a focus on *M. tuberculosis* activity. *In vitro* biological data suggest that vermitrasporin has strong anti-TB activity against both replicating and non-replicating *M. tuberculosis*. It also displayed moderate cytotoxicity against Vero cells and J774A.1 and antimicrobial activity against *S. aureus*, *C. albicans*, and *E. coli* and *M. smegmatis*.

4.2.4 Materials and methods

General experimental procedure

UV-vis spectra were obtained with a SpectraMax Plus 384 (Molecular Devices) at 25 °C. Optical rotation $[\alpha]_D$ were measured on a Perkin-Elmer 242 polarimeter at 25 °C. Infrared spectra were obtained with a Thermo Nicolet 6700 FT-IR spectrometer. All NMR experiments were obtained at 600 or 900 MHz Bruker DRX-600 and Bruker AVANCE II-900 equipped with a cryogenic sensitivity-enhanced triple-resonance 5mm inverse TCI cryoprobe. The NMR sample was prepared in a 3 mm NMR tube with 99.96% CDCl₃ or 99.96% MeOH-d₄. All NMR experiments were performed using standard Bruker pulse sequences. The mixing time for the 1D selective TOCSY and 2D ROESY was set at 90 and 200 msec, respectively. High-resolution ESI mass spectra were obtained using a Shimadzu IT-TOF LC mass spectrometer. The ¹H NMR full spin analysis used PERCH NMR software (v.2010.1, PERCH Solutions Ltd., Kuopio, Finland). The ¹H NMR spectra were processed with NUTS software (Acorn NMR Inc.), imported into PERCH as JCAMP-DX file and subjected to baseline correction, peak picking, and integration. The ¹H spin parameters in MeOH-d₄ were predicted using the PERCH Molecular Modeling System (MMS). After a manual examination of the ¹H assignments, the calculated ¹H chemical shifts, signal line widths, and *J*-couplings were refined by using the integral-transform (D) mode and the total-line-fitting (T)

mode until an excellent agreement between the observed and simulated spectra was reached. The CSEARCH ^{13}C NMR database was utilized to obtain predicted ^{13}C NMR shifts in $\text{MeOH-}d_4$. The structure of vermispurin was input as MDL MOLfile and compared with the experimental ^{13}C chemical shifts from a 225 MHz NMR ($\text{MeOH-}d_4$).

Fungal culture and extraction

MSX105528 was grown in a liquid medium (YESD) containing dextrose (2%), soy peptone (2%) yeast extract (1%). After 7 days incubation at 23 °C with agitation, the mycelia were inoculated into six-well plates containing, each well containing one of following: potato dextrose agar (PDA); dilute soy agar(DSA); agar 1.8%, mannitol 0.5%, soy grits (0.2%); dextrose-yeast extract agar (DYA) agar (1.8%), glucose (1%), yeast extract (0.1%), casein (0.2%); Czapek agar (CZA) Czapek agar Fisher brand 233910; (Mycological low pH agar, LPHA) Fisher brand DF0305173; Oatmeal agar (OMA) oatmeal agar, Fisher brand. Plates were incubated at 23 °C for 11 days and then frozen at -80 °C.

The plates containing the frozen cultures were lyophilized overnight. A custom robotics system was used to add methanol to freeze dried cultures and to dispense extracts into 96 well plates. Plates were bar coded to facilitate tracking and minimize errors. Methanol (10 ml) was placed into each well containing the freeze dried culture and left to soak overnight. The following day the methanol was removed and aliquots placed into 96-well plates and dried. Typically between 25-100 mg of extract was isolated from a 10 ml culture, depending on both the organism and the medium used for growth.

Isolation of the active principle

A total of 500 mg of MSX 105528 MeOH extract was obtained from a 100 ml culture of PDA agar as described above. Solid Phase Extraction (Varian, Bond Elut, C18, 500 mg, 6ml) generated six primary

fractions, with a volume of 40 ml each (20, 40, 60, 80, 100% MeOH, and 100% CHCl₃). The most active fraction, F-5 (MIC 0.7 μg/ml, 13 mg), was further fractionated using reverse-phase HPLC on a Waters Delta 600 system with a Water 996 photodiode array detector using a semi-preparative column (Waters, C18, 5 μm, 250 x 10 mm, 3 mL/min). Five subsequent injections and use of a linear solvent gradient of MeOH/H₂O (80:20, v/v) to MeOH over 60 min afforded 6.0 mg of vermisporin (peak at 50.8 min). General fraction monitoring for chromatographic separation was done by TLC analysis with precoated Alugram SIL G/UV plates (Macherey-Nagel, Düren, Germany).

Vermisporin

Colorless oil: R_F 0.31 (CH₂Cl₂/MeOH 96:4); [α]_D²⁵ +98° (c 0.001, MeOH); UV/Vis (MeOH) λ_{max} (log ε) 258 (3.03), 264 (3.27), 290 (3.89), 298 nm (4.06); IR (neat) ν_{max} 3378, 2955, 2927, 2870, 1673, 1609 cm⁻¹; ¹H/DEPTQ ¹³C NMR (900/225 MHz, MeOH-d₄), COSY and HMBC (900 MHz, MeOH-d₄) NMR, see Table 10.

Minimum Bactericidal Concentration (MBC)

The MBC is defined here as the lowest concentration resulting in more than 90% killing of the bacteria. MBC was determined by subculture onto 7H11 agar from a MABA testing plate just prior to the addition of Alamar Blue and Tween 80 to the test wells.

TB bioluminescence assay (ATP)

The ATP Bioluminescence assay Kit HS II (Roche, Cat. No. 11 699 709 001) was used for determining MICs vs. *M. tuberculosis*. It uses the ATP dependency of the light emitting luciferase catalyzed oxidation of luciferin. The plate was prepared as previously described for MABA plate preparation. After 7 days incubation, 50 μl from each 96-well plate was transferred to a white 96-well plate

(NUNC™). Upon addition of 50 µl cell lysis reagent from the kit, the plate was incubated at room temperature for 5 min. Viability was assessed by measuring of the luminescence (Victor3) after automated injection of 50 µl luciferase reagent.

The methods below were described in materials and methods, Chapter 3

Bacterial strain preparation for the screening (page 48)

Minimum inhibitory concentration (MIC) (page 48)

Low Oxygen Recovery Assay (LORA) (page 49)

Cytotoxicity (page 49)

MIC against drug-resistant isolates (page 49)

Spectrum of activity (page 50)

Chapter 5

General summary of aims and conclusions

5 General summary of aims and conclusions

To discover anti-TB drug leads from diverse natural sources, the present study hypothesized that implementing ethnomedical knowledge for the treatment of TB and combining it with the high throughput screening of a fungal extract library may assist in the discovery of new anti-TB drug leads. In order to support this hypothesis, three specific aims were set.

Aim 1. Selection of useful ethnobotanicals for anti-TB drug discovery by using the NAPRALERT, an online based natural product database

Aim 2. Biological and chemical assessment of an anti-TB ethnomedical mushroom, *Fomitopsis officinalis*

Aim 3. To search for a new TB drug lead from a fungal extract library

Summary Aim 1: The keywords “antimycobacterial activity” were used in Aim 1 for the initial NAPRALERT search and retrieved information related to (1) ethnomedical records of natural products, (2) *in vitro* and *in vivo* activity of plant extracts, and (3) antimycobacterial activity of isolates from natural sources. This yielded a total of 243 anti-TB ethnomedical references (1), containing 409 reports for the treatment of TB. The 409 reports were associated with 334 plant species in 103 families. There were 283 references related to antimycobacterial plant extracts (2), which contained 1867 entries of activity data against *M. tuberculosis*. The search also yielded 819 references for compounds tested against *Mycobacteria* (3), containing 1058 data entries for *M. tuberculosis*. In order to refine the raw mined data, a rational approach to prioritization of anti-TB ethnobotanicals was developed, using a scoring and indexing system.

Finally, 45 useful ethnobotanicals were selected and prioritized into 3 groups for further assessment in our TB drug discovery effort. Especially, Aim 3 of the study suggested that highly scored ethnobotanicals in group A (e.g. *Nidorella anomala*^{40, 64-66}, *Canscora decussata*^{41, 58-60}, and *Croton*

pseudopulchellus^{40, 61-63}) have higher probability of containing anti-TB metabolites because these selected ethnobotanicals have confirmed *in vitro* anti-TB activity. An example is the ethnobotanical *N. anomala* for which the extract demonstrated a MIC 100 µg/ml, but for which there are no reports of isolated compounds. *Croton* spp. is known for containing a volatile oil with violently purgative and irritating qualities, which might also explain the lack of scientific studies. The poisonous properties do not mean this plant has less potential to contain biologically useful compounds.

Unfortunately, access to most of the selected ethnobotanicals, which are mostly native to South Africa and East Asia, is very limited due to geographical and political restrictions. Further study will require collaborations to enable access, confirm their anti-TB activity *in vitro*, and enable purification and identification of new anti-TB leads.

Summary Aim 2: This aim focused on the investigation of the anti-TB ethnomedical mushroom, *F. officinalis*, which grows wild in the old growth forests of Oregon and Washington in the Pacific Northwest United States and Canada. In the NAPRALERT search from the aim 1, there was no *F. officinalis* in the result of data mining. Although there were numerous ethnomedical reports for the treatment of tuberculosis with this mushroom, those reports were mostly from non SCI journals, which led this mushroom had not been entered in the NAPRALERT database. In addition, there were several studies for isolation of numerous unusual triterpenoids from this mushroom, but never tested for anti-TB activity. This also indicates no data entry for the keywords “antimycobacterium activity” in the NAPRALERT database. However, if we simply apply anti-TB activity of the crude extract and ethnomedical reports founded from this present study, *F. officinalis* could score up to 9, which present one of the highest score in the score index.

In the present study to find anti-TB drug lead, from the EtOH extract of this polypore mushroom, two new anti-TB active coumarins were isolated and identified as 6-chloro-4-phenyl-2H-chromen-2-one (**1**)

and ethyl 6-chloro-2-oxo-4-phenyl-2H-chromen-3-carboxylate (**2**). The structures of the two isolates were confirmed by chemical synthesis along with spectroscopic methods. In addition, an analog for each of the isolates was synthesized, 7-chloro-4-phenyl-2H-chromen-2-one (**3**) and ethyl 7-chloro-2-oxo-4-phenyl-2H-chromen-3-carboxylate (**4**). Finally, the four compounds were chemically characterized, and their antimicrobial activities were determined as MIC from 22 to 50 $\mu\text{g/ml}$, indicating the content of coumarins in *Fomitopsis* is not responding to the main observed activity of the crude extract (MIC 100 - 200 $\mu\text{g/ml}$). The extensive antimicrobial activity assessment against *Mycobacterium* and Gram-positive/negative bacteria indicated these coumarins display anti-TB specific activity, which is a favorable property for an anti-TB agent although their activity did not justify their development as drug leads as they exhibited MICs from 22 to 50 $\mu\text{g/ml}$. However, structural modification may allow others to increase the potency as well as anti-TB selectivity.

Summary Aim 3a: In order to achieve Aim 3a, 12,905 fungal culture extracts were screened against *M. tuberculosis* in a state-of-the-art anti-TB assay. A total of 460 (3.6%) of the extracts effected $\geq 90\%$ inhibition in the MABA at 1.0 mg/ml and were further assessed for minimum inhibitory concentration (MIC) vs. *M. tuberculosis* and for Vero cell cytotoxicity. A total of 52 fungal extracts with anti-TB MICs of $< 300 \mu\text{g/ml}$ and $< 30\%$ inhibition of Vero cells at 1.0 mg/ml were further profiled by determining MICs against mono-drug resistant *M. tuberculosis* isolates and the activity against non-replicating *M. tuberculosis* cultures. The results of the study suggest that the inclusion of even a modest microbial extract library within a larger HTS campaign is likely to yield a manageable number of hits with biological profiles worthy of the effort required for bioassay-guided isolation.

Summary Aim3b: Accordingly, in Aim 3b, the anti-TB active fungal extract (MSX105528 MeOH extract, MIC 11 $\mu\text{g/ml}$) was selected from the previous HTS of a 12,905 fungal extract library, and culture conditions for MSX 105528 were optimized for activity against *M. tuberculosis*. An active principle was

isolated in a bioactivity-guided process using a combination of solid phase extraction (SPE) and high pressure liquid chromatography (HPLC). The activity was assigned to the pure isolate, vermitrasporin, one of possible stereoisomers of a known tetramic acid derivative (vermisporin) with decalin and oxirane moieties. There is no available report for the assessment of anti-TB activity of vermisporin, and the chemical characterization such as NMR and stereochemistry are not clearly described. For instance, Mikawa *et al.*, first chemically described vermisporin in the patent using $^1\text{H}/^{13}\text{C}$ NMR, IR, Optical Rotation, and UV, but the NMR chemical shift values and the absolute stereochemistry were not available in the patent.^{88a} Minowa *et al.*, determined the absolute configuration of the decalin moiety with X-ray crystallography of a degradation product of vermisporin, but not with vermisporin.^{88b} Koyama *et al.*, also claimed isolation of vermisporin along with tetramic acid derivatives (Spylidone and PF1052), but chemical assessment of vermisporin was not available.^{88c}

Therefore, an extensive biological and chemical assessment of vermitrasporin was conducted in this aim. *In vitro* biological assessments suggested that vermitrasporin has strong activity against *M. tuberculosis* as well as other microorganisms. Furthermore, activity against mono-drug resistant *M. tuberculosis* strains could suggest possible development of vermitrasporin to target drug resistant TB although the compound is moderately cytotoxic (IC₅₀ against Vero and J774A, 1.80 and 9.30 $\mu\text{g}/\text{ml}$ respectively). As the structure of vermisporin in the peer reviewed literature is not completely characterized, the isolate underwent an elaborate chemical characterization, which involved understanding of tautomerization with a tetramic acid moiety and elucidation of the relative configuration by a full spin analysis and NOE observation. The doubled resonances of ^1H and ^{13}C NMR spectrum indicated possible tautomerization of this vermitrasporin sample. Subsequently, CSEARCH analysis predicted an endo-enol form as the major tautomer of vermitrasporin in this particular case. In addition, a full spin analysis of the 900 MHz ^1H NMR spectrum was performed using PERCH iterator

software, and the full assignment of all ^1H resonances could be achieved including the multiplicities, which unambiguously assigned the relative configuration of the decalin portion of vermitrasporin. The suggested configuration was confirmed by the NOE correlation.

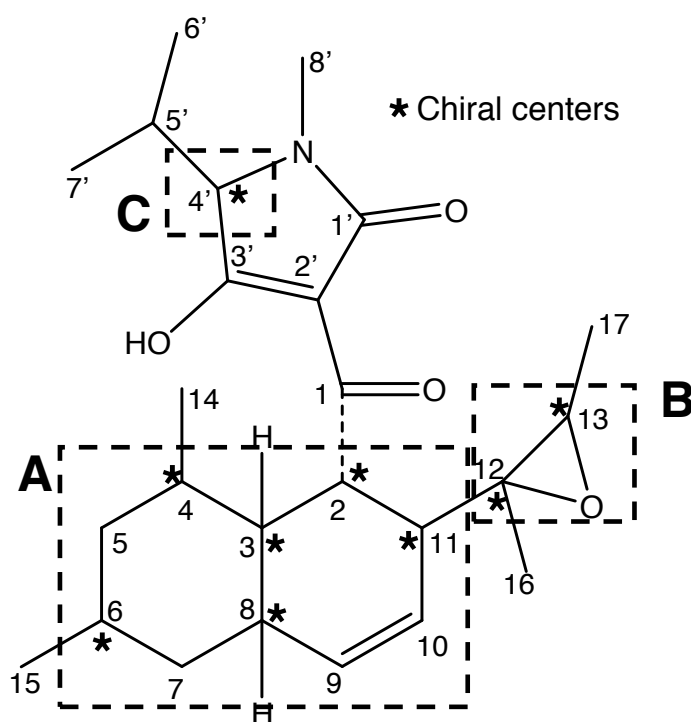


Figure 23. Chiral centers in vermitrasporin

However, the most important aspect in this chapter is that none of these analyses were sufficient to clarify the exact structure of vermitrasporin. The structure possesses a total of 9 chiral centers out of 25 carbons including the 9 methyl groups (Figure 23), which gives a total of 512 possible stereoisomers of vermitrasporin including enantiomers. Full ^1H NMR spin analysis with the PERCHit iterator established all ^1H chemical shifts and scalar coupling constants. Therefore, the relative configuration of the decalin moiety of vermitrasporin was established as of 2S^* , 3R^* , 4R^* , 6S^* , 8R^* , 11S^* configuration. The relative configuration of the oxirane ring was determined via NOE/ROE analysis, indicating a 12R^* ,

13R* configuration. In summary, all spectroscopic data of vermitrasporin are compatible with eight stereoisomers generated by the three chiral clusters (A, B, and C). Despite the lack of definitive data, the present study will provide the most informative data for the structural assessment for one of stereoisomers of vermisporin to date.

The anti-TB activity (MIC 0.56 – 0.74 $\mu\text{g/ml}$) suggests a possible development of vermitrasporin as a drug lead. However, the structural complexity (stereochemistry and tautomerization) will be the major difficulty for vermitrasporin to be developed as a drug lead. More elaborate spectroscopic studies, including NMR and X-ray crystallography of vermitrasporin, can be performed if significantly more material becomes available. In addition, potency and selectivity may be improved through chemical synthesis and structural modification.

In conclusion: Diverse natural sources as well as traditional medical knowledge are proven unique sources for many modern pharmaceuticals. Unfortunately, despite technological advances in the drug discovery such as computational chemistry, whole genome sequencing, bioinformatics, automated robotic HTS system, and modern spectroscopy devices (NMR and LCMS/MS) with much higher resolution and sensitivity, the number of new drugs in the market is insufficient to fight emerging infectious diseases, especially with the rapid development of drug resistance. This suggests that the lack of insufficient technology alone may not explain the paucity of newly discovered drugs. Consequently, drug discovery strategies based on natural products have recently once again appeared attractive.

Therefore, in order to find and utilize the best possible natural source for anti-TB drug lead discovery, this project uses an efficient integrated approach by implementing two distinctive procedures: ethnomedical knowledge and whole-cell based high throughput screening of a fungal extract library.

The former, which is considered a traditional drug discovery approach, proved to be a very valuable source for searching anti-TB drug leads and contributes the ancient and unique knowledge of traditional medicine. The latter, a modern high- technology approach, contributes state-of-the-art procedures and allows the handling of a high quantities of natural product sources. The combination of these two approaches enables us to extract the advantages of both techniques, old and new, and thereby receive unique and truly integrated data.

1. (a) Harries, A. D.; Dye, C., Tuberculosis. *Ann Trop Med Parasitol* **2006**, *100* (5-6), 415-431; (b) Smith, I., *Mycobacterium tuberculosis* pathogenesis and molecular determinants of virulence. *Clin Microbiol Rev* **2003**, *16* (3), 463-496; (c) van Soolingen, D.; Hoogenboezem, T.; de Haas, P. E.; Hermans, P. W.; Koedam, M. A.; Teppema, K. S.; Brennan, P. J.; Besra, G. S.; Portaels, F.; Top, J.; Schouls, L. M.; van Embden, J. D., A novel pathogenic taxon of the *Mycobacterium tuberculosis* complex, Canetti: Characterization of an exceptional isolate from Africa. *Int J Syst Bacteriol* **1997**, *47* (4), 1236-1245.
2. Abdallah, A. M.; Gey van Pittius, N. C.; Champion, P. A.; Cox, J.; Luirink, J.; Vandembroucke-Grauls, C. M.; Appelmelk, B. J.; Bitter, W., Type VII secretion-Mycobacteria show the way. *Nat Rev Microbiol* **2007**, *5* (11), 883-891.
3. Koul, A.; Arnoult, E.; Lounis, N.; Guillemont, J.; Andries, K., The challenge of new drug discovery for tuberculosis. *Nature* **2011**, *469* (7331), 483-490.
4. Stewart, G. R.; Robertson, B. D.; Young, D. B., Tuberculosis: a problem with persistence. *Nat Rev Microbiol* **2003**, *1* (2), 97-105.
5. (a) Rook, G. A.; Dheda, K.; Zumla, A., Immune responses to tuberculosis in developing countries: implications for new vaccines. *Nat Rev Immunol* **2005**, *5* (8), 661-667; (b) McShane, H., Tuberculosis vaccines: beyond bacille Calmette-Guerin. *Philos Trans R Soc Lond B Biol Sci* **2011**, *366* (1579), 2782-2789.
6. Russell, D. G., *Mycobacterium tuberculosis*: here today, and here tomorrow. *Nat Rev Mol Cell Biol* **2001**, *2* (8), 569-577.
7. Zhang, Y., Persistent and dormant tubercle bacilli and latent tuberculosis. *Front Biosci* **2004**, *9*, 1136-1156.
8. Boshoff, H. I.; Barry, C. E., 3rd, Tuberculosis - metabolism and respiration in the absence of growth. *Nat Rev Microbiol* **2005**, *3* (1), 70-80.
9. (a) Zink, A. R.; Sola, C.; Reischl, U.; Grabner, W.; Rastogi, N.; Wolf, H.; Nerlich, A. G., Characterization of *Mycobacterium tuberculosis* complex DNAs from Egyptian mummies by spoligotyping. *J Clin Microbiol* **2003**, *41* (1), 359-367; (b) Konomi, N.; Lebwohl, E.; Mowbray, K.; Tattersall, I.; Zhang, D., Detection of Mycobacterial DNA in Andean mummies. *J Clin Microbiol* **2002**, *40* (12), 4738-4740.
10. McCarthy, O. R., The key to the sanatoria. *J R Soc Med* **2001**, *94* (8), 413-417.
11. Domagk, G., Modern methods of chemotherapy of tuberculosis. *Ann R Acad Nac Med (Madr)* **1952**, *69* (4), 504-513.

12. (a) Dye, C., Global epidemiology of tuberculosis. *Lancet* **2006**, *367* (9514), 938-940; (b) Glaziou, P.; Floyd, K.; Raviglione, M., Global burden and epidemiology of tuberculosis. *Clin Chest Med* **2009**, *30* (4), 621-636, vii.
13. Global Tuberculosis Control. *WHO* **2010**.
14. Alcaide, F.; Santin, M., Multidrug-resistant tuberculosis. *Enferm Infecc Microbiol Clin* **2008**, *26* Suppl 13, 54-60.
15. WHO global tuberculosis control report 2010. Summary. *Cent Eur J Public Health* **2010**, *18* (4), 237.
16. Gandhi, N. R.; Moll, A.; Sturm, A. W.; Pawinski, R.; Govender, T.; Lalloo, U.; Zeller, K.; Andrews, J.; Friedland, G., Extensively drug-resistant tuberculosis as a cause of death in patients co-infected with tuberculosis and HIV in a rural area of South Africa. *Lancet* **2006**, *368* (9547), 1575-1580.
17. Schaaf, H. S.; Moll, A. P.; Dheda, K., Multidrug- and extensively drug-resistant tuberculosis in Africa and South America: epidemiology, diagnosis and management in adults and children. *Clin Chest Med* **2009**, *30* (4), 667-683, vii-viii.
18. Dmitriev, V. A., Global problem of tuberculosis and modern WHO strategy in its control. *Antibiot Khimioter* **2008**, *53* (5-6), 3-6.
19. Festenstein, F.; Grange, J. M., Tuberculosis and the acquired immune deficiency syndrome. *J Appl Bacteriol* **1991**, *71* (1), 19-30.
20. O'Boyle, S. J.; Power, J. J.; Ibrahim, M. Y.; Watson, J. P., Factors affecting patient compliance with anti-tuberculosis chemotherapy using the directly observed treatment, short-course strategy (DOTS). *Int J Tuberc Lung Dis* **2002**, *6* (4), 307-312.
21. Bastian, I.; Rigouts, L.; Van Deun, A.; Portaels, F., Directly observed treatment, short-course strategy and multidrug-resistant tuberculosis: are any modifications required? *Bull World Health Organ* **2000**, *78* (2), 238-251.
22. (a) Mwaba, P.; McNerney, R.; Grobusch, M. P.; O'Grady, J.; Bates, M.; Kapata, N.; Maeurer, M.; Zumla, A., Achieving STOP TB Partnership goals: perspectives on development of new diagnostics, drugs and vaccines for tuberculosis. *Trop Med Int Health* **2011**; (b) Keshavjee, S.; Girard, F.; Harrington, M.; Farmer, P. E., Time for a bold new vision at the Stop TB Partnership. *The Lancet* *376* (9749), 1283-1284.
23. (a) Ator, M. A.; Mallamo, J. P.; Williams, M., Overview of Drug Discovery and Development. In *Current Protocols in Pharmacology*, John Wiley & Sons, Inc.: 2001; (b) Swinney, D. C.; Anthony, J., How were new medicines discovered? *Nat Rev Drug Discov* **2011**, *10* (7), 507-519; (c) News Feature: A call to arms. *Nat Rev Drug Discov* **2007**, *6* (1), 8-12.

24. (a) Ginsberg, A. M., Drugs in development for tuberculosis. *Drugs* **2010**, *70* (17), 2201-2214; (b) Ginsberg, A. M.; Spigelman, M., Challenges in tuberculosis drug research and development. *Nat Med* **2007**, *13* (3), 290-294.
25. Matteelli, A.; Carvalho, A. C.; Dooley, K. E.; Kritski, A., TMC207: the first compound of a new class of potent anti-tuberculosis drugs. *Future Microbiol* **2010**, *5* (6), 8498-58.
26. Sensi, P., History of the development of rifampin. *Rev Infect Dis* **1983**, *5 Suppl 3*, S402-406.
27. Comroe, J. H., Jr., Pay dirt: the story of streptomycin. Part I. From Waksman to Waksman. *Am Rev Respir Dis* **1978**, *117* (4), 773-781.
28. Berdy, J., Bioactive microbial metabolites. *J Antibiot* **2005**, *58* (1), 1-26.
29. (a) Butler, M. S., The role of natural product chemistry in drug discovery. *J Nat Prod* **2004**, *67* (12), 2141-2153; (b) Butler, M. S.; Buss, A. D., Natural products-the future scaffolds for novel antibiotics? *Biochem Pharmacol* **2006**, *71* (7), 919-929.
30. Fischbach, M. A.; Walsh, C. T., Antibiotics for emerging pathogens. *Science* **2009**, *325* (5944), 1089-1093.
31. (a) Newman, D. J., Natural products as leads to potential drugs: an old process or the new hope for drug discovery? *J Med Chem* **2008**, *51* (9), 2589-2599; (b) Newman, D. J.; Cragg, G. M., Natural products as sources of new drugs over the last 25 years. *J Nat Prod* **2007**, *70* (3), 461-477; (c) Newman, D. J.; Cragg, G. M.; Snader, K. M., Natural products as sources of new drugs over the period 1981-2002. *J Nat Prod* **2003**, *66* (7), 1022-1037.
32. (a) Clardy, J.; Walsh, C., Lessons from natural molecules. *Nature* **2004**, *432* (7019), 829-837; (b) Henkel, T.; Brunne, R. M.; Müller, H.; Reichel, F., Statistical Investigation into the Structural Complementarity of Natural Products and Synthetic Compounds. *Angew Chem Int Ed* **1999**, *38* (5), 643-647.
33. Feher, M.; Schmidt, J. M., Property distributions: differences between drugs, natural products, and molecules from combinatorial chemistry. *J Chem Inf Comput Sci* **2003**, *43* (1), 218-227.
34. Sterling, T. R., New approaches to the treatment of latent tuberculosis. *Semin Respir Crit Care Med* **2008**, *29* (5), 532-541.
35. (a) Berning, S. E., The role of fluoroquinolones in tuberculosis today. *Drugs* **2001**, *61* (1), 9-18; (b) Adhvaryu, M. R.; Reddy, N.; Vakharia, B. C., Prevention of hepatotoxicity due to anti tuberculosis treatment: a novel integrative approach. *World J Gastroenterol* **2008**, *14* (30), 4753-4762.
36. Farnsworth, N. R.; Akerele, O.; Bingel, A. S.; Soejarto, D. D.; Guo, Z., Medicinal plants in therapy. *Bull World Health Organ* **1985**, *63* (6), 965-981.

37. Paing Soe, T. L., Khin Chit, Thaw Zin, and Ti Ti, The Role of Traditional Medicine in the Treatment of Multidrug-resistant Pulmonary Tuberculosis, Myanmar. *Regional Health Forum-WHO South-East Asia Region* **2006**, *10* (2).
38. Loub, W. D.; Farnsworth, N. R.; Soejarto, D. D.; Quinn, M. L., NAPRALERT: computer handling of natural product research data. *J Chem Inf Comput Sci* **1985**, *25* (2), 99-103.
39. (a) Case, R. J.; Franzblau, S. G.; Wang, Y.; Cho, S. H.; Soejarto, D. D.; Pauli, G. F., Ethnopharmacological evaluation of the informant consensus model on anti-tuberculosis claims among the Manus. *J Ethnopharmacol* **2006**, *106* (1), 82-89; (b) Inui, T.; Wang, Y.; Deng, S.; Smith, D. C.; Franzblau, S. G.; Pauli, G. F., Counter-current chromatography based analysis of synergy in an anti-tuberculosis ethnobotanical. *J Chromatogr A* **2007**, *1151* (1-2), 211-215; (c) Jaki, B. U.; Franzblau, S. G.; Chadwick, L. R.; Lankin, D. C.; Zhang, F.; Wang, Y.; Pauli, G. F., Purity-activity relationships of natural products: the case of anti-TB active ursolic acid. *J Nat Prod* **2008**, *71* (10), 1742-1748.
40. Lall, N.; Meyer, J. J., In vitro inhibition of drug-resistant and drug-sensitive strains of *Mycobacterium tuberculosis* by ethnobotanically selected South African plants. *J Ethnopharmacol* **1999**, *66* (3), 347-354.
41. Ghosal, S., Chemical constituents of Gentianaceae XVI: antitubercular activity of xanthones of *Cansocora decussata*. *J Pharm Sci* **1975**, *64*, 888.
42. Jain, R. C., Anti tubercular activity of garlic oil. *Indian J Pathol Microbiol* **1998**, *41* (1), 131.
43. Van Puyvelde, L., In vitro inhibition of mycobacteria by Rwandese medicinal plants. *Phytother Res* **1994**, *8* (2), 65-69.
44. Chopra, I. C., Antibacterial properties of volatile principles from *Alpinia galanga* and *Acorus calamus*. *Antibiot Chemther* **1957**, *7*, 378-383.
45. Cantrell, C. L.; Abate, L.; Fronczek, F. R.; Franzblau, S. G.; Quijano, L.; Fischer, N. H., Antimycobacterial eudesmanolides from *Inula helenium* and *Rudbeckia subtomentosa*. *Planta Med* **1999**, *65* (4), 351-355.
46. Saludes, J. P., Antibacterial constituents from the hexan fraction of *Morinda citrifolia* L (Rubiaceae). *Phytother Res* **2002**, *16* (7), 683-685.
47. Mc Cutcheon, A. R., Anti-mycobacterial screening of British Columbian medicinal plants. *Int J Pharmacog* **1997**, *35* (2), 77-83.
48. Frisbey, A., The occurrence of antibacterial substances in seed plants with special reference to *Mycobacterium tuberculosis* (Third report). *Mich State Univ Agr Appl Sci Quart Bull* **1953**, *35*, 392-404.

49. Watt, J. M., *Folklore, ethnomedical*. 1962.
50. Grange, J. M.; Davey, R. W., Detection of antituberculous activity in plant extracts. *J Appl Bacteriol* **1990**, *68* (6), 587-591.
51. Dopp, W., Tuberculostatic action of some plants extracts in vitro. *Pharmazie* **1950**, *5*, 603-604.
52. Salle, A. J., Studies on the antibacterial properties of *Eriodictyon californicum*. *Arch Biochem Biophys* **1951**, *32*, 121-123.
53. Azarowicz, E. N., Antibiotics in plants of Southern California active against *Mycobacterium tuberculosis* 607 and *Aspergillus niger*. *Antibiot Chemther* **1959**, *2*, 532-536.
54. FitzPatrick, F. K., Plant substances active against *Mycobacterium tuberculosis*. *Antibiot Chemther* **1954**, *4*.
55. Albert-Puleo, M., Physiological effects of cabbage with reference to its potential as a dietary cancer-inhibitor and its use in ancient. *J Ethnopharmacol* **1983**, *9* (213), 261-272.
56. Schramm, G., Plant and animal drugs of the old Chinese materia medica in the therapy of pulmonary tuberculosis. *Planta Med* **1956**, *4* (4), 97-104.
57. Gottshall, R., The occurrence of antibacterial substances active against *Mycobacterium tuberculosis* in seed plants. *J Clin Invest* **1949**, *28*, 920-923.
58. Madan, B.; Mandal, B. C.; Kumar, S.; Ghosh, B., *Canscora decussata* (Roxb.) Schult (Gentianaceae) inhibits LPS-induced expression of ICAM-1 and E-selectin on endothelial cells and carageenan-induced paw-edema in rats. *J Ethnopharmacol* **2003**, *89* (2-3), 211-216.
59. Madan, B.; Ghosh, B., *Canscora decussata* promotes adhesion of neutrophils to human umbilical vein endothelial cells. *J Ethnopharmacol* **2002**, *79* (2), 229-235.
60. (a) Chintalwar, G. J.; Chattopadhyay, S., Structural confirmation of decussatin, *Swertia decussata* xanthone. *Nat Prod Res* **2006**, *20* (1), 53-6; (b) Patro, B. S.; Chintalwar, G. J.; Chattopadhyay, S., Antioxidant activities of *Swertia decussata* xanthones. *Nat Prod Res* **2005**, *19* (4), 347-354.
61. (a) Farnsworth, N. R.; Blomster, R. N.; Messmer, W. M.; King, J. C.; Persinos, G. J.; Wilkes, J. D., A phytochemical and biological review of the genus *Croton*. *Lloydia* **1969**, *32* (1), 1-28; (b) Hedberg, I.; Hedberg, O.; Madati, P. J.; Mshigeni, K. E.; Mshiu, E. N.; Samuelsson, G., Inventory of plants used in traditional medicine in Tanzania. Part III. Plants of the families Papilionaceae-Vitaceae. *J Ethnopharmacol* **1983**, *9* (2-3), 237-260.

62. (a) Jones, K., Review of sangre de drago (*Croton lechleri*)--a South American tree sap in the treatment of diarrhea, inflammation, insect bites, viral infections, and wounds: traditional uses to clinical research. *J Altern Complement Med* **2003**, *9* (6), 877-896; (b) Gonzales, G. F.; Valerio, L. G., Jr., Medicinal plants from Peru: a review of plants as potential agents against cancer. *Anticancer Agents Med Chem* **2006**, *6* (5), 429-444.
63. Odalo, J. O.; Omolo, M. O.; Malebo, H.; Angira, J.; Njeru, P. M.; Ndiege, I. O.; Hassanali, A., Repellency of essential oils of some plants from the Kenyan coast against *Anopheles gambiae*. *Acta Trop* **2005**, *95* (3), 210-218.
64. Bohlmann, F.; Wegner, P.; Jakupovic, J., Unusual diterpenes and sesquiterpene xylosides from *Nidorella hottentotica*. *Phytochemistry* **1982**, *21* (5), 1109-1114.
65. (a) Cantrell, C. L.; Lu, T.; Fronczek, F. R.; Fischer, N. H.; Adams, L. B.; Franzblau, S. G., Antimycobacterial cycloartanes from *Borrchia frutescens*. *J Nat Prod* **1996**, *59* (12), 1131-1136; (b) Rajab, M. S.; Cantrell, C. L.; Franzblau, S. G.; Fischer, N. H., Antimycobacterial activity of (E)-phytol and derivatives: a preliminary structure-activity study. *Planta Med* **1998**, *64* (1), 2-4.
66. (a) Inui, T.; Wang, Y.; Nikolic, D.; Smith, D. C.; Franzblau, S. G.; Pauli, G. F., Sesquiterpenes from *Oplopanax horridus*. *J Nat Prod* **2010**, *73* (4), 563-567; (b) Li, H.; O'Neill, T.; Webster, D.; Johnson, J. A.; Gray, C. A., Anti-mycobacterial diynes from the Canadian medicinal plant *Aralia nudicaulis*. *J Ethnopharmacol* **2012**, *140* (1), 141-144.
67. Githiori, J. B.; Hoglund, J.; Waller, P. J.; Baker, R. L., Anthelmintic activity of preparations derived from *Myrsine africana* and *Rapanea melanophloeos* against the nematode parasite, *Haemonchus contortus*, of sheep. *J Ethnopharmacol* **2002**, *80* (2-3), 187-191.
68. Githiori, J. B.; Hoglund, J.; Waller, P. J.; Leyden Baker, R., Evaluation of anthelmintic properties of extracts from some plants used as livestock dewormers by pastoralist and smallholder farmers in Kenya against *Heligmosomoides polygyrus* infections in mice. *Vet Parasitol* **2003**, *118* (3-4), 215-226.
69. (a) Stamets, P., Antipox Properties of *Fomitopsis officinalis* (Vill.) Bondartsev et Singer (Agarikon) from the Pacific Northwest of North America. *Int J Med Mushr* **2005**, *7* (3), 495 - 506; (b) Stamets, P., Potentiation of cell-mediated host defense using fruitbodies and mycelia of medicinal mushrooms. *Int J Med Mushr* **2002**, *5* (2), 179 - 192; (c) Grazywnowicz, K., Medicinal mushrooms in Polish folk medicine. *Int J Med Mushr* **2001**, *3* (2-3); (d) Wu, X.; Yang, J. S.; Yan, M., Four new triterpenes from fungus of *Fomes officinalis*. *Chem Pharm Bull (Tokyo)* **2009**, *57* (2), 195-197.

70. (a) Anderson, C., Metabolic intermediates in the biological oxidation of lanosterol to eburicoic acid. *Phytochem* **1971**, *10* (11), 2713-2717; (b) Anderson, C., Minor triterpenoids of *Fomes officinalis*. *Phytochem* **1972**, *11* (9), 2847-2852; (c) Epstein, W., Structure and stereochemistry of officinalic acid, a novel triterpenes from *Fomes officinalis*. *J. Am. Chem. Soc* **1979**, *101* (10), 2748-2750; (d) Wu, X., New lanostane-type triterpenes from *Fomes officinalis*. *Chem Pharm Bull* **2004**, *52* (11), 1375-1377.
71. (a) Napolitano, J. G.; Gödecke, T.; Rodriguez-Brasco, M. F.; Jaki, B. U.; Chen, S. N.; Lankin, D. C.; Pauli, G. F., The Tandem of Full Spin Analysis and qHNMR for the Quality Control of Botanicals Exemplified with *Ginkgo biloba*. *J Nat Prod* **2012**, *75* (2), 238-248; (b) Molina-Salinas, G. M.; Rivas-Galindo, V. M.; Said-Fernandez, S.; Lankin, D. C.; Munoz, M. A.; Joseph-Nathan, P.; Pauli, G. F.; Waksman, N., Stereochemical analysis of leubethanol, an anti-TB-active serrulatane, from *Leucophyllum frutescens*. *J Nat Prod* **2011**, *74* (9), 1842-1850; (c) Scher, J. M.; Schinkovitz, A.; Zapp, J.; Wang, Y.; Franzblau, S. G.; Becker, H.; Lankin, D. C.; Pauli, G. F., Structure and anti-TB activity of trachylobanes from the liverwort *Jungermannia exsertifolia* ssp. *cordifolia*. *J Nat Prod* **2010**, *73* (4), 656-663.
72. Cresente-Campo, J., Microwave-Promoted, One-Plot, Solvent-Free Synthesis of 4-Arylcoumarins from 2-Hydroxybenzophenones. *Eur J Org Chem* **2010**, *2010* (21), 4130-4137
73. Tawada, H., ChemInform Abstract: Synthesis of 3-Ureido Derivatives of Coumarin and 2-Quinolone as Potent Acyl-CoA: Cholesterol Acyltransferase Inhibitors. *Chem Pharm Bull* **1995**, *26* (45), 616-625.
74. Gabbutt, C. D.; Heron, B. M.; Instone, A. C., The synthesis and electronic absorption spectra of 3-phenyl-3(4-pyrrolidino-2-substituted phenyl)-3H-naphtho[2,1-b]pyrans: further exploration of the ortho substituent effect. *Tetrahedron* **2006**, *62* (4), 737-745.
75. (a) Collins, L.; Franzblau, S. G., Microplate Alamar Blue assay versus BACTEC 460 system for high-throughput screening of compounds against *Mycobacterium tuberculosis* and *Mycobacterium avium*. *Antimicrob Agents Chemother* **1997**, *41* (5), 1004-1009; (b) Franzblau, S. G.; Witzig, R. S.; McLaughlin, J. C.; Torres, P.; Madico, G.; Hernandez, A.; Degnan, M. T.; Cook, M. B.; Quenzer, V. K.; Ferguson, R. M.; Gilman, R. H., Rapid, low-technology MIC determination with clinical *Mycobacterium tuberculosis* isolates by using the microplate Alamar Blue assay. *J Clin Microbiol* **1998**, *36* (2), 362-366.
76. Cho, S. H.; Warit, S.; Wan, B.; Hwang, C. H.; Pauli, G. F.; Franzblau, S. G., Low-oxygen-recovery assay for high-throughput screening of compounds against nonreplicating *Mycobacterium tuberculosis*. *Antimicrob Agents Chemother* **2007**, *51* (4), 1380-1385.
77. Falzari, K.; Zhu, Z.; Pan, D.; Liu, H.; Hongmanee, P.; Franzblau, S. G., In vitro and in vivo activities of macrolide derivatives against *Mycobacterium tuberculosis*. *Antimicrob Agents Chemother* **2005**, *49* (4), 1447-1454.

78. (a) NCCLS, *Methods for Dilution Antimicrobial Susceptibility Test for Bacteria That Grow Aerobically*. 2nd ed.; Villanova, PA, 1990; (b) NCCLS, *Performance Standards for Antimicrobial Susceptibility Testing*. Villanova, PA, 1991; Vol. 3rd Informational Supplement.
79. Molinari, G., Natural products in drug discovery: present status and perspectives. *Adv Exp Med Biol* **2009**, *655*, 13-27.
80. Mayr, L. M.; Bojanic, D., Novel trends in high-throughput screening. *Curr Opin Pharmacol* **2009**, *9* (5), 580-588.
81. Sivendran, S.; Jones, V.; Sun, D.; Wang, Y.; Grzegorzewicz, A. E.; Scherman, M. S.; Napper, A. D.; McCammon, J. A.; Lee, R. E.; Diamond, S. L.; McNeil, M., Identification of triazinoindol-benzimidazolones as nanomolar inhibitors of the *Mycobacterium tuberculosis* enzyme TDP-6-deoxy-d-xylo-4-hexopyranosid-4-ulose 3,5-epimerase (RmlC). *Bioorg Med Chem* **2010**, *18* (2), 896-908.
82. (a) Ananthan, S.; Faaleolea, E. R.; Goldman, R. C.; Hobrath, J. V.; Kwong, C. D.; Laughon, B. E.; Maddry, J. A.; Mehta, A.; Rasmussen, L.; Reynolds, R. C.; Secrist, J. A., 3rd; Shindo, N.; Showe, D. N.; Sosa, M. I.; Suling, W. J.; White, E. L., High-throughput screening for inhibitors of *Mycobacterium tuberculosis* H37Rv. *Tuberculosis* **2009**, *89* (5), 334-353; (b) Maddry, J. A.; Ananthan, S.; Goldman, R. C.; Hobrath, J. V.; Kwong, C. D.; Maddox, C.; Rasmussen, L.; Reynolds, R. C.; Secrist, J. A., 3rd; Sosa, M. I.; White, E. L.; Zhang, W., Antituberculosis activity of the molecular libraries screening center network library. *Tuberculosis* **2009**, *89* (5), 354-363.
83. Anthony, K. G.; Strych, U.; Yeung, K. R.; Shoen, C. S.; Perez, O.; Krause, K. L.; Cynamon, M. H.; Aristoff, P. A.; Koski, R. A., New Classes of Alanine Racemase Inhibitors Identified by High-Throughput Screening Show Antimicrobial Activity against *Mycobacterium tuberculosis*. *PLoS One* **2011**, *6* (5), e20374.
84. Lin, G.; Li, D.; Chidawanyika, T.; Nathan, C.; Li, H., Fellutamide B is a potent inhibitor of the *Mycobacterium tuberculosis* proteasome. *Arch Biochem Biophys* **2010**, *501* (2), 214-220.
85. Shu, Y. Z., Recent natural products based drug development: a pharmaceutical industry perspective. *J Nat Prod* **1998**, *61* (8), 1053-1071.
86. Harvey, A. L., Natural products as a screening resource. *Curr Opin Chem Biol* **2007**, *11* (5), 480-484.
87. Chin, N. X.; Neu, H. C., In vitro antimicrobial activity of the new antibiotic vermispurin. *Eur J Clin Microbiol Infect Dis* **1992**, *11* (8), 755-757.

88. (a) Mikawa, T.; Miyadoh, S.; Ohkishi, H.; Sato, Y.; Sezaki, M.; Takahashi, N., Noval antibiotic vermispurin, process for the production thereof and pharmaceutical composition comprising it as an active antibacterial agent. U.S 4,933,180 (Cl. A61K3570; G12P 102), Feb **1988**, June **1990**. (b) Minowa, N.; Kodama, Y.; Hariyama, K.; Mikawa, T., A degradation study of vermispurin and determination of its absolute configuration. *Heterocycles* **1998**, *48*, 1639-1642. (c) Koyama, N.; Nagahiro, T.; Yamaguchi, Y.; Ohshiro, T.; Masuma, R.; Tomoda, H.; Omura, S., Spylidone, a novel inhibitor of lipid droplet accumulation in mouse macrophages produced by *Phoma* sp. FKI-1840. *J Antibiot* **2005**, *58* (5), 338-345.
89. Royles, B. J. L., Naturally Occurring Tetramic Acids: Structure, Isolation, and Synthesis. *Chem Rev* **1995**, *95* (6), 1981-2001.
90. (a) Yamaguchi, T.; Saito, K.; Tsujimoto, T.; Yuki, H., Nmr Spectroscopic Studies on Tautomerism in Schiff-Bases of Tenuazonic Acid Analogs. *B Chem Soc Jpn* **1976**, *49* (4), 1161-1162; (b) Yamaguchi, T.; Saito, K.; Tsujimoto, T.; Yuki, H., NMR Spectroscopic Studies on Tautomerism in Tenuazonic Acid Analogs. *J Heterocyclic Chem* **1976**, *13* (3), 533-537; (c) Saito, K.; Yamaguchi, T., Nmr Spectroscopic Studies of Tautomerism in Tetramic Acid Analogs and Their Anilides .3. Polar-Solvent Effects on Tautomeric Populations. *Bull Chem Soc Jpn* **1978**, *51* (2), 651-652.
91. Jones, R. C. F.; Sumaria, S., A synthesis of 3-acyl-5-alkyl tetramic acids. *Tetrahedron Lett* **1978**, *19* (34), 3173-3176.
92. Nolte, M. J.; Steyn, P. S.; Wessels, P. L., Structural investigations of 3-acylpyrrolidine-2,4-diones by nuclear magnetic resonance spectroscopy and X-ray crystallography. *J Chem Soc Perkin Trans 1* **1980**, 1057-1065
93. Jeong, Y. C.; Moloney, M. G., Synthesis of and tautomerism in 3-acyltetramic acids. *J Org Chem* **2011**, *76* (5), 1342-1354.
94. Janke, E. M. B. I.; Schlund, S.; Paasche, A.; Engels, B.; Dede, R. d.; Hussain, I.; Langer, P.; Rettig, M.; Weisz, K., Tautomeric Equilibria of 3-Formylacetylacetone: Low-Temperature NMR Spectroscopy and ab Initio Calculations. *J Org Chem* **2009**, *74* (13), 4878-4881.
95. Steyn, P. S.; Wessels, P. L., Tautomerism in tetramic acids: ¹³C NMR determination of the structures and ratios of the tautomers in 3-acetyl-5-isopropylpyrrolidine-2,4-dione. *Tetrahedron Letts* **1978**, *19* (47), 4707-4710.
96. Wolfgang, R., Do high-quality ¹³C-NMR spectral data really come from journals with high Impact Factors? *TrAC Trends Anal Chem* **2009**, *28* (7), 914-922.

APPENDICES

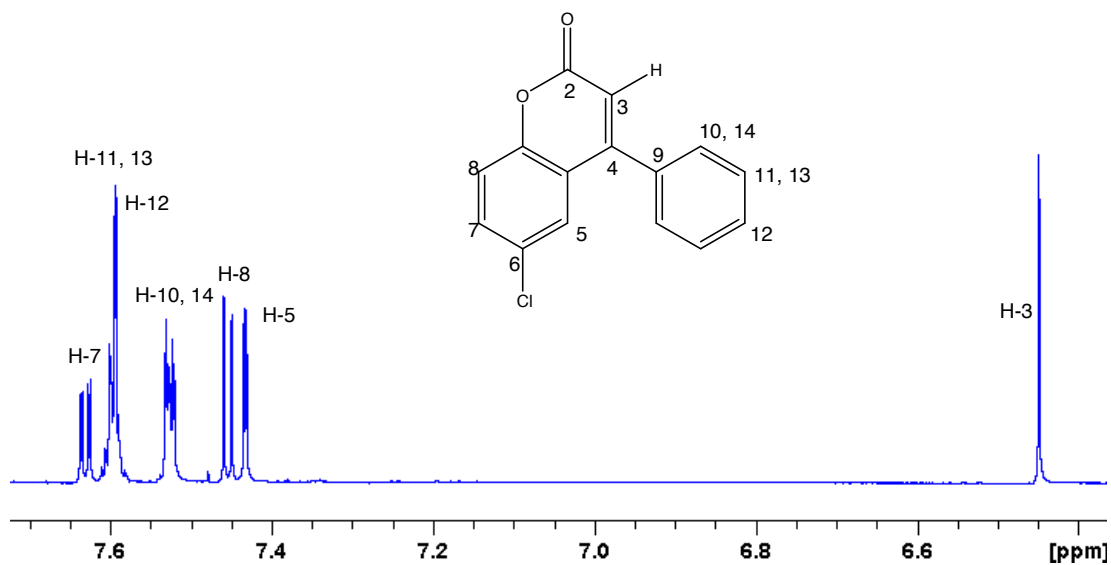


Figure 24. ¹H NMR spectrum of isolated **1** (900 MHz, 3 mm tube, 0.5 mg in 200 μ l MeOH-*d*₄), 6-chloro-4-phenyl-2H-chromen-2-one.

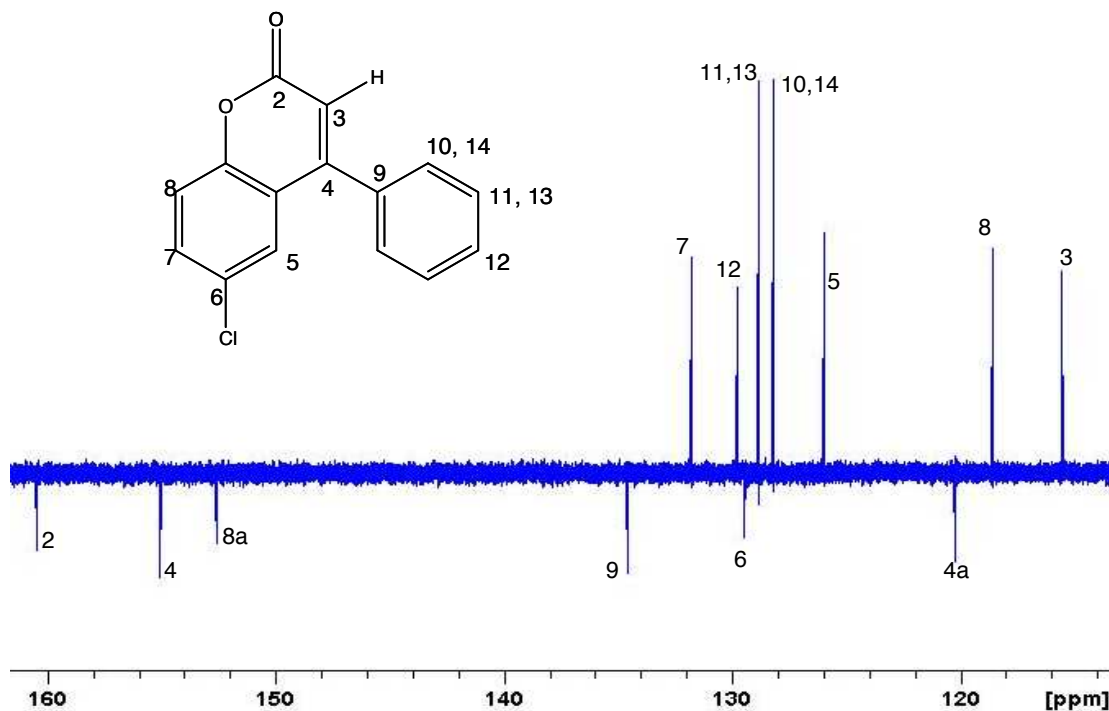


Figure 25. ¹³C DEPTQ NMR spectrum of isolated **1** (225 MHz, 3 mm tube, 0.5 mg in 200 μ l MeOH-*d*₄), 6-chloro-4-phenyl-2H-chromen-2-one.

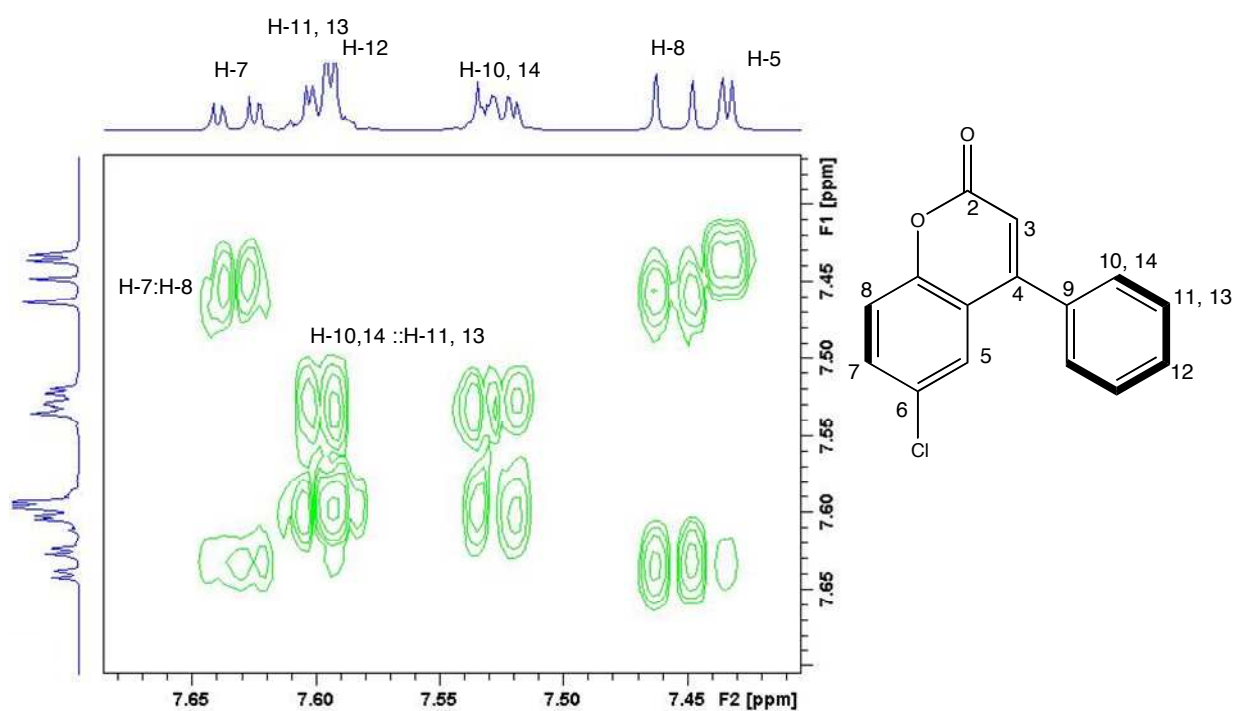


Figure 26. ^1H - ^1H COSY NMR spectrum of isolated **1** (900 MHz, 3 mm tube, 0.5 mg in 200 μl $\text{MeOH-}d_4$), 6-chloro-4-phenyl-2H-chromen-2-one.

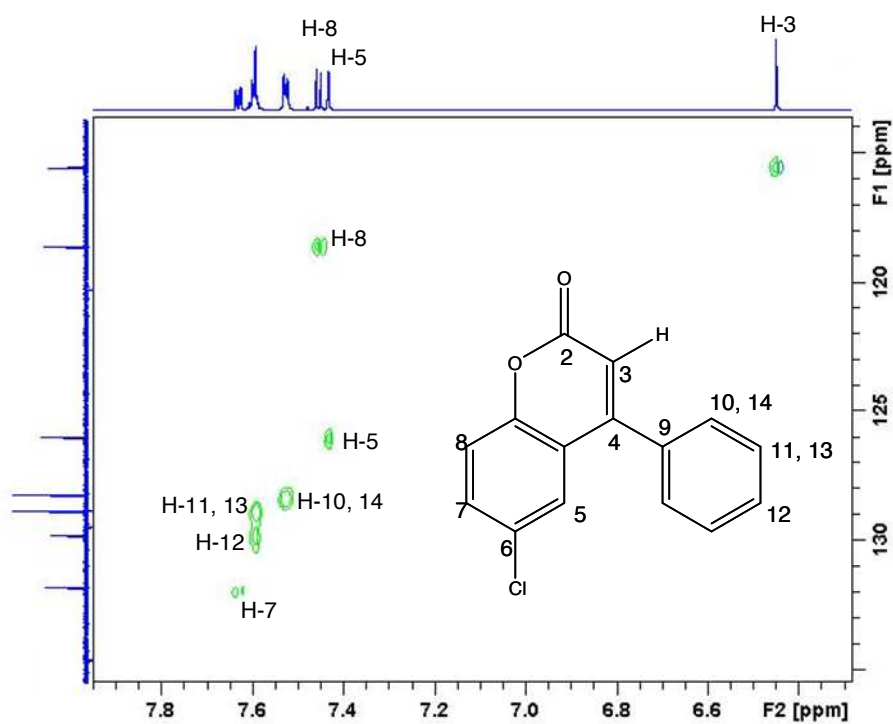


Figure 27. HSQC NMR spectrum of isolated **1** (600 MHz, 3 mm tube, 0.5 mg in 200 μl $\text{MeOH-}d_4$), 6-chloro-4-phenyl-2H-chromen-2-one.

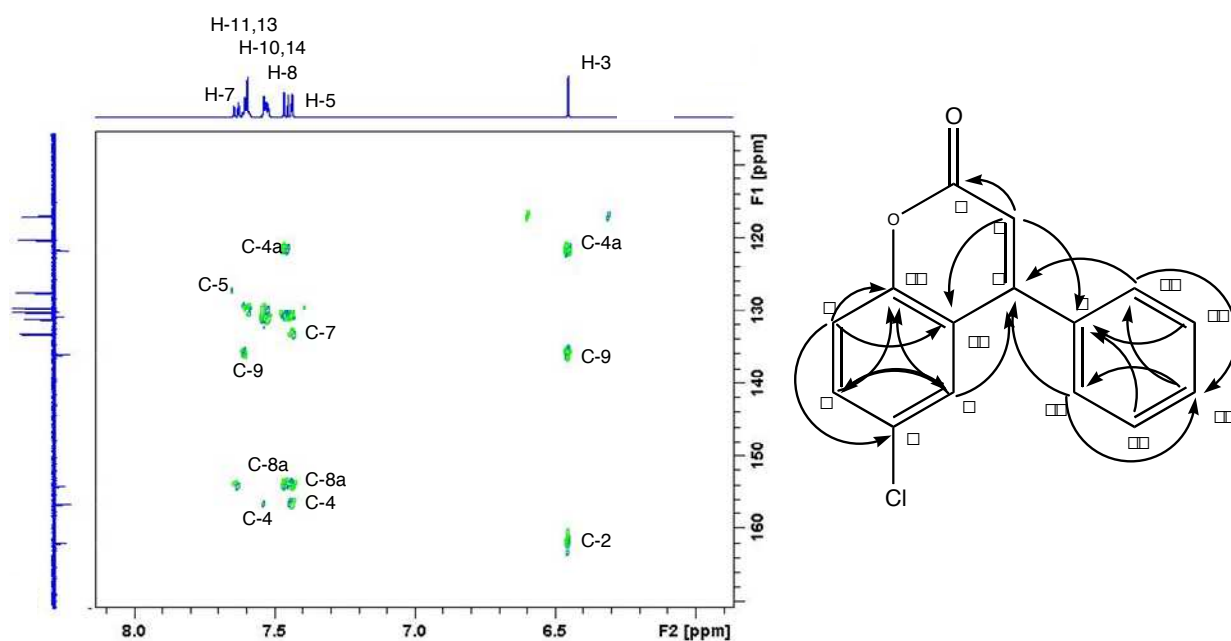


Figure 28. HMBC NMR spectrum of isolated **1** (600 MHz, 3 mm tube, 0.5 mg in 200 μ l MeOH- d_4), 6-chloro-4-phenyl-2H-chromen-2-one.

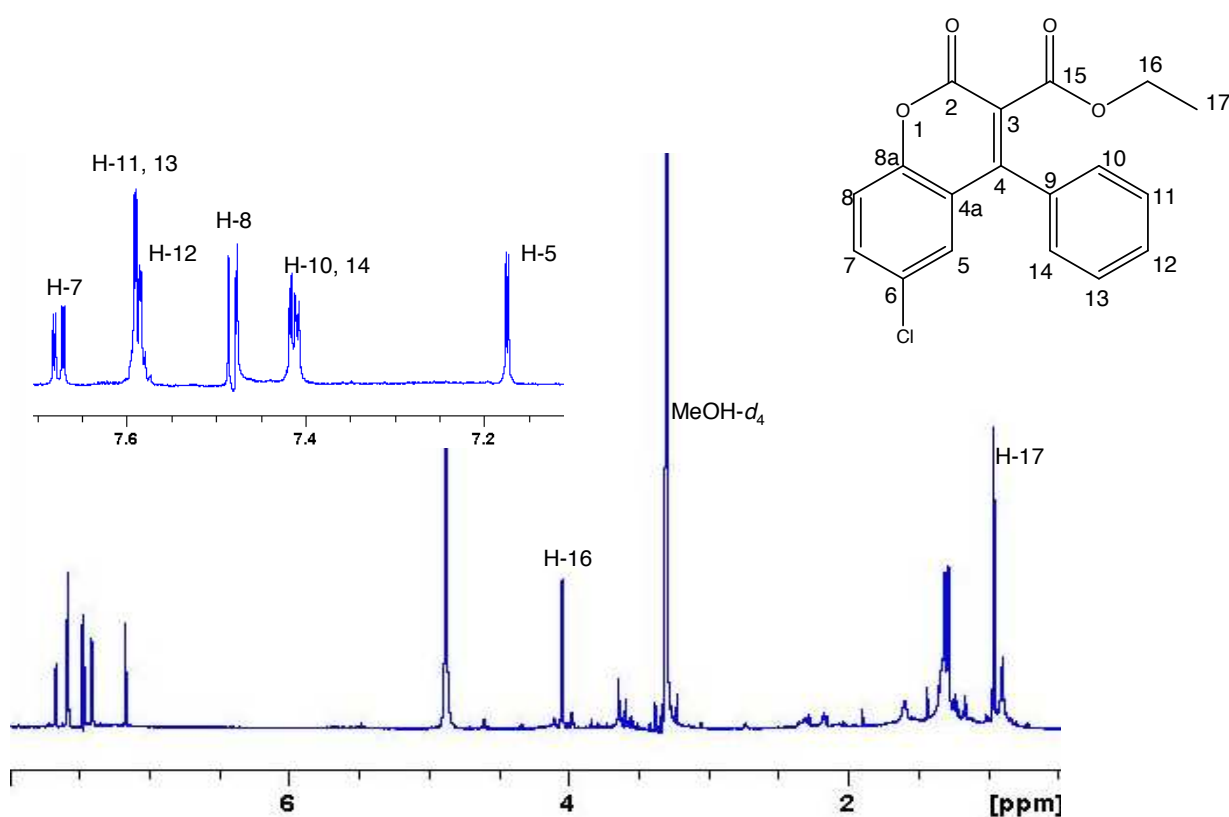


Figure 29. ^1H NMR spectrum of isolated **2** (900 MHz, 1.7 mm tube, 0.2 mg in 50 μ l MeOH- d_4), ethyl 6-chloro-2-oxo-4-phenyl-2H-chromen-3-carboxylate.

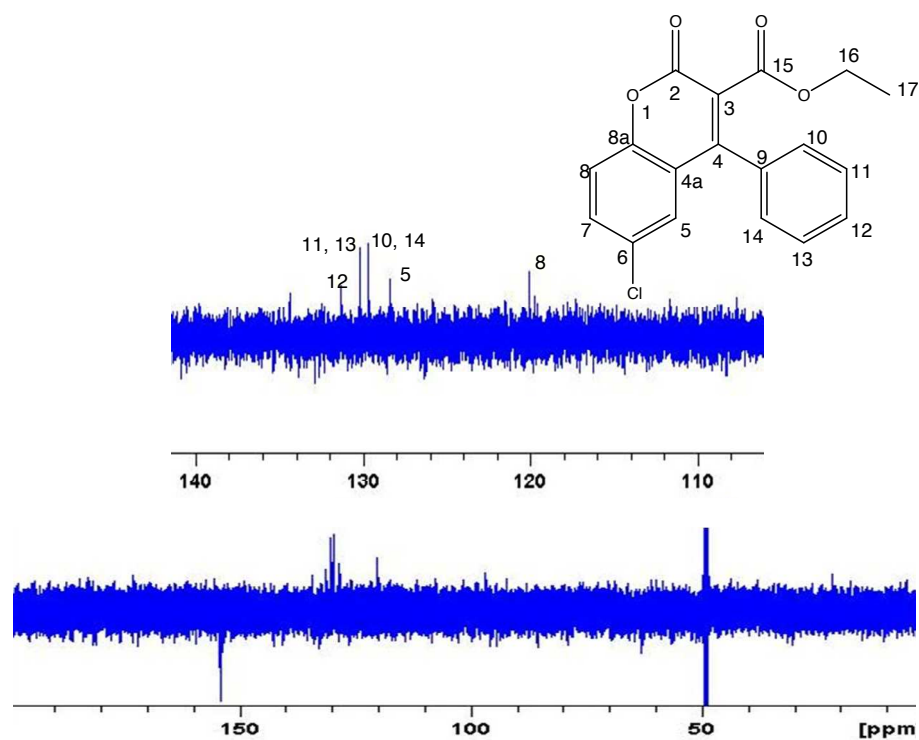


Figure 30. ^{13}C DEPTQ NMR spectrum of isolated **2** (225 MHz, 1.7 mm tube, 0.2 mg in 50 μl $\text{MeOH-}d_4$), ethyl 6-chloro-2-oxo-4-phenyl-2H-chromen-3-carboxylate.

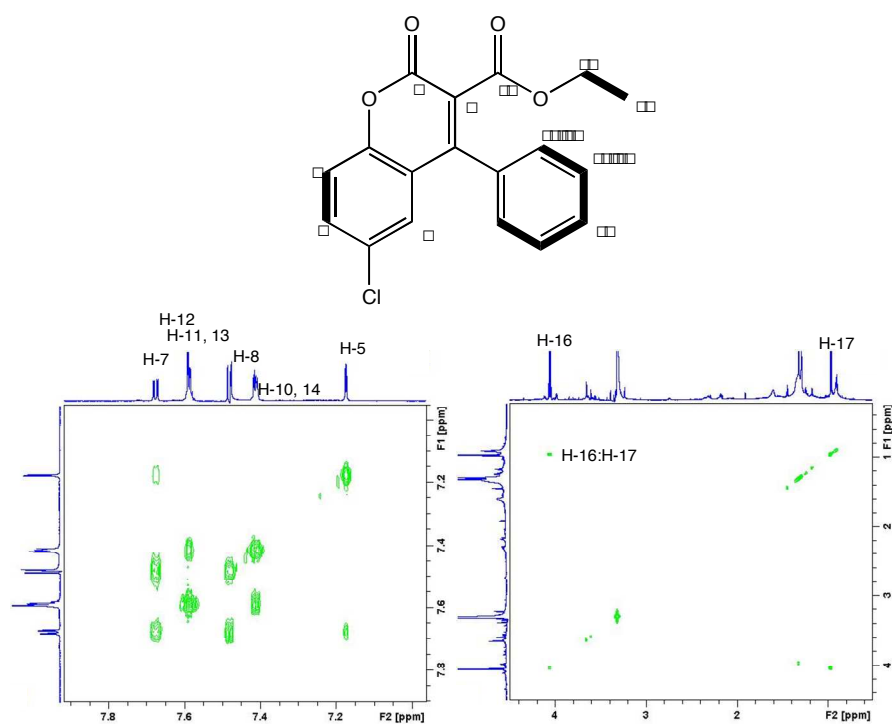


Figure 31. ^1H - ^1H COSY NMR spectrum of isolated **2** (900MHz, 1.7 mm tube, 0.2 mg in 50 μl $\text{MeOH-}d_4$), ethyl 6-chloro-2-oxo-4-phenyl-2H-chromen-3-carboxylate.

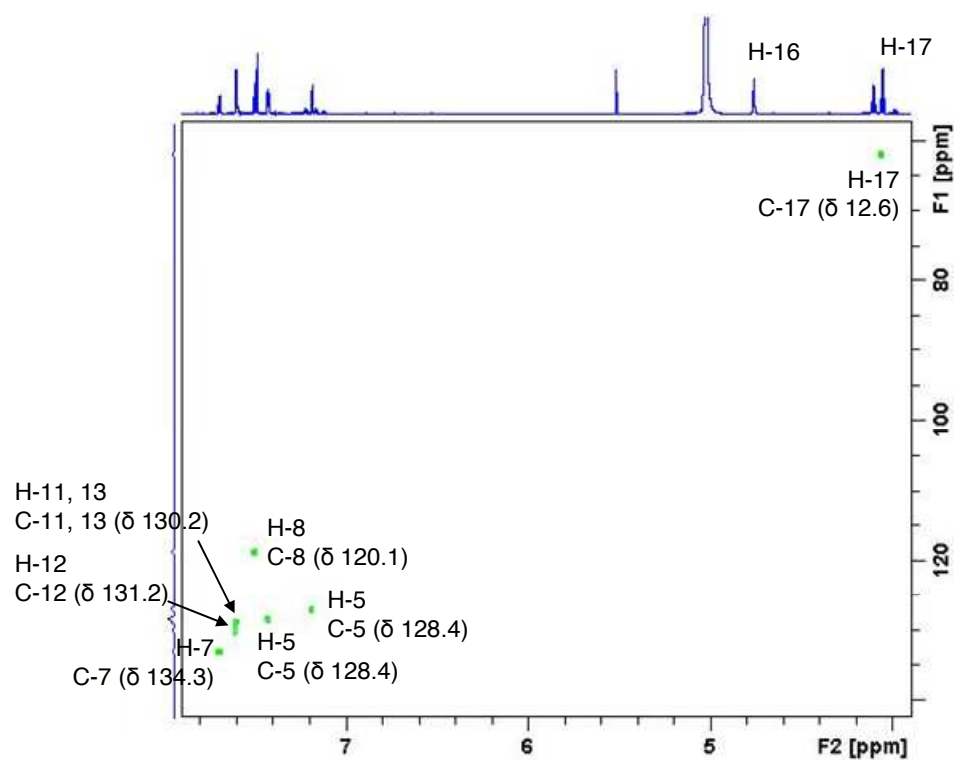


Figure 32. HSQC NMR spectrum of isolated **2** (900 MHz, 3 mm tube, 0.2 mg in 200 μ l MeOH- d_4), ethyl 6-chloro-2-oxo-4-phenyl-2H-chromen-3-carboxylate.

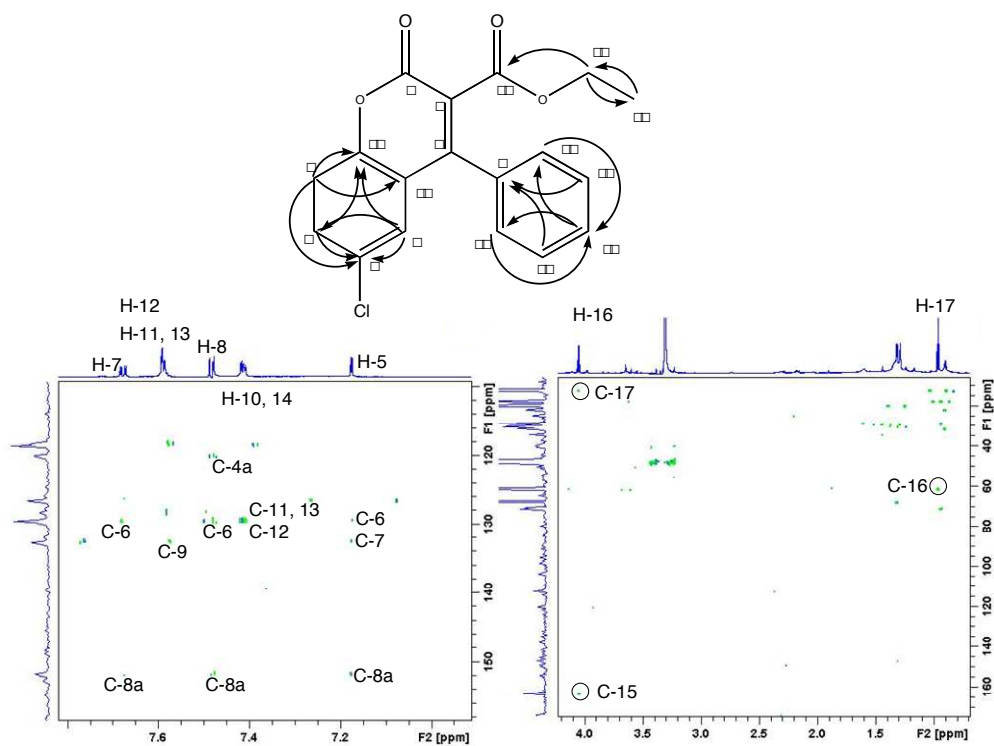


Figure 33. HMBC NMR spectrum of isolated **2** (900MHz, 1.7 mm tube, 0.2 mg in 50 μ l MeOH- d_4), ethyl 6-chloro-2-oxo-4-phenyl-2H-chromen-3-carboxylate.

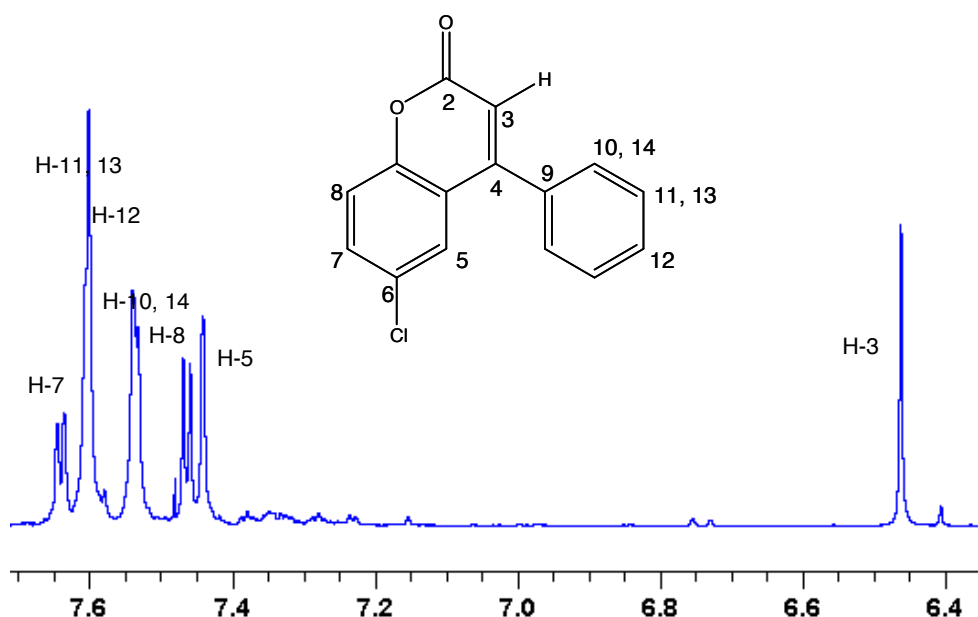


Figure 34. ¹H NMR spectrum of synthetic **1** (900 MHz, 3 mm tube, 2 mg in 200 μ l MeOH-*d*₄), 6-chloro-4-phenyl-2H-chromen-2-one.

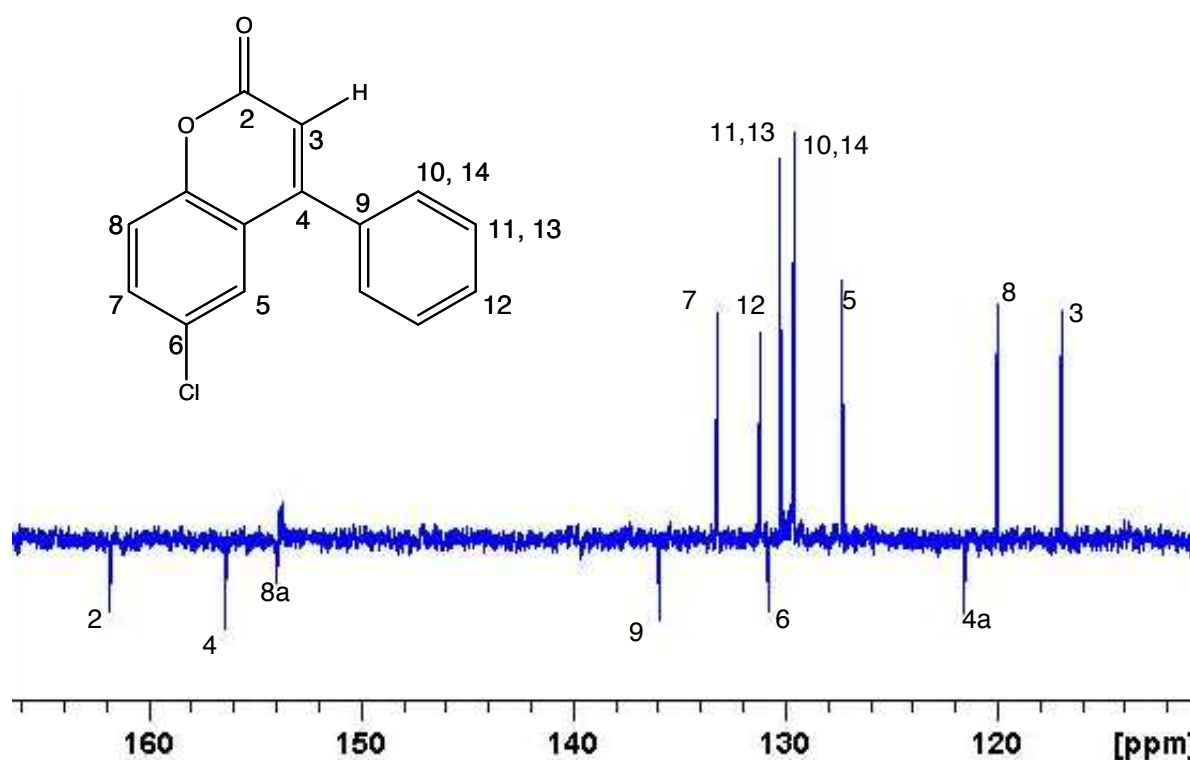


Figure 35. ¹³C DEPTQ NMR spectrum of synthetic **1** (225 MHz, 3 mm tube, 2 mg in 200 μ l MeOH-*d*₄), 6-chloro-4-phenyl-2H-chromen-2-one.

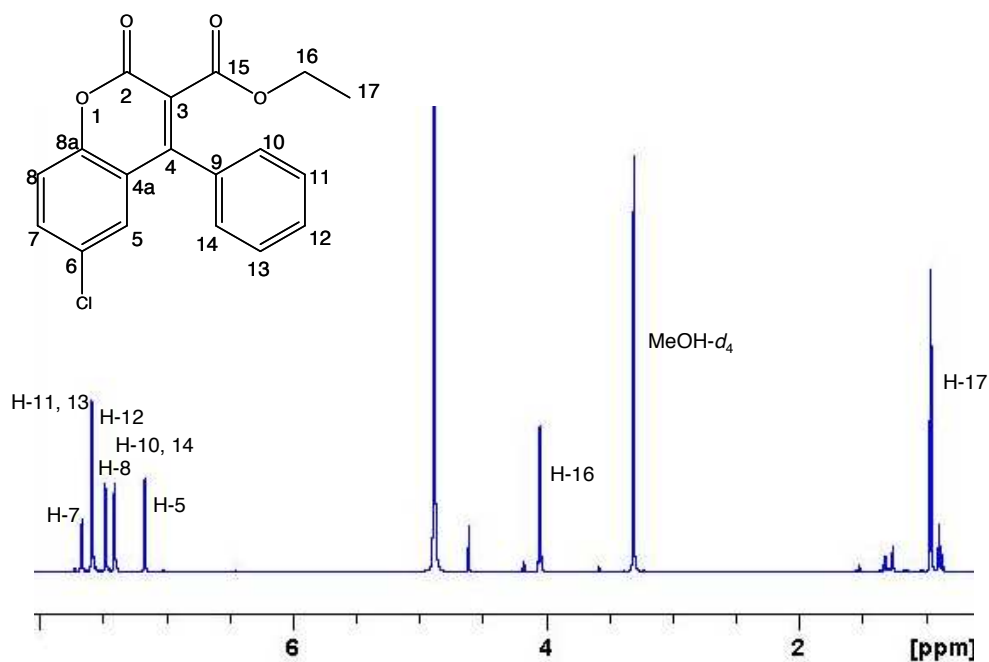


Figure 36. ¹H NMR spectrum of synthetic **2** (900 MHz, 3 mm tube, 2 mg in 200 μ l MeOH-*d*₄), ethyl 6-chloro-2-oxo-4-phenyl-2H-chromen-3-carboxylate.

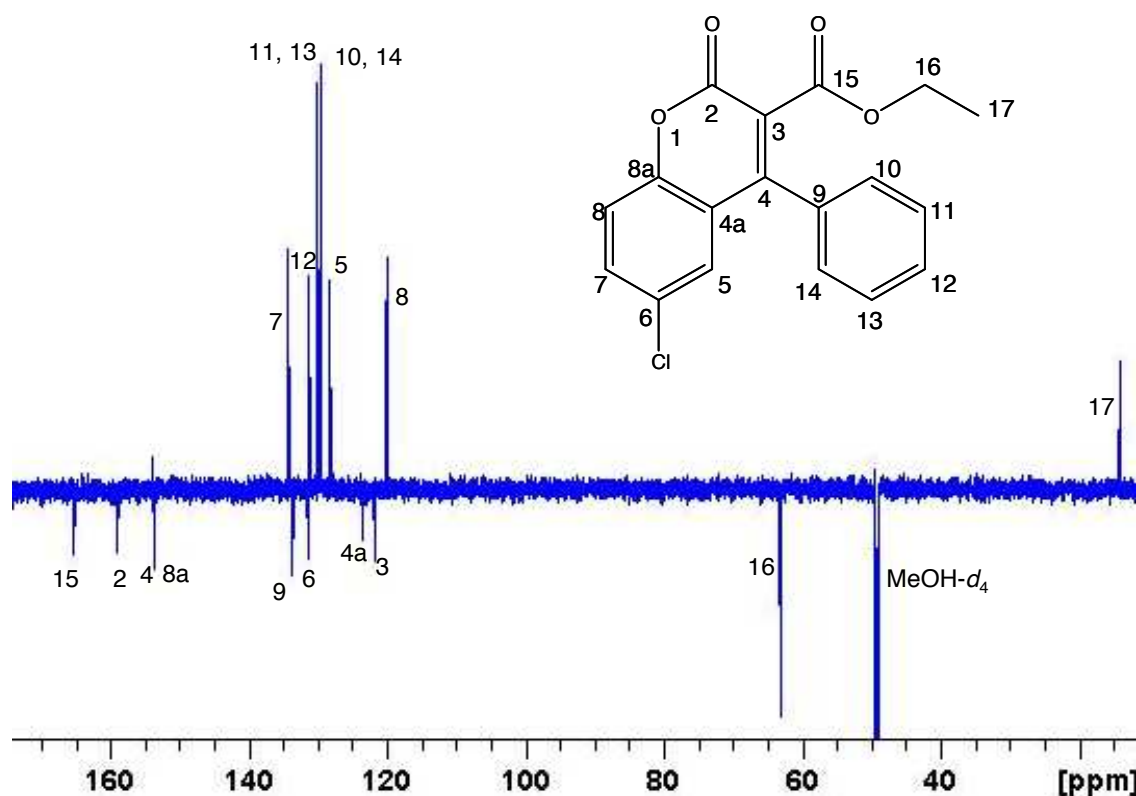


Figure 37. ¹³C DEPTQ NMR spectrum of synthetic **2** (225 MHz, 3 mm tube, 2 mg in 200 μ l MeOH-*d*₄), ethyl 6-chloro-2-oxo-4-phenyl-2H-chromen-3-carboxylate.

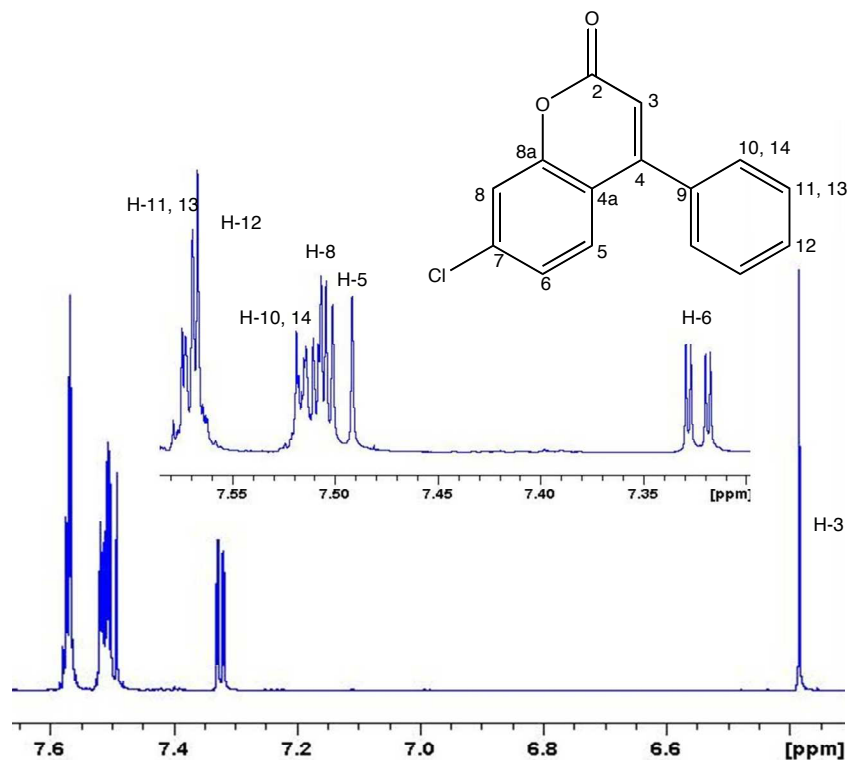


Figure 38. ¹H NMR spectrum of synthetic **3** (900 MHz, 3 mm tube, 2 mg in 200 μ l MeOH-*d*₄), 7-chloro-4-phenyl-2H-chromen-2-one.

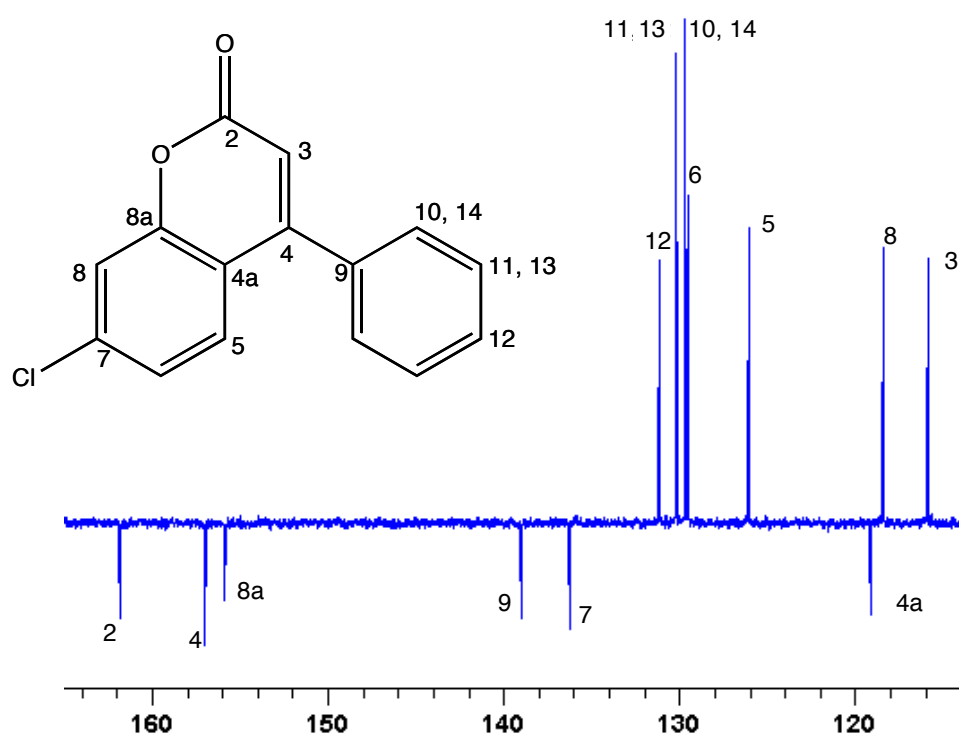


Figure 39. ¹³C DEPTQ NMR spectrum for synthetic **3** (225 MHz, 3 mm tube, 2 mg in 200 μ l MeOH-*d*₄), 7-chloro-4-phenyl-2H-chromen-2-one.

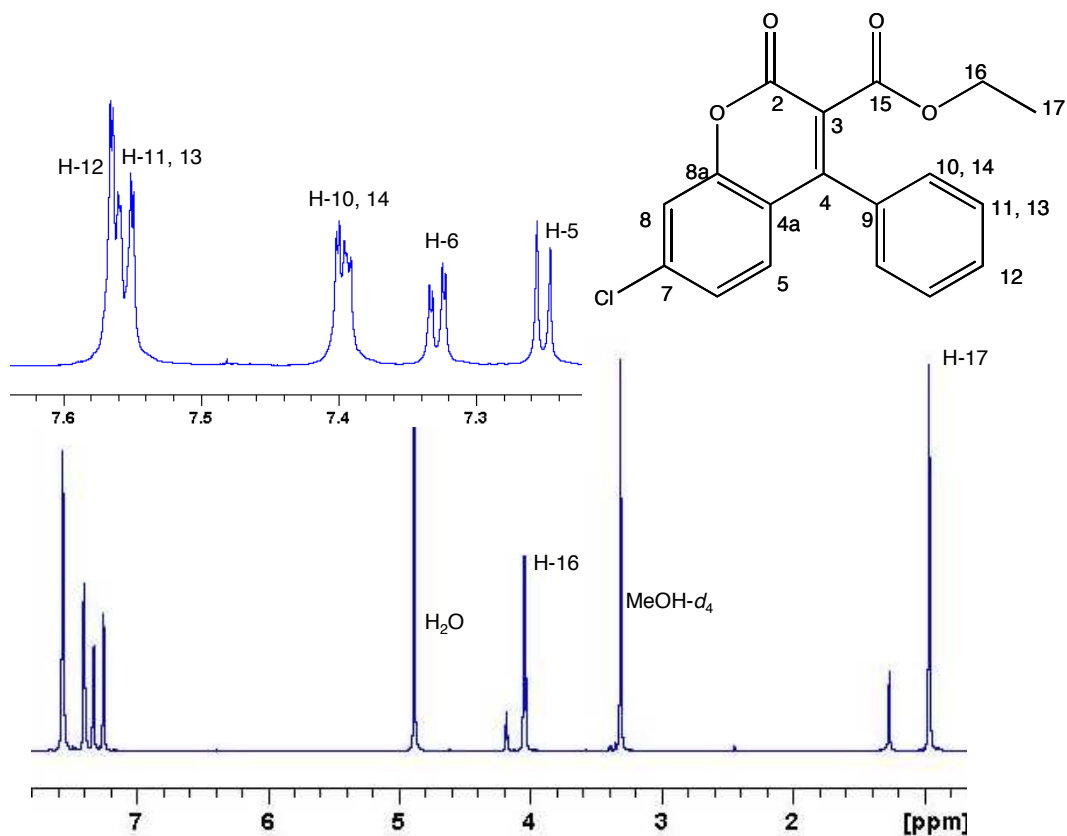


Figure 40. ^1H NMR spectrum of synthetic **4** (900 MHz, 3 mm tube, 2 mg in 200 μl MeOH- d_4), ethyl 7-chloro-2-oxo-4-phenyl-2H-chromen-3-carboxylate.

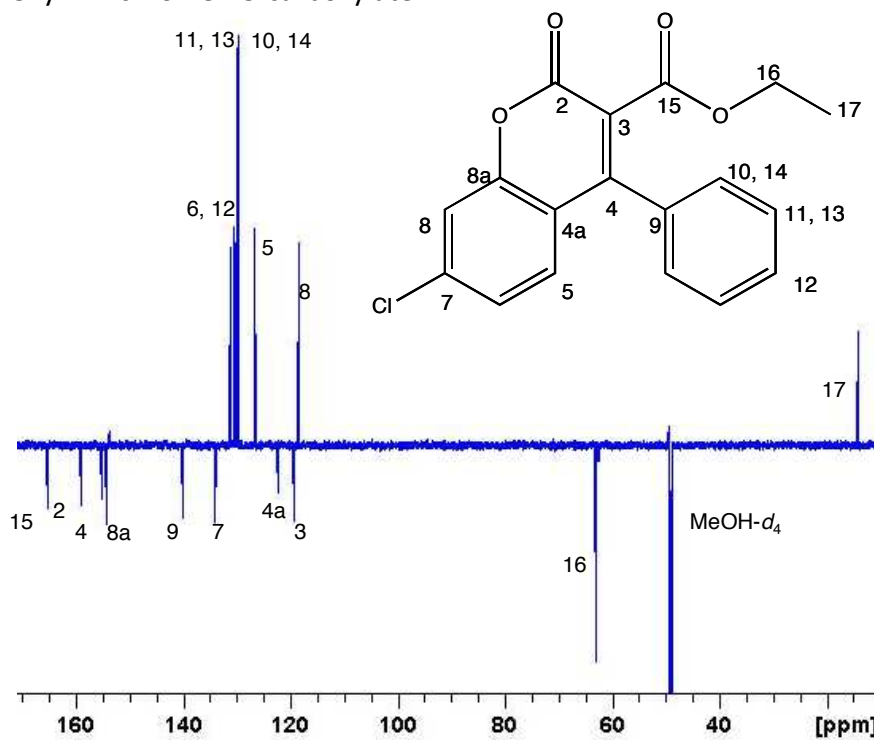


Figure 41. ^{13}C DEPTQ NMR spectrum of synthetic **4** (225 MHz, 3 mm tube, 2 mg in 200 μl MeOH- d_4), ethyl 7-chloro-2-oxo-4-phenyl-2H-chromen-3-carboxylate

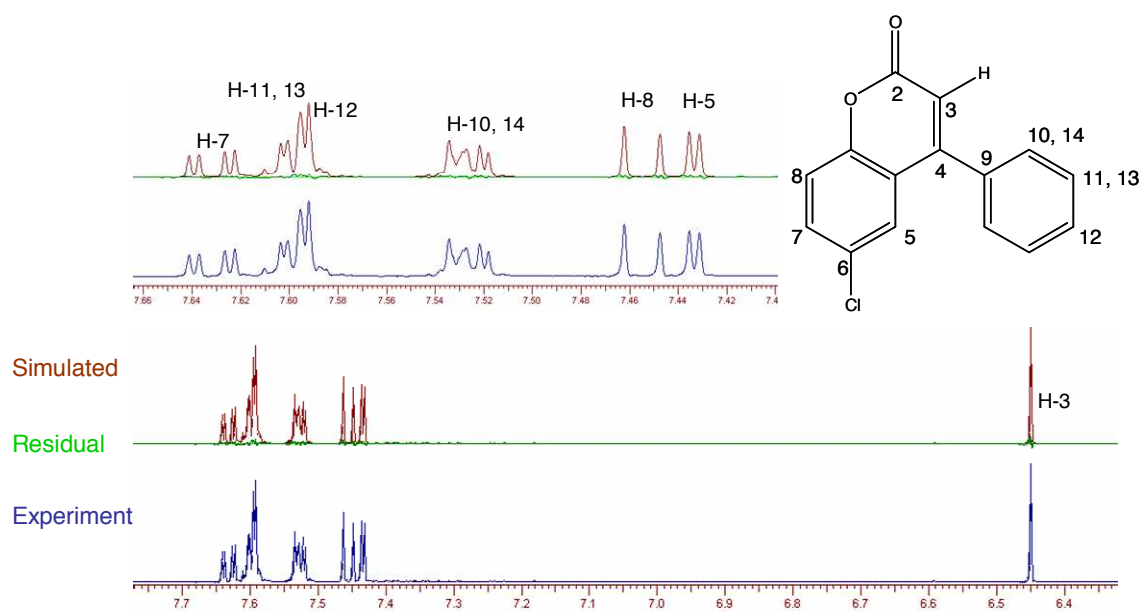


Figure 42. Full ^1H NMR spin analysis by PERCH iteration of 900 MHz data of the synthetic **1**, 6-chloro-4-phenyl-2H-chromen-2-one (simulated spectra in red: experimental spectra in blue: residual in green) Total RMS = 0.05%

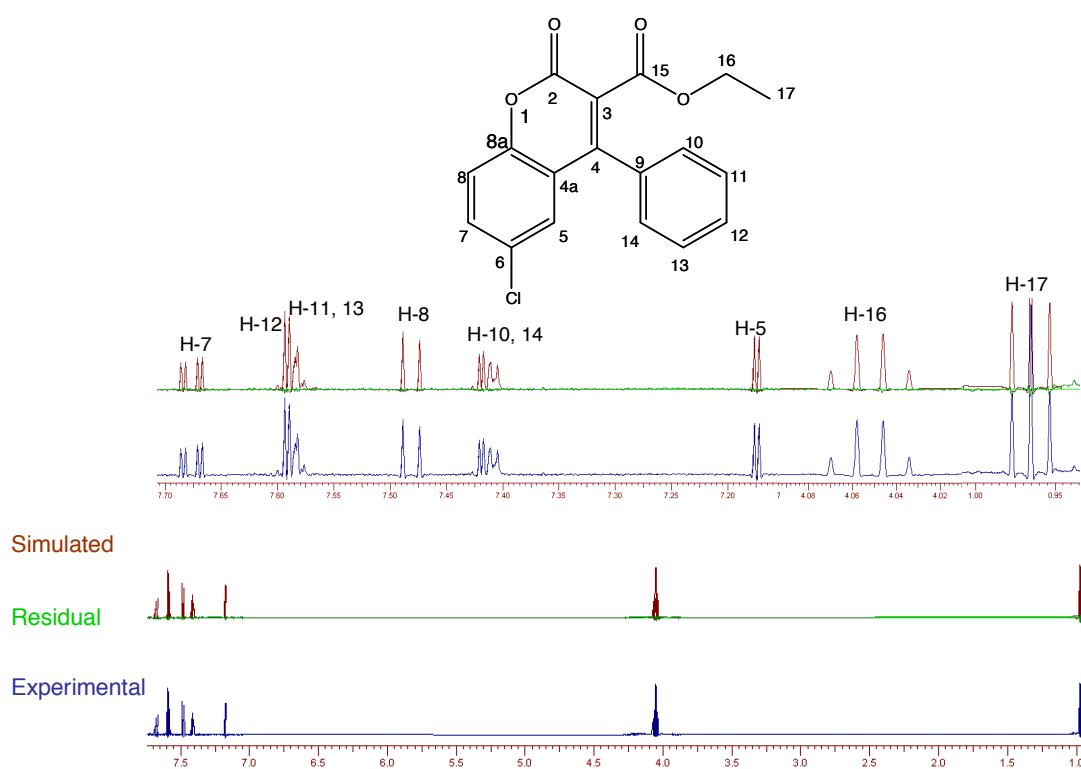


Figure 43. Full ^1H NMR spin analysis by PERCH iteration of 900 MHz data of the synthetic **2**, ethyl 6-chloro-2-oxo-4-phenyl-2H-chromen-3-carboxylate (simulated spectra in red: experimental spectra in blue) Total RMS = 0.19%

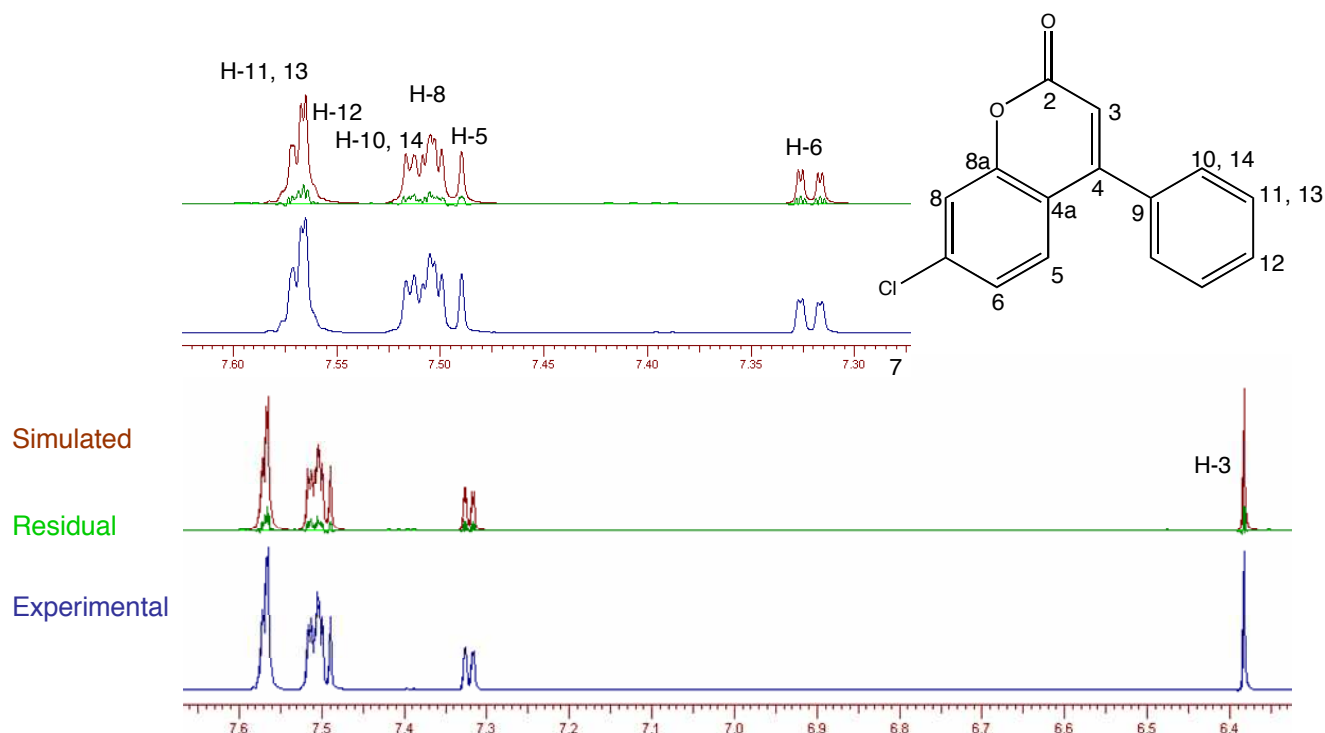


Figure 44. Full ^1H NMR spin analysis by PERCH iteration of 900 MHz data of the synthetic **3**, 7-chloro-4-phenyl-2H-chromen-2-one (simulated spectra in red: experimental spectra in blue) Total RMS = 0.04%

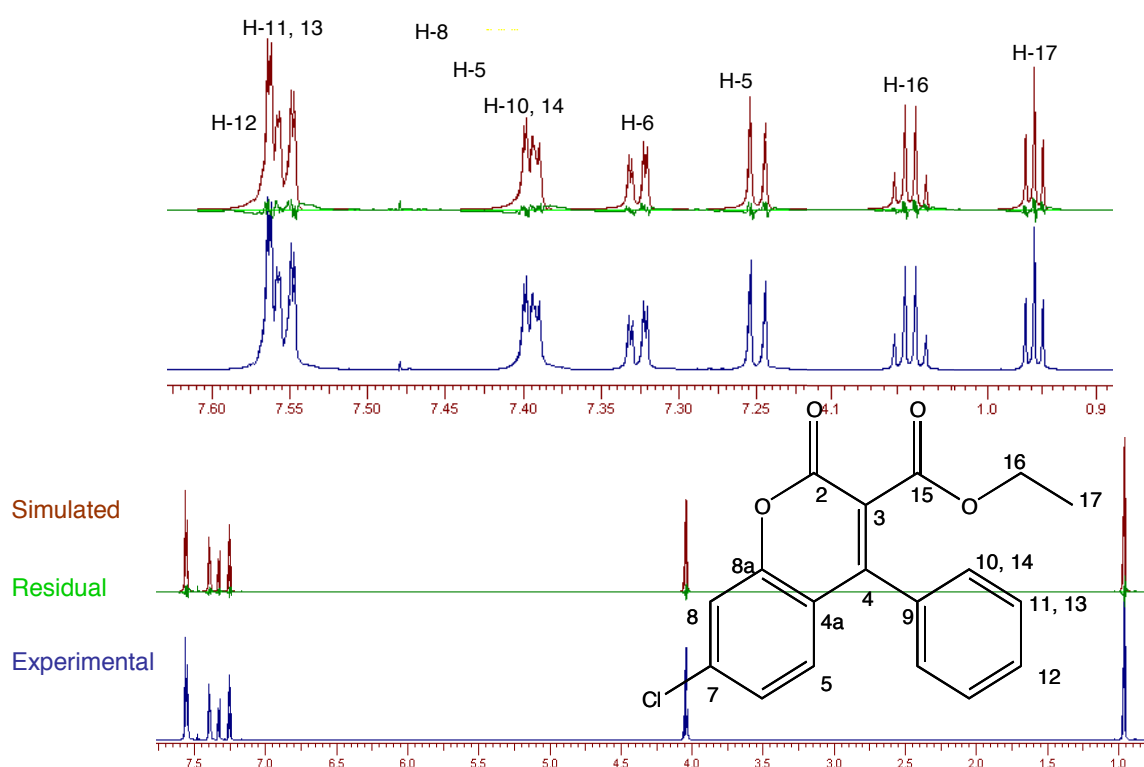


Figure 45. Full ^1H NMR spin analysis by PERCH iteration of 900 MHz data of the synthetic **4**, ethyl 7-chloro-2-oxo-4-phenyl-2H-chromen-3-carboxylate (simulated spectra in red: experimental spectra in blue) Total RMS = 0.05%

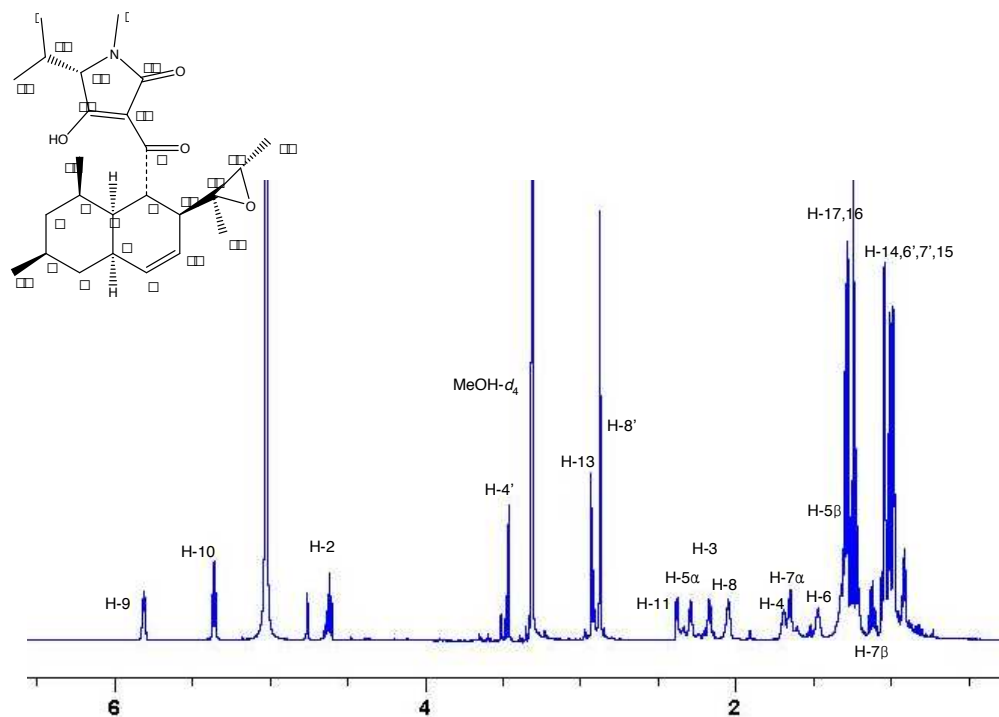


Figure 46. ^1H NMR spectrum of Vermitrasporin (900 MHz, 3 mm tube, 1 mg in 200 μl MeOH- d_4)

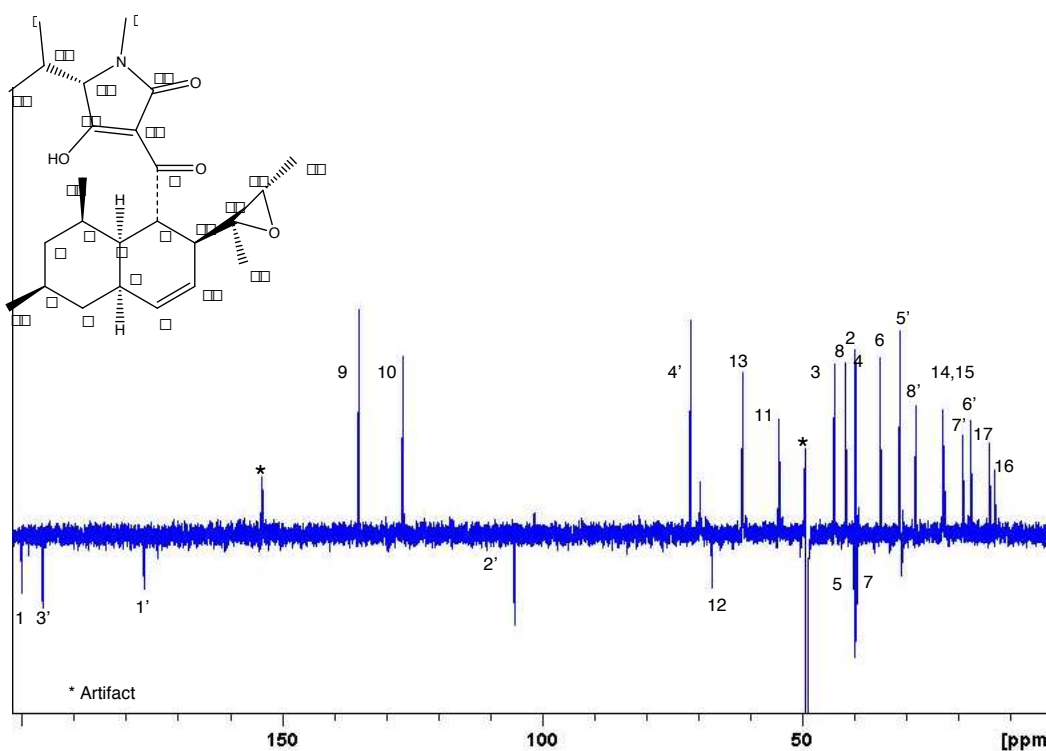
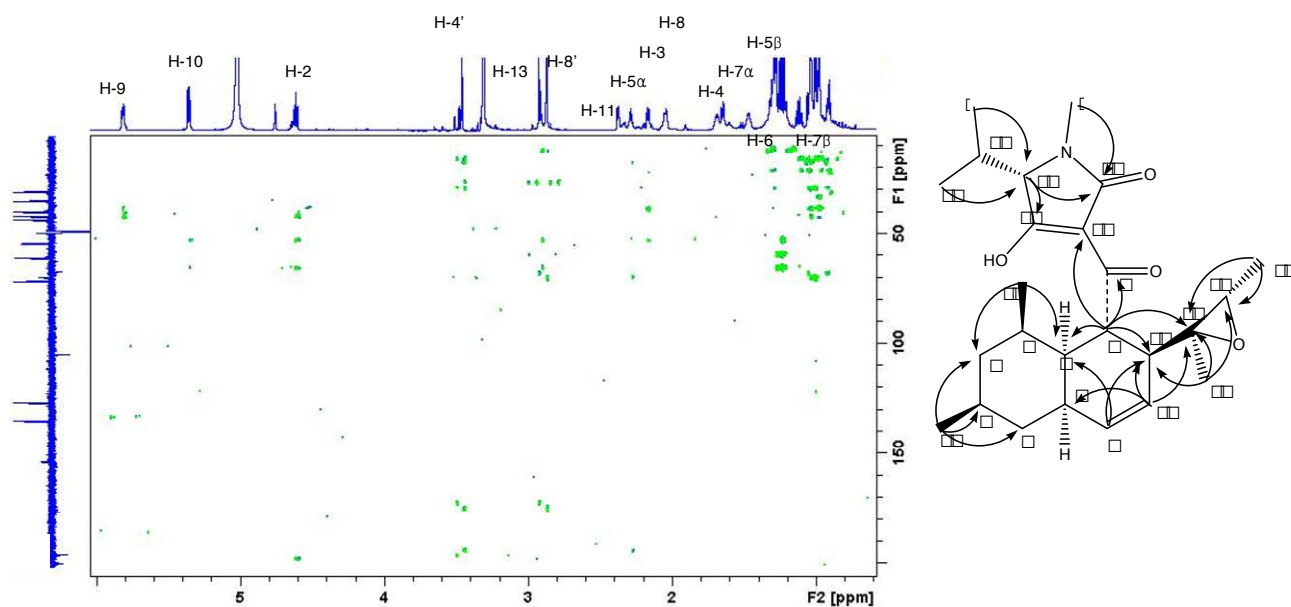
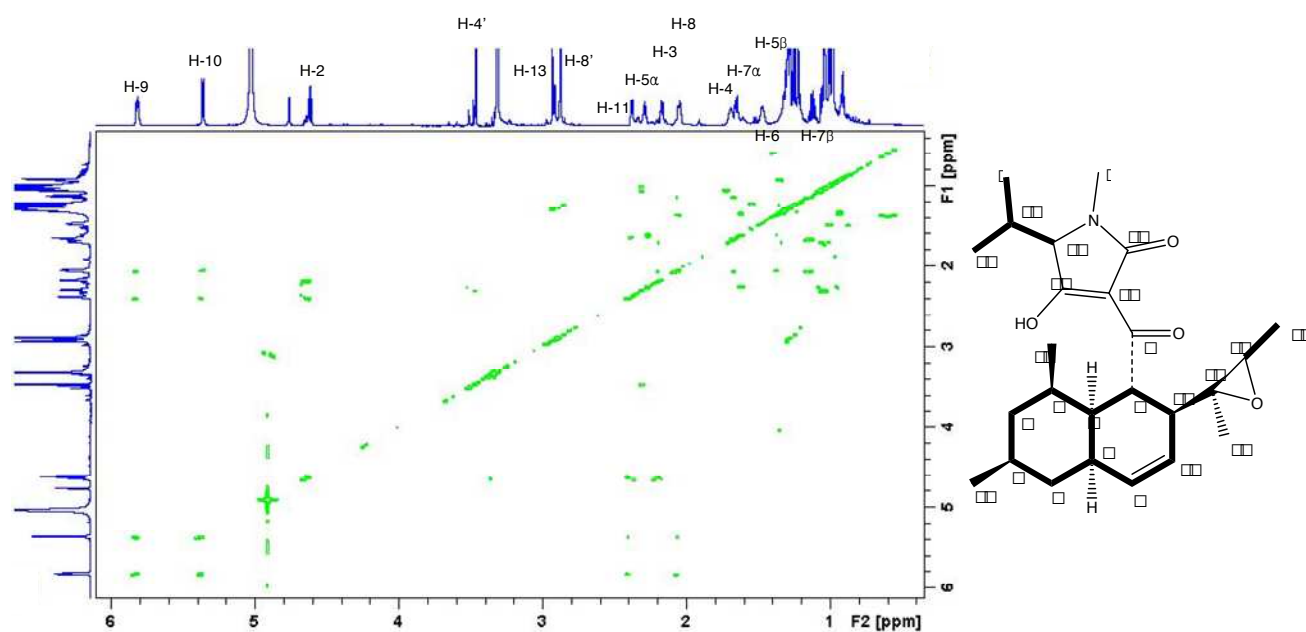


Figure 47. ^{13}C DEPTQ NMR spectrum of Vermitrasporin (225 MHz, 3 mm tube, 1 mg in 200 μl MeOH- d_4)



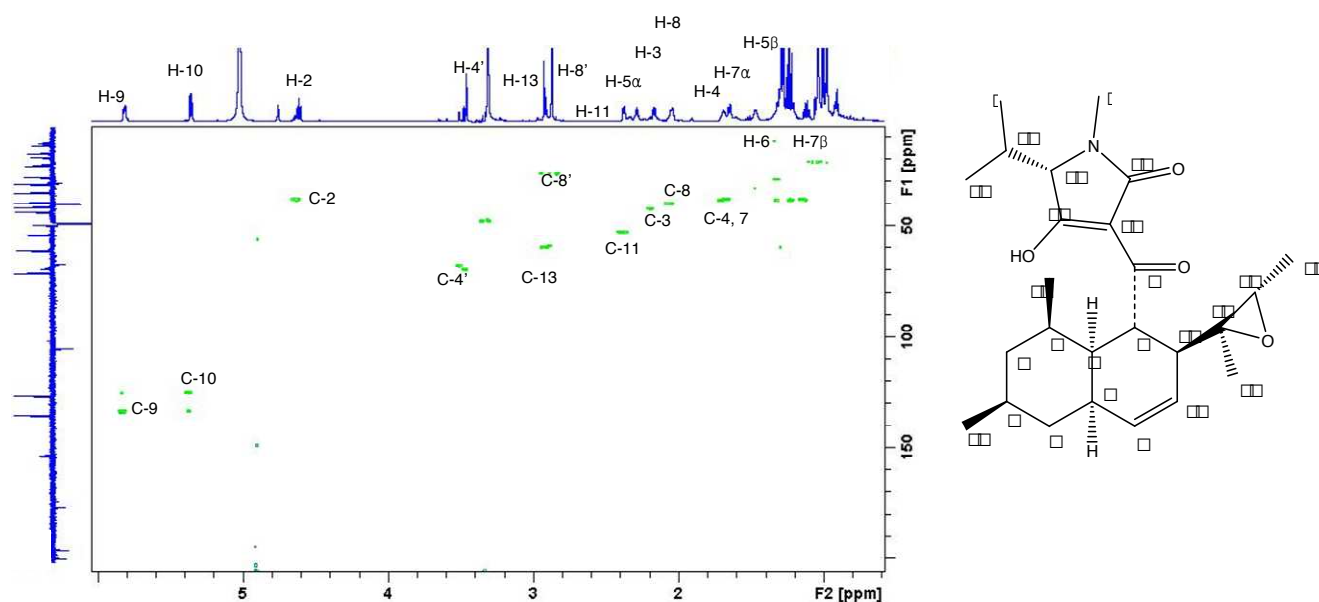


Figure 50. HSQC NMR spectrum of Vermitrasporin (900 MHz, 3 mm tube, 1 mg in 200 μ l MeOH- d_4)

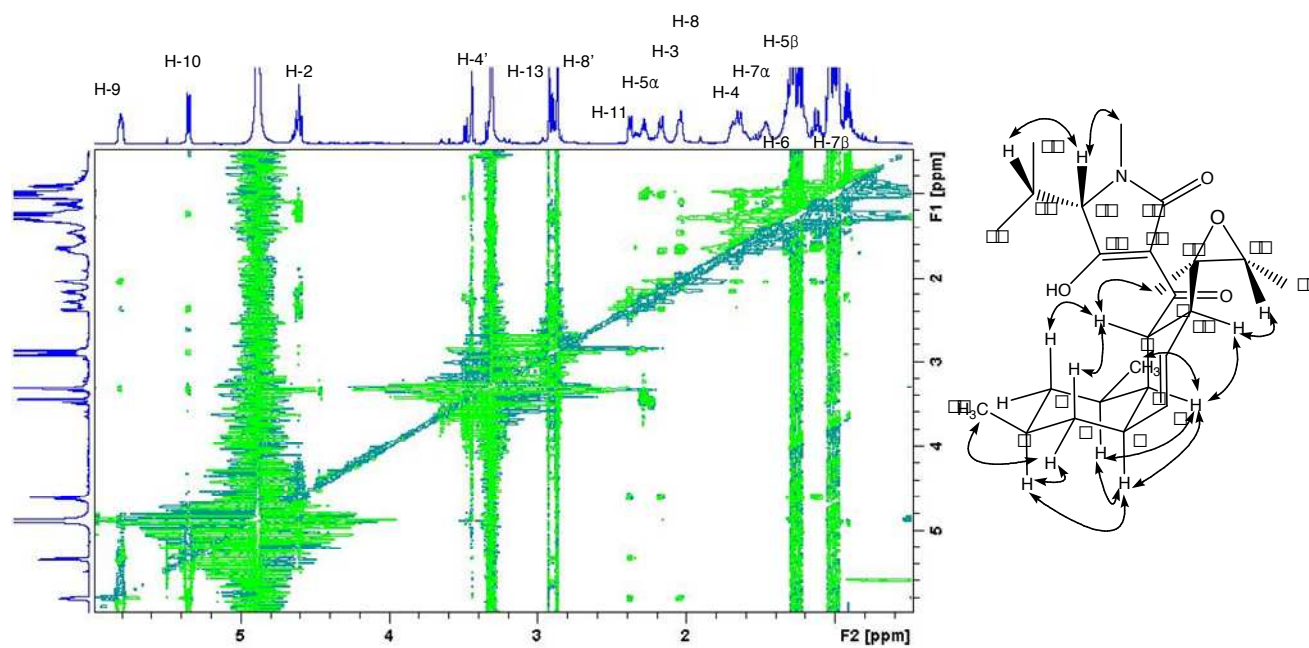


Figure 51. ROESY NMR spectrum of Vermitrasporin (600 MHz, 3 mm tube, 1 mg in 200 μ l MeOH- d_4)

VITA

NAME: Chang Hwa Hwang

EDUCATION: B.S., Biological Research, University of Illinois at Chicago, Chicago, 2003
Ph.D., Pharmacognosy, University of Illinois at Chicago, Chicago, Illinois, 2012

TEACHING EXPERIENCE: College of Pharmacy, University of Illinois at Chicago; Teaching Assistant for professional level classes in the college, 2007-2008

HONORS: UIC Chancellor's Leadership Award for Graduate Research, University of Illinois at Chicago, Chicago, Illinois, 2010

PROFESSIONAL MEMBERSHIPS: American Society of Pharmacognosy
American Society of Microbiology

POSTER PRESENTATIONS: **Chang Hwa Hwang**, Sang Hyun Cho, Yuehong Wang, Marcelle Hon, Cedric Pearce, Guido F. Pauli, and Scott G. Franzblau. "HIGH THROUGHPUT SCREENING OF FUNGAL EXTRACTS FOR ANTI-TUBERCULOSIS ACTIVITY". 51st Annual Meeting of American Society of Pharmacognosy, San Diego. 30 July 2011

Chang Hwa Hwang, Birgit U. Jaki, Guido F. Pauli, and Scott G. Franzblau. "UTILIZING ETHNOBOTANICAL INFORMATION FROM THE NAPRALERT DATABASE FOR TUBERCULOSIS DRUG DISCOVERY". 51st Annual Meeting of American Society of Pharmacognosy, San Diego. 30 July 2011

Chang Hwa Hwang, Birgit U. Jaki, Sang Hyun Cho, Yeun Kim, Minjee Kim, Cedric Pearce, Scott G. Franzblau, and Guido F. Pauli. "ISOLATION, IDENTIFICATION, AND BIOLOGICAL EVALUATION OF THE ANTI-TB ACTIVE NATURAL PRODUCT VERMISPORIN." 51st Annual Meeting of American Society of Pharmacognosy, San Diego. 30 July 2011

Chang Hwa Hwang, Sang Hyun Cho, Cedric Pearce, and Scott G. Franzblau "HIGH THROUGHPUT SCREENING OF FUNGAL CULTURES FOR ANTI-TUBERCULOSIS ACTIVITY" 48th Annual Meeting of American Society of Pharmacognosy, Portland, Maine. 17 July 2007

Xiaomei Wei, Skylar Carlson, Urszula Tanouye, **Chang Hwa Hwang**, Minjee Kim, Saba rezea, Sanghyun Cho, Scott Franzblau, Brian Murphy. "Induction of Anti-mycobacterial Agents from putatively inducible biosynthetic pathways of marine actinobacteria" 51st Annual Meeting of American Society of Pharmacognosy, San Diego. 30 July 2011

Xiaomei Wei¹, Urszula Tanouye, **Chang Hwa Hwang**, Yeuhong Wang, Sanghyun Cho, Scott Franzblau, Brian T. Murphy. "Identification of anti-tuberculosis secondary metabolites from deep Lake Michigan sediment strain *Micromonospora tulbaghia*. University of Illinois at Chicago, College of Pharmacy, Research Day, 2012

PUBLICATIONS: Moraski GC, Markley LD, Chang M, Cho S, Franzblau SG, **Hwang C**, Boshoff H, Miller MJ. "Generation and exploration of new classes of antitubercular agents: The optimization of oxazolines, oxaxoles, thiazolines, thiazoles to imidazo[1,2-a]pyridines and isomeric 5,6-fused scaffolds. *Bioorg Med Chem.* 2012, 20(7):2214-20.

Cho SH, Warit S, Wan B, **Hwang C**, Pauli GF, "Franzblau Low-oxygen-recovery assay for high-throughput screening of compounds against Nonreplicating *Mycobacterium tuberculosis*". *Antimicrob. Agents. Chemother.* 2007, 51(4):1380-5.

MANUSCRIPTS **Hwang C**, Cho SH, Wang Y, Pearce CJ, Pauli GF, Franzblau SG. "High Throughput Screening of Fungal Extract Library for Anti-tuberculosis Activity". To be submitted to *J. Antibiot.*
IN

PREPARATION: **Hwang C**, Jaki BU, Napolitano JG, Lankin DC, McAlpine JB, Cho SH, Pearce CJ, Franzblau SG, Kim Y, and Pauli GF. "Chemical and Biological Evaluation of Vermisporin, an Anti-TB Natural Product". To be submitted to *J. Antibiot.*

Hwang C, Jaki BU, Klein LL, Lankin DC, Napolitano JG, McAlpine JB, Cho SH, Franzblau SG, Stamets PE, and Pauli GF. "Two Naturally Occurring Anti-mycobacterial Coumarins from the Polypore Mushroom, *Fomitopsis officinalis*". To be submitted to *J. Nat. Prod.*